KU Leuven
Biomedical Sciences Group
Faculty of Medicine
Department of Cardiovascular Sciences
Center for Molecular and Vascular Biology

DNA METHYLATION STUDIES IN SPINA BIFIDA

Anne ROCHTUS

Promoter: Prof. Dr. K. Freson, University of Leuven, Belgium
Co-promoter: Prof. Dr. C. Van Geet, University of Leuven, Belgium

Jury members: Prof. Dr. K. Jansen, University of Leuven, Belgium
Prof. Dr. A. Van Eynde, University of Leuven, Belgium
Prof. Dr. O.F. Brouwer, University Medical Center Groningen, The Netherlands
Prof. Dr. W. Steegenga, Wageningen University, The Netherlands

Dissertation presented in partial fulfilment of the requirements for the degree of
Doctor in Biomedical Sciences
Leuven, September 1st 2016

To the Children with Neural Tube Defects

A meeting was held quite far from Earth!
It's time again for another birth.
Said the Angels to the LORD above,
This Special Child will need much love.

His progress may be very slow,
Accomplishments he may not show.
And he'll require extra care
From the folks he meets down there.

He may not run or laugh or play,
His thoughts may seem quite far away,
In many ways he won't adapt,
And he'll be known as handicapped.

So let's be careful where he's sent,
We want his life to be content.
Please LORD, find the parents who
Will do a special job for you.

They will not realize right away
The leading role they're asked to play,
But with this child sent from above
Comes stronger faith and richer love.

And soon they'll know the privilege given
In caring for their gift from Heaven.
Their precious charge, so meek and mild,
Is HEAVEN'S VERY SPECIAL CHILD.

Edna Massionilla

TABLE OF CONTENTS

LIST OF ABBREVIATIONS

A/B	Exon A/B = *GNAS-A/B*:TSS DMR
AHO	Albright Hereditary Osteodystrophy
AS1	*GNAS* antisense = *GNAS-AS1*:TSS DMR
BSP	Bisulfite Sequencing PCR
BWS	Beckwith Wiedemann Syndrome
CGH	Whole genome array competitive genomic hybridization
CGI	CpG islands
CNS	Central Nervous System
DLHP	Dorsolateral Hinge Point
DMR	Differentially Methylated Region
DNMT	DNA methyltransferase
GD	Gestational Day
HDAC	Histone Deacetylase
HLPC	Quantitative high-performance liquid chromatography
HOX	Homeobox
HM450k	Human Methylation 450k BeadChip
IGF1	Insulin-Like Growth Factor
LINE-1	Long Interspersed Nuclear Element 1
MGS	Meckel-Gruber Syndrome
MHP	Median Hinge Point
MMC	Myelomeningocele
MOMS	Management of Myelomeningocele Study
MSI	Microsatellite Instability
MS-MLPA	Methylation specific-multiplex ligation-dependent probe amplification
MSP	Methylation-Specific PCR
MTHFD	Methenyltetrahydrofolate Dehydrogenase
MTHFR	Methylene Tetrahydrofolate Reductase
MTR	Methionine synthase
Mtrr	Murine methionine synthase reductase

NESP	Neuroendocrine secretory protein 55 = *GNAS-NESP*:TSS DMR
Non-LTR	Non-Long Terminal Repeat
NTD	Neural Tube Defect
PCP	Planar Cell Polarity
PHP	Pseudohypoparathyroidism
PONTI	Prevention of Neural Tube Defects by Inositol
PPHP	Pseudopseudohypoparathyroidism
PTH	Parathyroid Hormone
SAH	S-adenosylhomocysteine
SAM	S-adenosylmethionine
Shh	Sonic Hedgehog
SINE	Short Interspersed Elements
SRS	Silver-Russell Syndrome
TET	Ten-Eleven-Translocation proteins
tHcy	total Homocysteine
THF	Tetrahydrofolate
TNDM	Transient Neonatal Diabetes Mellitus
TSH	Thyroid Stimulating Hormone
XL	Extra-large stimulatory G protein = *GNAS-XL*:Ex1 DMR

GENERAL INTRODUCTION

It is not the strongest of the species that survives,
nor the most intelligent,
but the one most responsive to change.
Charles Darwin (1809)

CHAPTER 1

Introduction to neural tube defects

“nervorum propagines tam varie per tumorem dispersas”
Nicolaas Tulp (1641)

1.1 The history of neural tube defects

The first signs for Neural Tube Defects (NTDs) in humans are ancient. Anthropologists discovered spines with stigmata typical for infants born with meningomyeloceles. As these children were born in time periods where medical treatment was scarce, we can only suppose that most of them did not survive. But the large number of anthropological figures sculpted in stone and terracotta, makes us assume that persons survived with an otherwise devastating condition. The figures are often seated in the typical forward posture of a paraplegic individual with a thoraco-lumbar kyphotic spine [1].

Figure 1. Figures from Meso-American cultures. From left to right: a terracotta figure from Colima, Mexico (circa 200 A.D.), a terracotta figure from Chancay, Peru (circa 1000 A.D.) and a child from the Olmec culture (circa 1500 B.C., Meso-America). The forward position with paraplegic legs and thoracolumbar kyphosis is indicative of individuals with a neural tube defect.

The earliest definition of spina bifida is from the Dutch clinician Peter van Forest (1522-1597) [2]. Some years later, the Dutch surgeon Nicolaas Tulp (1593-1674), famous as the main figure in Rembrandt's painting "The Anatomy Lesson of Dr. Tulp", introduced the term "spina bifida" as *"nervorum propagines tam varie per tumorem dispersas"* (the prolongations of the nerves scattered in different directions through the tumor). Tulp was in charge of the anatomy and dissection lessons for the Surgeons' Guild in Amsterdam and was a friend of Rembrandt van Rijn. In his most famous work *Observationes Medicae* (1641) he described a number of cases with an excellent drawing of the condition, possibly by Rembrandt. He presented how the myelomeningocele sac should be dissected. But as his patients died, he recommended caution in the approach of patients, as consequences could be terrible. For more than 200 years, surgeons around the world tried various surgical procedures, but concluded that spina bifida was untreatable. Infections and

septicemia were almost invariably fatal. After the introduction of aseptic surgical techniques in the 1870s, discussions on the best surgical treatment recommenced and survival rates improved. In 1952, Nulsen, Spitz and Holter developed the first modern ventriculoperitoneal shunts. With all their problems, shunts transformed the future for patients with spina bifida and hydrocephalus. The medical revolution continued and in 2003, the National Institutes of Health began the “Management of Myelomeningocele Study (MOMS)” to investigate health consequences of pre- versus postnatal repair. Interestingly, fetal repair reduced the need for shunting and improved motor outcomes at 30 months but had higher maternal and fetal risks.

We owe gratitude to our previous colleagues ameliorating the management of this devastating disorder. As a result, many children now live independently.

1.2 Clinical presentation of neural tube defects

NTDs result from failure of spontaneous neural tube closure between the 3rd and 4th week of development. The most common NTDs are anencephaly and myelomeningocele (commonly named spina bifida), which are often referred to as 'open' NTDs because the neural tube does not close completely. Craniorachischisis, which results from failure over the entire body axis, is an additional relatively rare form of open NTD. The 'closed' or skin-covered NTDs include encephalocele, meningocele and occult spinal dysraphisms (commonly called spina bifida occulta).

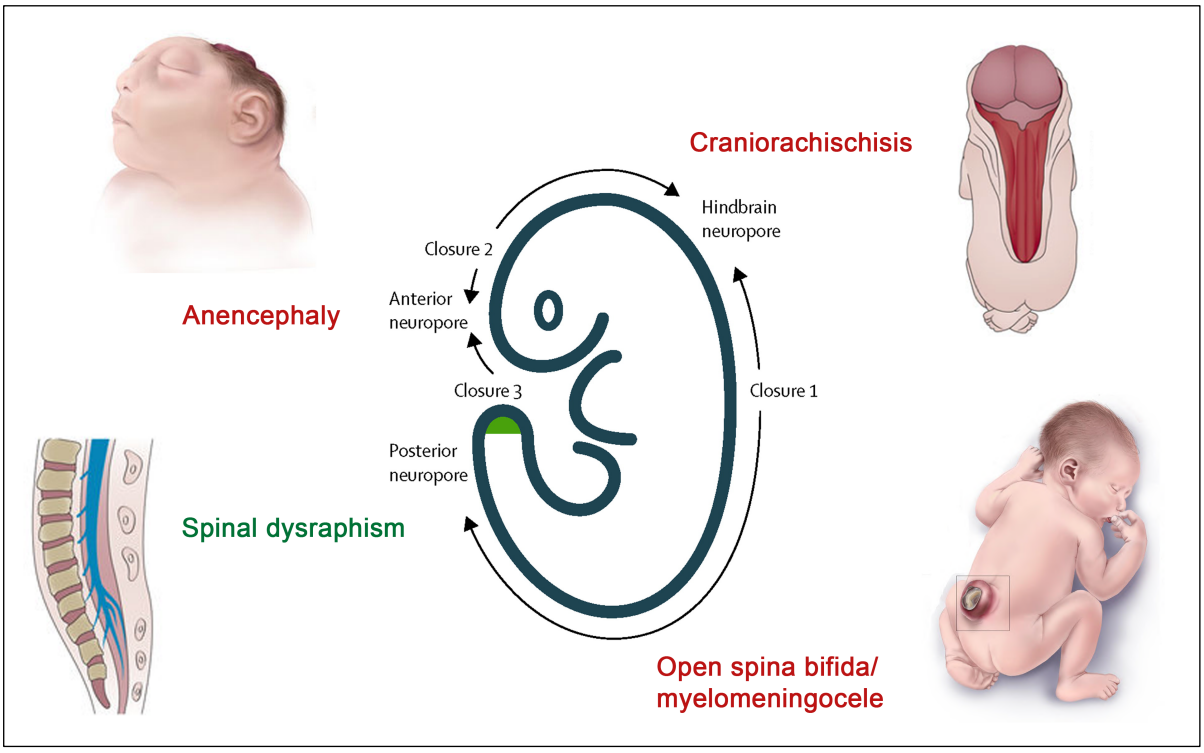

Figure 2. Subtypes of mammalian neural tube defects related to stages of neural tube closure. The main 'open' NTDs that result from a defective primary neurulation are presented in red. The main 'closed' NTD that resuls from a defective secondary neurulation is presented in green (Figure adapted from [3]).

In spina bifida, the spinal cord (myelon), the coverings (meninges) and vertebral arches develop abnormally. Both the spinal cord and brain are affected. Sensory and motor functions at and below the level of the spinal cord defect are impaired, leading to paralysis (Table 1), bowel and bladder dysfunction. Nearly all infants have the Arnold-Chiari II malformation, which includes hindbrain herniation, brain-stem abnormalities, low-lying venous sinuses and a small posterior fossa.

Table 1: Rehabilitation needs for patients with NTDs according to their functional motor level.

Functional motor level	Expected muscle function	Functional ability	Equipment use	Orthotic use
Thoracic	Abdominals, paraspinals, quadratus lumborum	Nonfunctional ambulation/standing, early use of wheelchair	Standing frame, wheelchair, parapodium	Trunk-hip-knee-ankle-foot orthosis
High lumbar L1-L3	Hip flexion, hip adduction	Limited household ambulation, early use of wheelchair	Wheelchair, walker, forearm crutches	Reciprocating gait orthosis, hip-knee-ankle-foot orthosis
Midlumbar L3-L4	Knee extension	Household, limited community ambulation, wheelchair	Wheelchair, walker, forearm crutches	Knee-ankle-foot orthosis
Low lumbar L4-L5	Hip abduction, knee flexion, ankle dorsiflexion, ankle inversion, toe extension	Household, community ambulation, wheelchair for long distances	Wheelchair, forearm crutches	Ankle-foot orthosis
Sacral S1-S2	Hip extension, ankle plantar flexion, ankle eversion, toe flexion	Community ambulation	-	Supramalleolar-foot orthosis, foot orthotic

The severity of the neurologic disability in the lower limbs is correlated with the level of the injury to the spinal cord.

Traditionally, postnatal surgery is performed within 48 hours after birth to minimize the risk of meningitis. Recently, a number of centres implemented prenatal surgery, with promising results on motor outcome [4]. As the Arnold-Chiari malformation obstructs the outflow of cerebrospinal fluid and causes hydrocephalus, almost all infants with lumbosacral spina bifida need ventriculoperitoneal shunting, which is often associated with surgical revisions to address failure or infection. Regular evaluation of neurological function by a specialized multidisciplinary team is essential for neurologic and physical function. Deterioration can occur very insidious and can be caused by undiagnosed shunt malfunction, hydromyelia, tethered cord, as well as orthopedic and urologic complications.

In addition to surgery and regular clinical and neurological follow-up, patients need careful monitoring of urologic and bowel functions. The abnormal neurological control of the bladder may result in urinary retention with overflow and vesico-ureteral reflux, recurrent urinary tract infections and deterioration of the renal function. Therefore, urodynamic studies and ultrasonography are performed to detect urological complications and the introduction of clean intermittent

catheterization dramatically reduced renal failure. As the innervation of the bowel and anus also often are affected, patients require bowel management treatment such as oral laxatives, suppositories and enemas.

Overall, management of patients with NTDs is very complex and requires a multidisciplinary team to provide the best medical care. Integrated effort from many disciplines, including a specialized nurse, a pediatric neurologist and neurosurgeon, an orthopedic surgeon, an urologist, a physical therapist, a psychologist and a social worker, results in the best opportunity for coordinated and high-quality care.

1.3 Epidemiology of neural tube defects

NTDs affect an average of one in 1000 pregnancies. The incidence varies by geographical location and ethnicity, and is obviously under influence of population-specific risk alleles, dietary habits and environmental exposures [5]. Twin concordance rates, which are higher for monozygotic (7.7%) than dizygotic (4.0%) twins, attest for a genetic contribution. In addition, a lot of environmental factors are known to influence neural tube closure. It has been clear for forty years that maternal folic acid supplementation prevents both NTD recurrence [6] and occurrence [7], which quickly led to the recommendation of supplementation of 400 µg folic acid to women who are planning to become pregnant. Despite this recommendation, many NTDs are not prevented. As only a minority of women takes supplements and a lot of pregnancies are unplanned, mandatory fortification of cereal grains was introduced in the United States in 1998. The incidence in the US decreased from 2 per 1000 in the 1960s to 1 per 2000 nowadays. Mandatory fortification of folic acid resulted in a lower prevalence of NTDs than voluntary folic acid supplementation [8]. In Europe, mandatory folic acid fortification does not yet exist. A recent population based study in Europe showed a total prevalence of NTD of 9.1 per 10 000 births, which did not decrease after two decades of recommendations for folic acid supplementation [6,9]. Mandatory folic acid fortification should be considered more effective means for NTD prevention in Europe. Each year approximately 5000 fetuses are affected with a NTD in Europe and after prenatal diagnosis, termination of pregnancy is the most common outcome for fetuses with NTDs. Below are prevalence rates listed for Belgium, the Netherlands and all European member countries of Eurocat.

Table 2: Prevalence of neural tube defects and subtypes in Belgium, the Netherlands and all full member countries of Eurocat.

Registry	Anomaly	Total N	Prevalence	LB	FD	TOPFA
Belgium	Neural Tube Defects	648	8.74	31.0%	7.9%	61.1%
	Anencephaly	245	3.31	4.9%	7.8%	87.3%
	Encephalocele	53	0.72	34.0%	7.5%	58.5%
	Spina Bifida	350	4.72	48.9%	8.0%	43.1%
The Netherlands	Neural Tube Defects	483	9.10	53.2%	14.3%	32.5%
	Anencephaly	165	3.11	18.8%	27.3%	53.9%
	Encephalocele	35	0.66	57.1%	20.0%	22.9%
	Spina Bifida	283	5.33	72.8%	6.0%	21.2%
Total Europe	Neural Tube Defects	16973	9.67	32.2%	7.3%	60.5%
	Anencephaly	6588	3.75	11.4%	12.0%	76.6%
	Encephalocele	1813	1.03	37.5%	6.3%	56.3%
	Spina Bifida	8572	4.88	47.1%	3.9%	49.0%

Prevalence is stated per 10 000 births. LB: life births; FD: fetal deaths/still births from 20 weeks gestation; TOPFA: termination of pregnancy for fetal anomaly following prenatal diagnosis. Data are extracted from Eurocat from 1980 - 2012. Genetic conditions are excluded from the data.

Every public intervention is characterized by concerns on benefits and risks. Folic acid has been used for more than forty years, and throughout its use, some old and new concerns exist [10]. The major concern is the possibility that a high dose of folic acid masks anemia caused vitamin B12 deficiency, but to date there is little evidence. Secondly, many studies investigated a link between folate, DNA methylation and cancer risk. It has been suggested that folic acid might prevent some cancers and might promote others, but currently there is no evidence that demonstrates a causal link between fortification and cancer.

1.4 Embryology of neural tube defects

To gain insight into the embryological basis of NTDs, it is essential to understand the morphogenetic processes and molecular mechanisms that underlie neural tube closure.

The human nervous system originates from the primitive ectoderm that also develops into epidermis [11]. The ectoderm, endoderm and mesoderm form the three primary germ layers that are developed by the 3rd week. The endoderm, particularly the notochordal plate and the intra-embryonic mesoderm, induces the overlying ectoderm to develop the neural plate in the 3rd week of development. The neural plate is converted into a tube by a two-stage process: primary and secondary neurulation. Primary neurulation initiates discontinuously at several discrete levels of the body axis (Figure 2). This process has been most intensively investigated in mice. Murine neural tube closure initiates at the hindbrain/cervical boundary (closure 1), and spreads caudally and rostrally from this site. Separate closure initiation sites occur at the midbrain-forebrain (closure 2) and at the rostral limit of the forebrain (closure 3). Neural tube closure in humans is similar to mice, but closure 2 may be absent [11]. Interestingly, mouse embryos that lack closure 2 (described in the SELH/Bc inbred strain) achieve total cranial closure in around 80% of cases [12], indicating that closure 2 is not obligatory for brain formation. The process of primary neurulation generates the entire neural tube, with closure of the anterior neuropore on day 24 and the posterior neuropore on day 26. The posterior neuropore fuses with the process of secondary neurulation, a process in which the stem cells in the tail bud differentiate to form cells of neural fate. As the process of secondary neurulation does not require bending of the neural plate, defects are never open but involve tethering of the neural tube to surrounding tissues. On the other hand, failure of primary closure leads to exposure of the neuroepithelium to the environment, with degeneration of neural tissue and neuronal deficit. My study included patients with abnormalities in primary neurulation of the spinal cord, failures that result in ‘open’ spina bifida (myelomeningocele).

The following morphogenetic events are essential for successive neurulation:
1) initiation of neural tube closure; 2) neural fold elevation and apposition; and 3) adhesion and fusion of the neural folds. As failure of these mechanisms may result in NTDs, insights in these processes are discussed below.

1. Initiation of neural tube closure

Immediately preceding neural tube closure, the initially elliptical neural plate becomes longer and narrower to form a keyhole-shaped structure with broad cranial and narrow spinal regions. Convergent extension is the driving force for this process. Cells move towards the midline and sequential intercalation of cells narrows and lengthens the neural plate along the anterior-posterior body-axis. The process of convergent extension depends on the Planar Cell Polarity Pathway (PCP) or non-canonical Wnt signaling. Disruption of this pathway results in a wide neural plate, which makes neural fold fusion impossible. This results in craniorachischisis, the most severe NTD, with an open neural tube from the brain to the spinal cord. Mouse embryos with homozygous mutations in genes implicated in the PCP pathway (*Dishevelled, Vangl2, Scribble*, or *Celsr1)* exhibit failure of closure 1 (Figure 2), which results in craniorachischis. Interestingly, *Vangl2,* results in different phenotypes depending of its combination with other mutant genes: *Vangl2* with *Ptk7* and *Grhl3* results in open spina, whereas exencephaly occurs when *Vangl2* is combined with a loss of the *Cthrc1* gene [13]. These findings illustrate that a combination of related gene defects can produce different NTD phenotypes. In humans however, mutations of PCP genes are only associated with a few cases of NTDs [14]. Notably, also in humans, mutations in PCP genes are associated with different NTD phenotypes such as cranial, spinal and both open and closed NTD.

2. Neural fold elevation and apposition

Bending of the neuroepithelium of the spinal cord occurs at two sites: the median hinge point (MHP) and the paired dorsolateral hinge points (DLHPs). The MHP overlies the notochord and *Sonic Hedgehog (Shh)* has been implicated as the signal from the notochord that induces the floor plate of the neural tube. The paired DLHPs create longitudinal grooves that bring the neural fold tips face each other in the dorsal midline. Experiments with mice showed that *Shh* inhibits DLHP formation at the upper spinal cord, the strength of *Shh* signaling lessens down the neuraxis,

whereby DLHP formation occurs at lower spinal levels. This signal creates different combinations of bending points as closure progresses down the neural axis. At the upper levels bending occurs at the MHP, at intermediate spinal levels at both MHP and DLHP and at the lowest spinal levels solely at DLHPs. As *Shh* overexpression inhibits dorsolateral bending, this leads to NTDs [11]. Some mouse mutants such as *Gli3, Ptc1, opb* and *Zic2* inhibit negative regulators of *Shh* signaling which results in severe NTDs [15].

3. Adhesion and fusion of the neural folds

Adhesion and fusion of apposed neural folds is essential for neural tube closure. The mechanisms of adhesion and fusion are poorly understood. It has been suggested that cellular protrusions consisting of extracellular carbohydrate material at the tips of the neural folds may be related to the adhesive properties of the cells. The protrusions seem to interdigitate when the folds appose, what provides an initial contact that facilitates subsequent cell adhesion [15]. In support of this idea, *Efna5* and *Epha7* mice mutants with mutations in the ephrin family of cell-surface ligands, exhibit exencephaly due to a lack of fusion in apposed folds [15,16].

1.5 Genetic and environmental factors contribute to neural tube defects

Both genetic and environmental factors are involved in the etiology of NTDs. The high recurrence risk for siblings (2-5%) indicates a strong genetic component, but the majority of NTDs are sporadic, with relatively few reports of multi-generational families, suggesting a multifactorial polygenic pattern of inheritance. Studies indicated numerous candidate genes and environmental factors, and introduced further complexity by potential gene-gene and gene-environment interactions. Although it is well established that there is a genetic component underlying NTDs, the genetic players still remain largely unknown. In order to unravel the underlying etiology, candidate genes for NTDs are mainly selected based on their biological plausibility from syndromes that include a NTD, but mostly from animal models with NTDs. In addition, environmental risk or preventive factors for NTDs point at genes that might influence neurulation such as genes involved in the folate metabolism or glucose homeostasis.

Lessons from genetic syndromes that include a NTD

The study of syndromes with NTDs and their associated anomalies contributes to our understanding of the potential pathogenic mechanisms underlying NTDs. NTDs are associated with genetic syndromes that include Meckel-Gruber syndrome, Joubert syndrome, Currarino syndrome, and Mohr syndrome [17]. They are also caused by various chromosomal abnormalities. Deletions and duplications of smaller chromosome segments and single-gene conditions are also important to identify human genes that contribute to NTDs. The proportion of patients with NTDs classified as isolated, multiple birth defects or syndromes varies widely among different studies. It has been estimated that 3-10% of NTDs are associated with chromosomal abnormalities [18-20]; this does not include single-gene conditions. Specific associated defects that occur with greatest frequency are facial clefting, cardiac defects, anotia/microtia, limb defects, anophtalmia/microphtalmia, abdominal wall defects, and renal anomalies. Less common associated defects include holoprosencephaly, amniotic bands and polydactyly. As midline anomalies are often associated defects, two hypotheses tried to explain the co-occurrence of structural anomalies with NTDs: the *schisis associated* and the *midline developmental field concept*. The *schisis associated concept* supposes that associated defects may be

considered defects of closure such as cleft lip, cleft palate, cardiac defects, omphalocele, and diaphragmatic hernia. The *midline developmental field concept* suggests a vulnerability of midline structures. However, none of both theories are supported by strong evidence.

An example of how syndromal NTDs might help to unravel NTD etiology is Meckel-Gruber syndrome (MGS). MGS is considered to be the most frequent syndromic NTD. It includes polycystic kidneys, postaxial polydactyly and central nervous system defects, usually microcephaly and encephalocele. The diseased genes are involved in the correct function of primary cilia. Primary cilia are hair-like extensions from the cell surface that have a fundamental role in extracellular signal transduction, cell fate control, tissue patterning and morphogenesis. Recently, it has become clear that cilia are involved in the *Wnt* and *Shh* signaling pathways. In MGS, disruption of these pathways results in hyperactivation of the PCP pathway and defects in convergent extension. In this way, research of MGS, provided an incredible insight into neural tube patterning during early embryogenesis [21].

Lessons from animal models with NTDs

Only higher vertebrates have a process of neurulation in which neural folding and fusion creates a closed neural tube. Therefore, embryos with NTDs are only seen in higher animals, including amphibians, birds, and mammals. The mouse is the most extensively studied mammalian experimental model. Multiple sources give rise to the mutant mouse strains: spontaneous, mutagen-induced and gene trap-induced mutations disrupted the function of an (un)known gene, thereby inducing NTDs. Various mouse mutants develop NTDs at different levels of the body-axis, covering the conditions observed in humans, and therefore provide a suitable model for human NTDs.

Studies in mouse give evidence that more than 250 genes regulate successful neural tube closure in mice. This large number of mouse mutants demonstrates the genetic complexity that must underlie early development of the central nervous system (CNS). The genes are involved in diverse cellular functions (such as control of cell proliferation, cytoskeletal and transcriptional regulation) and multiple

molecular pathways. Hereby, we discuss the most valuable key points and lessons from mouse models of NTDs.

1. *Embryonic lethality and coexisting pathology*
2. *Is there a link between gene and NTD type?*
3. *Gene-gene interactions – a multifactorial concept?*
4. *Gene-environment interactions – prevention possible?*
5. *Role of folate pathway gene mutations in NTDs in mice?*
6. *Most commonly affected biochemical pathways or cell functions?*

1. *Embryonic lethality and coexisting pathology*

Before concluding that a given mouse mutant exhibits NTDs, care must be taken to ensure that embryonic lethality and/or degeneration processes are not likely to be responsible for preventing normal development beyond neurulation. As the CNS is not necessary for in utero survival, embryonic/fetal lethality in a mouse mutant with NTDs must indicate a coexisting pathology. A particular problem of interpretation rises when embryos die in the period in which the neural tube closes around gestational day (GD) 8-10. Also in mouse embryos that die on GD10-11, the neural tube is open past the time that it should be closed, but the extreme body malformations suggest that the NTD is secondary to other developmental defects. Therefore, the discussion focuses mainly on the mutants that survive past GD12 [16,22].

2. *Is there a link between genetic causation and NTD type?*

The majority of the mouse mutants present with exencephaly (80%), although a number also exhibit spinal defects. In humans, cranial and caudal NTDs have a comparable incidence. The intriguingly high proportion of mice with exencephaly compared to humans might be explained by the fact that the human embryo has a proportionally smaller brain than the mouse embryo at the corresponding neurulation-stage. The smaller brain poses less challenge for cranial neural tube closure, and might have made closure 2 unnecessary [23]. This however might also result in significant differences between mouse and human neural tube closure and many of the mouse candidate genes are not involved in NTDs of humans.

3. *Gene-gene interaction – a multifactorial concept?*

The mouse genes that produce NTDs mostly require homozygous effects. But for example PCP gene mutants are double heterozygotes that act additively in genetic combinatorial mechanisms [16,22]. In addition, it might be that homozygosity produces craniorachischis, whereas compound heterozygotes can produce both craniorachischisis and other NTD phenotypes. Another interesting finding comes from homozygous null mutants that die before GD10 or on GD10-12 with a highly penetrant syndromic NTD. Interestingly, heterozygotes or mutants with partial gene function at these genes have only a NTD, viable and non-syndromic. In this way also genes from mouse mutants that die before GD12 might be candidate genes for human NTDs [16]. In humans, the genetic risk for cranial or caudal NTDs is thought to be oligogenic [24]. The SELH/Bc mouse strain nicely illustrates this oligogenic, multifactorial inheritance pattern for NTDs. Four loci act additively: *Exen1, Exen2, Exen3* and *Exen4.* In this model, the genes act approximately equal, additive and interchangeable. The curly tail model is an example of a more hierarchical model in which genetic variants at three “modifier” genes increase NTD risk in the mutant mice. In this situation, the modifier genes do not act on it’s own.

All these findings support the multifactorial occurrence model for human NTDs, with a relatively sporadic occurrence and low recurrence risk, as the causative genetic variants segregate apart in subsequent generations [24]. The combination of two or more different genetic variants and environmental factors in a single individual would provide the interaction necessary to disturb neurulation.

4. *Gene-environment interactions – prevention possible?*

On the basis of findings that maternal folic acid supplementation prevented up to 70% of human NTDs, the folate response has been investigated in mouse mutants [25]. Up to date, only a dozen mutant strains have been tested. Half of the tested strains responded well to folic acid and half did not. Dietary folic acid supplementation produced a wide range of responses, with prevention ranging between 35% and 85%, but also with an apparent exacerbation in some cases. Prevention was in no strain 100%. A reduction was seen for both cranial and caudal NTDs. Importantly, all the mutants had additional major developmental anomalies, insensitive for folic acid treatment. The variation in response might result from a wide

variety in dosing of folic acid, with sometimes a 100-fold higher dose used in mutants compared to humans [25]. Notably, the mouse mutants that are prevented by folic acid have no obvious connection to folate metabolism.

In the light of the 30% human NTDs that do not respond at maternal folic acid supplementation, unresponsive mouse mutants and the research for other maternal supplements are of special interest. Three mouse mutants that are non-responders to folic acid, have a strong response to other maternal nutrients. In the *Axd* mutant, spina bifida was reduced by 50% by supplementation of methionine; in the *ct* mutant spina bifida reduced by 70-85% after inositol; and exencephaly in the SELH/Bc strain reduced by 55-85% when the mother was fed Purina 5001 instead of Purina 5015 [25]. Surprisingly, given that human NTDs are mostly non-syndromal (85%) and responsive to folic acid, all the folic acid-responsive mouse mutants are syndromic whereas unresponsive mutants are mainly nonsyndromic.

5. Role of folate pathway gene mutations in NTDs in mice?

Mutations in folate-pathway genes do not cause a phenotype like that of the majority of human NTDs. Null mutants have been described for 10 genes involved in the folic acid metabolism. Only for the folate-receptor mutant *Folr1* folic acid deficiency contributes to neurulation [25]. Untreated *Folr1*-mutants die by GD10, but survive after folic acid supplementation to GD18 and 5-30% have exencephaly. Null mutants for 6 genes (*Cbs, Folr2, Mthfd1, Mthfd2, Mthfr, Shmt1)* have normal neural tube closure. These findings do not exclude a possible role in combination with other genes. Three other null mutants (*Mtr, Mtrr* and *Rfc1)* die before GD9. For these genes, it might be interesting to investigate NTD phenotype in hypomorphs.

In conclusion, mouse mutants suggest that folic acid supplementation does not simply compensate for a genetic lesion in the folate pathway or for dietary folic acid deficiency. A large number of genes can respond to folic acid. Mouse models support the importance of gene-environment interactions, whereby a genetic variant and suboptimal folate supply interact for an increased liability.

6. Most commonly affected biochemical pathways or cell functions?

The numerous mouse genes are involved in diverse biological classes and molecular pathways. As described previously, mouse mutants involved in apoptosis and cell-cycle mutants give rise to cranial NTDs. Actin function is also essential for cranial

neural tube closure in mice. Mutations in PCP genes are linked to craniorachischis. Mutants are involved in both inter- as intracellular signaling, in a variety of pathways. Some are involved in gene transcription. Intriguingly, new affected biochemical pathways and cellular functions are still being identified. For example, mutations in protease-activated receptor cascade, inositol metabolism and defects in primary cilia are linked to NTDs. Also, several groups of genes are involved in epigenetic processes. There are 11 mouse mutants: *Dnmt3b, Dnmt3l* responsible for de novo methylation; *Crebbp*, *Ep300, Cited2, Tcfap2a, Hdac4* and *Sirt1* are involved in histone deacetylation and chromatin silencing; *Cecr2, Kat2a, Smarca4* and *Smarcc1* also regulate chromatin remodeling.

In the light of all these findings, it is unclear whether mouse genes offer good candidate genes for human NTDs. The majority of mouse NTDs are syndromic and highly penetrant. Human NTDs on the other hand are nonsyndromic and multifactorial. Attention focused on the human orthologues of the mouse mutants, with very few significant findings to date [26,27]. Therefore, if mouse NTD genes have a role in human NTDs, the mutations in humans might be partial or regulatory.

Lessons from studies that link NTDs with environmental factors

Many non-genetic factors including hyperthermia, drugs, malnutrition, chemicals, maternal obesity and diabetes are associated with NTDs in humans (Table 3).

Table 3: Non-genetic factors linked to the causation of NTDs in human pregnancy.

Category	Teratogenic agent	Proposed teratogenic mechanism
Folate antagonists	Carbamazepine	Inhibition of cellular folate uptake
	Fumonisin	Inhibition of cellular folate uptake
	Trimethoprim	Disturbance of folate metabolism
Glycemic dysregulation	Maternal diabetes mellitus	Increased cell death in neuroepithelium
	Maternal gestational diabetes	Increased cell death in neuroepithelium
	Maternal obesity	Unknown
Histone deacetylase inhibitors	Valproic acid	Disruption of key signaling pathways in neurulation
Micronutrient deficiencies	Folate	Disturbance of folate metabolism
	Inositol	Disturbance of phosphorylation events downstream of protein kinase C
	Vitamin B12	Disturbance of folate metabolism
	Zinc	Unknown
Thermal dysregulation (hyperthermia in week 3-4 of pregnancy)	Maternal fever Hot tubs Sauna use	Unknown

In addition to environmental factors, many sociodemographic factors are associated with NTD risk. For example a lower socioeconomic status and education, higher maternal and paternal age, parental occupation such as cooks, cleaners, farm workers and gardeners are linked to a higher NTD risk [28].

As inositol supplementation reduced NTD incidence in the *ct* mouse mutant, recently the Prevention of Neural Tube Defects by Inositol (PONTI) study investigated inositol usage in human pregnancy for NTD prevention [29]. There were no adverse effects of inositol supplementation during pregnancy. This pilot study encourages further evaluating of inositol supplementation for primary prevention of NTDs [29].

1.6 Epigenetics: the missing links for neural tube defects?

Neural tube closure is influenced by a complex multifactorial etiology including both genetic and environmental factors. Although more than 250 genes are known to cause NTDs in mice and many candidate genes are investigated in patient cohorts, the molecular basis underlying most human NTDs is still unknown [30]. Up to 70% of NTDs can be prevented by an optimal maternal red blood cell folate concentration [31].

Several lines of evidence support the link between NTDs and epigenetics; especially with an impaired methylation cycle [32]. The basis of the epigenetic control layer is complex; DNA methylation, histone modifications and non-coding RNA are the main investigated mechanisms that do alter gene expression independently of nucleotide sequence [33]. The methylation hypothesis suggests that folate prevents NTDs by stimulating cellular methylation reactions. Folate is central to the one-carbon metabolism that produces pyrimidines and purines for DNA synthesis and for the generation of the methyldonor S-adenosyl-methionine. Disturbances in the one-carbon metabolism, like maternal hyperhomocysteinemia and the homocysteine remethylation *MTHFR 677C>T* variant are known risk factors for NTDs [31]. Folate deficiency may increase NTD risk by decreasing DNA methylation, but to date, human studies vary widely in study design in terms of analyzing different clinical subtypes of NTDs, using different methylation quantification assays and using DNA isolated from diverse types of tissues. Some studies have focused mainly on global DNA methylation differences while others have quantified specific methylation differences for imprinted genes, transposable elements and DNA repair enzymes. Findings of global DNA hypomethylation and *LINE-1* hypomethylation suggest that epigenetic alterations may disrupt neural tube closure.

Epigenetic mechanisms serve as key regulatory elements during vertebrate embryogenesis. DNA methyltransferases (*DNMT*) play a central role in mammalian development. They are inherent to DNA-reprogramming, the genome-wide erasure of epigenetic footprints with resetting of the methylation signature that is essential for

vertebrate embryogenesis. This process takes place in the same time window as neural tube folding [32].

Multiple model systems support the hypothesis that abnormal methylation contributes to NTDs. Mice deficient for *DNMT3B* or treated with methyl cycle inhibitors have cranial NTDs [34,35], which underscores the necessity of proper remethylation for neural tube closure. In addition, mutations in several epigenetic regulators in mice have been shown to result in NTDs [16,22]. Histone deacetylation inhibitors (e.g. valproate) influence neural crest development and neural tube closure in humans, zebrafish and chick embryos [36-39]. All these findings suggest an underlying disturbed methylation cycle in NTDs.

It is clear that epigenetic regulators play key roles in neural tube closure [32]. However, it is still unclear which DNA regions are more sensitive to methylation changes during embryogenesis and can lead to NTDs. Chapter 2 provides a literature review on the relation between folate, DNA methylation changes and NTDs [40].

1.7 Zebrafish as a model for neural tube defects

Similarities between zebrafish and human embryonic neurulation provide evidence that the zebrafish could be a useful model system for analyzing neural tube development [41]. Zebrafish form a neural tube that does not require bending and fusion of the neural plate, but the genetic programs of notochord formation and development are shared. Advantages like external fertilization, large clutch size, rapid development and optical transparency, render zebrafish as a good model to characterize novel candidate genes. The neural plate is present by 6-7 hours post fertilization (hpf) and the first neurons form by 16 hpf.

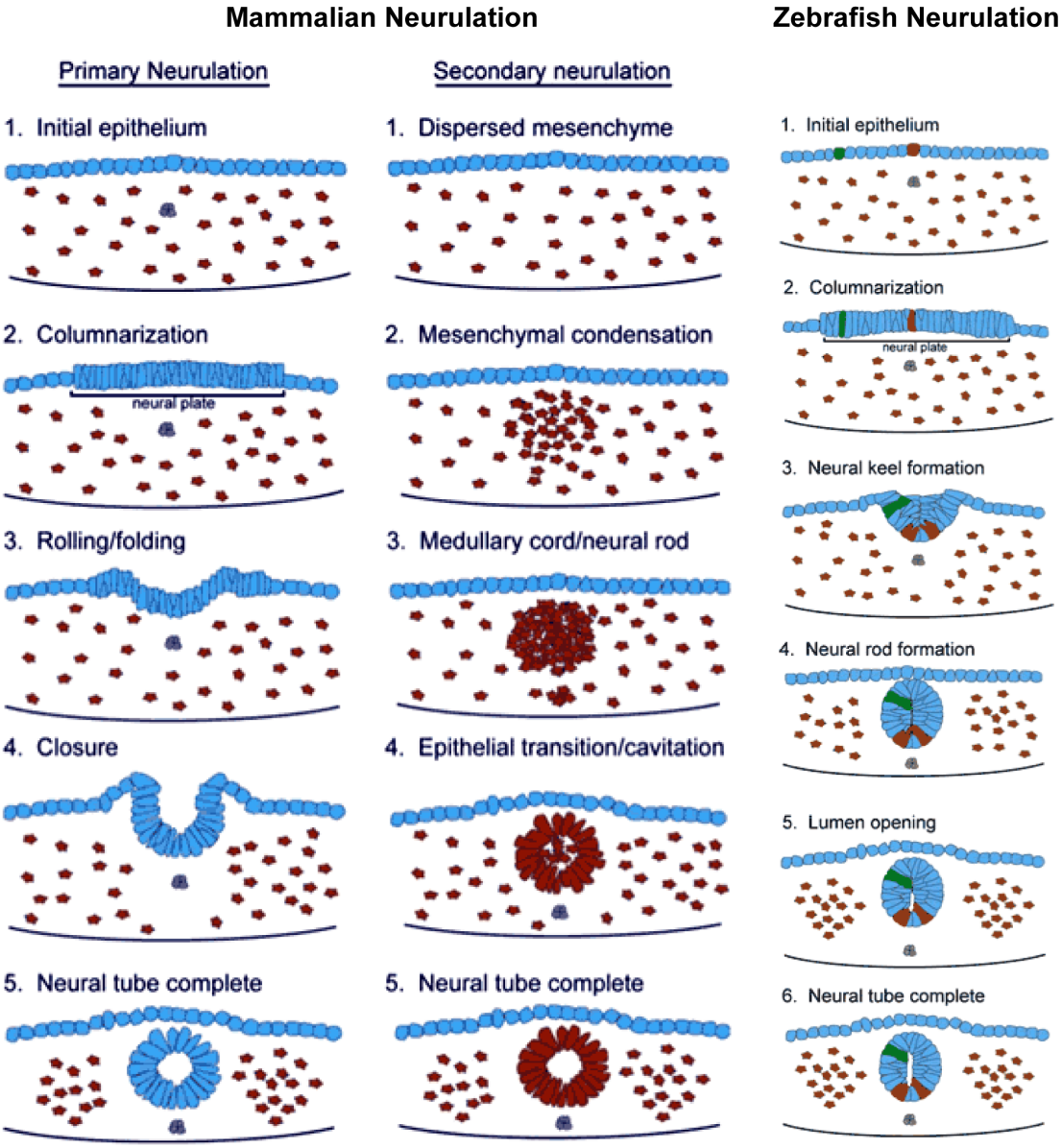

Figure 3: Comparison of mammalian and zebrafish neurulation. Mammalian neurulation involves both primary and secondary neurulation. In primary neurulation, epithelial cells columnarize to form the neural plate. The neural plate rolls and folds the lateral edges into a dorsal position. In secondary neurulation the mesenchymal cells (brown) form a rod, which undergoes epithelial transition to form the neural tube. Zebrafish neurulation has many similarities to mammalian primary neurulation. Both begin with an epithelial sheet that columnarizes to form the neural plate. In the zebrafish, the lateral edges of the neural plate thicken and undergo subsequently a sinking movement forming the *neural keel*, which is a solid mass of cells. The two sides of mammalian neural folds fuse to close the tube, while in zebrafish the two sides of the neural keel come together and form the *neural rod*, which lumen opens subsequently. Adapted from [41] with permission.

For example, in humans, mutations in the PCP gene *VANGL1* were identified in few patients with NTDs [42] and were next characterized as loss of function variants in *Vangl2* depleted zebrafish [43]. In addition, other members of the PCP pathway were analyzed in zebrafish and were shown to cause severe gastrulation defects or shortening of the trunk as well as mediolateral expansion of somites [44]. Valproic acid, an anti-epileptic drug, is an important risk factor for spina bifida in humans and the drug also induces developmental defects in neurulation in zebrafish and Xenopus [36]. Valproic acid is an inhibitor of histone deacetylases (HDACs). HDAC inhibitors elevate histone acetylation, which is associated with “open” chromatin structure and active gene transcription. On the other hand, histone deacetylation is associated with “closed” and transcriptionally silent chromatin. Especially HDAC inhibitors increase the transcription of certain genes involved in cessation of cell proliferation and differentiation of tissues or apoptosis.

Based on all these findings, zebrafish provide a model system for the study of potential mutations and drugs associated with human NTDs.

CHAPTER 2

Folate, DNA methylation and neural tube defects

Published paper
Anne Rochtus, Katrien Jansen, Chris Van Geet, Kathleen Freson. *Nutri-epigenomic studies related to neural tube defects: does folate affect neural tube closure via changes in DNA methylation?*
Mini Rev Med Chem. 2015;15(13):1095-102.

Abstract

Neural tube defects (NTDs), affecting 1-2 per 1000 pregnancies, are severe congenital malformations that arise from the failure of neurulation during early embryonic development. The methylation hypothesis suggests that folate prevents NTDs by stimulating cellular methylation reactions. Folate is central to the one-carbon metabolism that produces pyrimidines and purines for DNA synthesis and for the generation of the methyldonor S-adenosyl-methionine. This review focuses on the relation between the folate-mediated one-carbon metabolism, DNA methylation and NTDs. Studies will be discussed that investigated global or locus-specific DNA methylation differences in patients with NTDs. Folate deficiency may increase NTD risk by decreasing DNA methylation, but to date, human studies vary widely in study design in terms of analyzing different clinical subtypes of NTDs, using different methylation quantification assays and using DNA isolated from diverse types of tissues. Some studies have focused mainly on global DNA methylation differences while others have quantified specific methylation differences for imprinted genes, transposable elements and DNA repair enzymes. Findings of global DNA hypomethylation and LINE-1 hypomethylation suggest that epigenetic alterations may disrupt neural tube closure. However, current research does not support a linear relation between red blood cell folate concentration and DNA methylation. Further studies are required to better understand the interaction between folate, DNA methylation changes and NTDs.

2.1 Nutri-epigenomics: epigenetic changes induced via diets

Epigenetics is the study of mitotically or meiotically heritable changes in gene expression that do not result from changes in the underlying DNA sequence. DNA methylation changes, histone modifications and alteration in expression patterns of non-coding RNAs are the main investigated mechanisms that modulate chromatin structure and contribute to the regulation of the major molecular processes in the cell nucleus, including transcription, replication, repair and RNA processing. Epigenetic modifications are dynamic throughout life and can be heavily influenced by external factors such as food nutrients, drugs, alcohol and many more. DNA methylation patterns strongly control gene expression. As they are dynamic during cellular differentiation and can be changed in disease, they offer a particular potential as a biomarker. Moreover, as they can be inherited mitotically in somatic cells, they provide the link between changes induced by the environment and alterations in gene expression that eventually might lead to a disease phenotype [45]. This review will only focus on epigenetic modifications induced by DNA methylation that is proven to be essential for normal development, tissue differentiation and tissue homeostasis.

DNA methylation is a covalent modification of genomic DNA, which adds a methyl group to the base cytosine (Figure 1). In eukaryotes it mostly occurs at cytosines next to guanine, termed CpG dinucleotides. The symmetry of CpG dinucleotides provides a mechanism for transmitting epigenetic information through DNA replication and cell division. Once established by the *de novo* DNA methyltransferases *DNMT3A* and *DNMT3B*, the maintenance methyltransferase *DNMT1* enables propagation through cell division [46]. Epigenetic memory implies stability of the modified base. The stability and instructive potential of DNA methylation varies dependent on sequence context and CpG density [46]. Almost all mammalian CpG dinucleotides (99%), including those

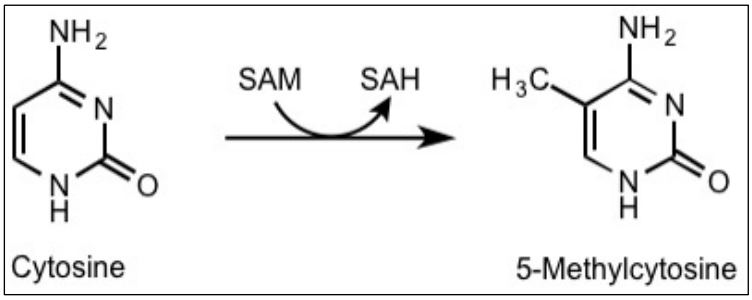

Figure 1. DNA methylation at C5 of the cytosine pyrimidine ring, converting them to 5-methylcytosine. SAM: S-adenosyl-methionine, SAH: S-adenosyl-homocysteine.

located in gene bodies, repetitive elements and the majority of inactive or repressed regulatory elements, are fully methylated [47]. Methylation is generally associated with transcriptional silencing [48]. Conversely, unmethylated CpGs reside either in CpG rich regions, termed CpG islands (CGI), or are located at active promoters, enhancers and boundary elements. CGIs overlap with about 60% of human promoters that are typically unmethylated. Methylation of CGIs is generally associated with gene repression. Loss of methylation occurs both passively as actively. Active demethylation occurs in the germline and early embryo and also during somatic differentiation. The ten-eleven-translocation (TET) proteins are implicated in active DNA de-methylation, by their ability to oxidize 5-methylcytosine to 5-hydroxymethylcytosine and further to formyl- and carboxylmethylcytosine. These products can be removed by DNA repair processes or via replication [46]. The identification and quantification of DNA methylation turnover is critical for interpreting DNA methylation marks but also for concepts of epigenetic memory, as the stability of the modified base could be impaired by pathways of active demethylation. Epigenetic marks appear to be controlled by the genetic sequence [49]. Epigenome-wide methylation studies revealed that both DNA methylation and gene expression mainly follow genetic sequence, providing evidence for shared genetic and epigenetic mechanisms. Epigenetic modifications are informative indicators of underlying regulatory activity. However, the establishment, turnover and recognition of DNA methylation by transcription factors and how defects in these mechanisms contribute to disease, still remain largely unknown.

Nutri-epigenomics is an emerging discipline that examines the role of dietary influences on gene expression. Nutrition can influence DNA methylation because the mammalian one-carbon metabolism is highly dependent on dietary methyl donors and cofactors. Diet-DNA methylation interactions have been associated with the development of cancer and diverse complex diseases. The ‘developmental origins of health and disease’ hypothesis suggests that increased susceptibility to disease is partly shaped during fetal programming [50]. This developmental time period, including gametogenesis and early embryogenesis, is especially prone to environmental influences as genomic DNA from the pre-implantation embryo undergoes extensive demethylation, with lineage-specific remethylation after implantation. Methylation patterns need to be maintained over many rounds of rapid

cellular proliferation during fetal and early postnatal development. S-adenosylmethionine (SAM) supplies methyl groups used for DNA methylation. Therefore, early malnutrition could affect these embryonic methylation patterns resulting in gene expression changes or genome instability, thereby contributing to disease susceptibility, even if these changes in methylation only occur in a subset of cells of a single tissue. The viable yellow allele of murine Agouti ($A^{vy)}$ has been one of the most thoroughly characterized mice models for such diet-induced DNA methylation interactions. This model perfectly illustrates the influence of a mother's diet during pregnancy on the adult phenotype of her offspring, directly linked to changes in DNA-methylation [51].

2.2 Folate influences DNA methylation via the one-carbon metabolism

Folate is a water soluble B-vitamin (vitamin B9) that is essential for DNA and RNA synthesis and different methylation reactions. Natural diet contains folate monoglutamates and polyglutamates that need to be hydrolyzed to monoglutamates for intestinal absorption. The monoglutamate form, 5-methyltetrahydrofolate (5-methyl THF), is the predominant folate in blood circulation. 5-methyl THF is taken up into cells by tissue-specific folate receptors and is sequestered after polyglutamylation. Polyglutamated folates do not cross cellular membranes and are thus retained within the cell [31,52,53]. Inside the cell, folate functions both as an acceptor and a donor of one-carbon units in several critical pathways. These pathways include synthesis or catabolism of amino acids (serine, glycine, histidine, and methionine) and synthesis of nucleotides (thymidine and purines). Folates are also critical in the methylation cycle through their role in methionine synthesis, the precursor of SAM. This is the major methyl donor for many important methylation reactions including DNA methylation and synthesis of creatine, phospholipids and neurotransmitters. The folate and homocysteine pathways are shown in Figure 2 (chemical structures are illustrated in Figure 3). The interaction between these biochemical pathways eventually results in the methylation of DNA, proteins and lipids for which folate is an essential intermediate compound.

2.3 Relation between folate, DNA methylation and neural tube defects

Neural tube defects (NTDs), affecting 1-2 per 1000 pregnancies, are severe congenital malformations that arise from the failure of neurulation during early embryonic development. Neural tube closure takes place between the 3rd and 4th week of *in utero* development and is influenced by a complex multifactorial etiology including both genetic and environmental factors [28]. Multiple environmental factors such as parental occupation, maternal obesity and maternal nutrition have been related to NTDs. The maternal folate status was associated with NTD risk as early as 40 years ago [54]. Two studies in the early 1990s provided unequivocal evidence that maternal supplementation with folic acid, the more stable synthetic form of folate, during pregnancy prevented both NTD recurrence [6] and occurrence [7], which led to the recommendation of supplementation of 400 µg folic acid in women of child-bearing age. Up to 70% of NTDs can be prevented by an optimal maternal red blood cell folate concentration. However, the exact mechanism how folate can prevent NTDs is not understood [31]. More and more studies suggest that not only folate but also its associated methylation metabolism are involved in the etiology of NTDs. Indeed, a low red blood cell folate concentration results in reduced remethylation of homocysteine to methionine with subsequent lower levels of SAM and hyperhomocysteinemia. Studies have shown that this type of metabolic profile with decreased methylation capacity is reflected in the maternal blood of NTD-affected pregnancies. The only well-characterized genetic risk factor for human NTDs is the 677C>T (rs1801133) change in the 5,10-methylene tetrahydrofolate reductase gene (*MTHFR*). The *MTHFR* 677C>T variant leads to hyperhomocysteinemia and global DNA hypomethylation, which is more pronounced under low folate conditions [31,55-58]. However, the exact mechanism by which the *MTHFR* variant would affect neural tube closure is not known, although several hypotheses are possible [59]: 1) increased homocysteine may be toxic for the embryo, 2) homocysteine accumulation that leads to increased oxidative stress or endoplasmic reticulum stress, 3) altered distribution of folates that interfere with DNA synthesis and 4) decreased availability of SAM that disrupts methylation reactions.

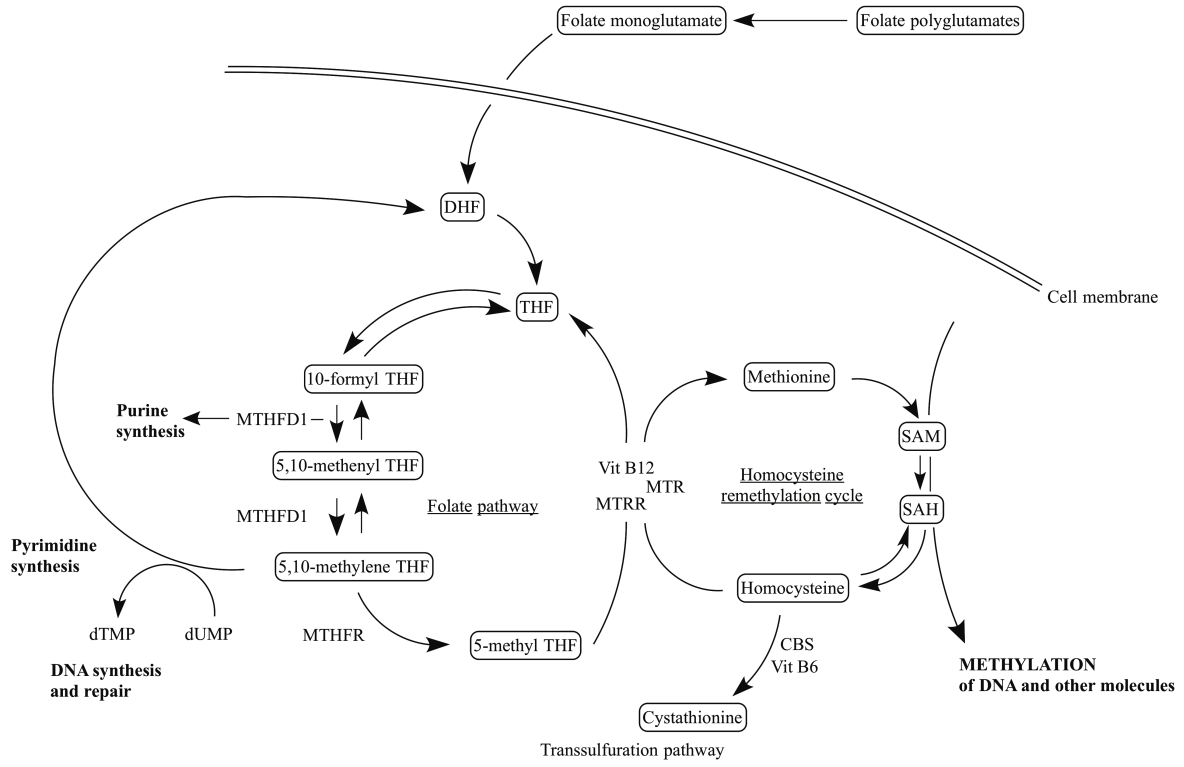

Figure 2. Folate dependent homocysteine remethylation and its interaction with S-adenosyl-methionine transmethylation reactions. The folate-mediated one-carbon-metabolism is required for the synthesis of purines, thymidylate, and the remethylation of homocysteine to methionine. The monoglutamate form 5-methyl tetrahydrofolate is the predominant folate in the blood circulation and is taken up into cells by tissue specific folate receptors or carriers. The more stable synthetic folic acid enters the remethylation cycle after reduction to dihydrofolate and then tetrahydrofolate. DHF: dihydrofolate; MTHFD: methenyltetrahydrofolate dehydrogenase; MTHFR: methylenetetrahydro-folate reductase; MTR: methionine synthase; SAH: S-adenosylhomocysteine; SAM: S-adenosyl-methionine; THF: tetrahydrofolate.

An altered folate metabolism affects both DNA biosynthesis and DNA methylation. Therefore, the *MTHFR* variant has also been investigated in several cancers [60] though results are complex and inconsistent. Interestingly, a hypomorphic mutation of the murine methionine synthase reductase (*Mtrr*) gene results in intrauterine growth restriction, developmental delay and congenital malformations, including NTDs [61]. Moreover, the *Mtrr* genotype of either maternal grandparent determined the developmental potential of their wild-type progeny via an altered DNA methylation pattern, intrauterine growth defects and congenital malformations. Several other lines of evidence suggest that maternal relatives compared to paternal relatives are more likely to have one or more genotypes associated with decreased folate metabolism [62]. Neural tube closure requires precise coordination of cell proliferation, survival, differentiation and migration. Therefore, it is expected that impairment in folate levels with subsequent altered one-carbon metabolism could

easily disrupt any of these processes. Instead of folate or vitamin B12 deficiency, several studies reported hyperhomocysteinemia as a biomarker for NTDs [63,64].

2.4 DNA methylation studies related to neural tube defects

The methylation hypothesis suggests that folate prevents NTDs by stimulating cellular methylation reactions. It is expected that changes in cytosine methylation are not randomly distributed in the DNA but are preferentially located at loci that are more sensitive to these processes. Imprinted genes and transposable DNA elements are both associated with high CpG density and, therefore, recent studies have quantified the methylation of such CpGs [51,65]. Neural tube closure depends on highly coordinated morphologic events and multiple biologic interactions that include proteins that regulate cytoskeletal organization, cell cycle, neurogenesis, cell viability and cell surface-extracellular matrix interactions. A tight regulation of DNA repair is critical for normal embryogenesis and therefore, DNA methylation disturbances and genomic instability are believed to result in neural tube closure defects.

Imprinted genes are expressed in a parent-of-origin specific manner, controlled by epigenetic marks. To date, more than 70 imprinted genes have been identified in the human genome [66]. Their parental-specific 'marks' or imprints are established during germ cell development, mainly via allele-specific methylation. Imprint marks resist the first wave of demethylation that occurs in the pre-implantation embryo following fertilization [67]. CpG methylation of imprinted genes is necessary for their monoallelic (parent-specific) gene expression. The allele-specific methylation of imprinted genes typically occurs at the differentially methylated regions (DMRs). DMRs can differ in size between one single CpG to an entire gene locus [68].

Transposable elements are repetitive mobile elements that can move along chromosomal DNA and can be classified as DNA transposons (that transpose by a direct DNA "cut-and-paste" mechanism) or retrotransposons (that transpose via an RNA intermediate). Non-long terminal repeat (non-LTR) retrotransposons that include long interspersed nuclear element 1 (LINE-1) and short interspersed

elements (SINEs, including Alu sequences) constitute the main class of transposable elements, which accounts for approximately one-third of the human genome. The extremely high density of transposable elements, in comparison to our exon coding genome (2%), results in their ability to affect genomic stability and influence genome evolution. There are > 500 000 LINE-1 copies and > 1 million Alu copies in the human genome, integrated into the ancestral genome more than 150 and 80 million years ago, respectively. About 12% of all CpGs fall within LINE-1 and about 25% fall within Alu sequences. It is hypothesized that the host genome methylates retrotransposon DNA as a defense mechanism to limit detrimental transcription. Their CpG methylation is necessary for transcriptional silencing and there is evidence that they are sensitive to nutrient exposures [69].

DNA repair mechanisms prevent chromosome instability and DNA mutagenesis during time periods of rapid embryonic proliferation and differentiation. Silencing of DNA repair genes has been linked to altered promoter methylation in different tumor cell types. Especially for neurons, repair mechanisms are important for non-replicating DNA. In addition to DNA mismatch repair mechanisms, the adult brain contains high levels of DNA methyltransferase to restore the original pattern of methylation after deamination of 5-methylcytosine to thymine and cytosine to uracil [70]. Microsatellite instability (MSI) is a signal of genomic instability and reflects the status of DNA mismatch repair mechanisms [71].

2.5 Are changes in DNA methylation modifying risk factors for neural tube defects?

A literature search in PubMed until June 2014 was performed for the meta-analysis using a search strategy designed to identify studies evaluating DNA methylation alterations related to NTDs. PubMed search parameters ("DNA Methylation") AND ("Neural Tube Defects") resulted in only 18 studies. For inclusion in this review, studies also had to meet the following criteria: 1) being a randomized control trial, cohort, case-control or cross-sectional study using human tissues and 2) investigating global DNA methylation or specific methylation differences of candidate genes for NTDs in patient samples with a NTD. This selection further resulted in 9

studies that investigated DNA methylation in relation to NTDs using human samples (overview in Table 1). These studies will next be discussed in more detail.

Methylation is the key regulator of imprinted gene expression and the methylation patterns of imprinted genes are sensitive to malnutrition in early development. Several studies quantified the methylation of **imprinted genes** in patients with NTDs. They focused mainly on the insulin-like growth factor 2 (*IGF2*), a maternally imprinted gene that has a key role in fetal and placental development. By binding to the insulin-like growth factor receptor, *IGF2* activates intracellular signaling cascades that promote cell growth and survival. *Liu et al* [72] investigated *H19* and *IGF2* methylation in brain tissue of patients with NTDs by methylation-specific PCR (MSP) and bisulfite sequencing PCR (BSP). Methylation of the *H19* differentially methylated region 1 (DMR1) was higher for patients with NTDs compared to controls (73.3% vs 58.3%; $P<0.05$). There was no significant difference for *IGF2* DMR0 methylation between patients with NTDs and controls. In addition to *IGF2* methylation in brain, *Wu et al* [73] investigated *IGF2* methylation in placental and lung tissue of patients with NTDs. But only in neural tissue the *IGF2* DMR0 was significantly hypermethylated in patients (19.3% vs 16.7% in controls; $P=0.001$). DMR0 methylation was not significantly different in placental or lung tissue and DMR2 was not differentially methylated in brain, placental or lung tissue. The average methylation level of DMR0 was much higher in lung and placental tissues (54.6% and 55.7%, respectively), representing tissue-specific methylation differences. *IGF2* mRNA expression was negatively correlated with the methylation level of DMR0 ($R^2=0.893$) in HCT15 cells. *Stolk et al* [74] investigated *H19*, *IGF2* and *KCNQ1OT1* methylation in peripheral white blood cells of patients with NTDs but found no significant differences.

Changes in the methylation pattern of **transposable elements** affect genomic stability. Therefore, *Wang et al* [75] investigated and found LINE-1 hypomethylation in neural tissues from patients with NTDs and this difference was more pronounced for cranial compared to caudal NTDs (52.43%, 57.32% and 59.03% for anencephaly, spina bifida and control samples, respectively; $P<0.001$). LINE-1 promotor hypomethylation might result in decreased chromosomal instability in NTDs due to increased retrotransposition. There was no correlation between LINE-1

hypomethylation and the maternal nutrition status of folate, vitamin B12 or homocysteine levels. The underlying mechanism might be explained by: 1) the induction of an imbalance in DNA synthesis and repair or 2) the alteration of DNA methylation. However, more studies are needed to provide further insights in these hypotheses.

Global DNA hypomethylation and chromosomal aberrations have been linked in several cancers, implying that global DNA hypomethylation may play an important role in inducing chromosomal instability [76]. Global DNA methylation studies related to complex diseases such as NTDs are still limited. *Wang et al* [75] were the first to investigate global DNA methylation in neural tissue of patients with NTDs. They found significant methylation differences between anencephaly, spina bifida and control samples (4.79%, 5.26% and 5.95%, respectively). Hypomethylation was most pronounced in patients with a cranial NTD. This study also found a significantly reduced maternal plasma vitamin-B12 concentration, lower plasma concentrations of folate and higher concentrations of homocysteine, supporting the link between an impaired one-carbon-metabolism and increased risk for NTDs. However, no significant correlation was found between global methylation levels and maternal plasma concentrations of folate, vitamin B-12 or homocysteine. A second study performed by *Chang et al* [77], investigated tissue-specific global DNA methylation in multiple tissues of second-trimester NTD and control human fetuses. The distribution of DNA methylation in NTD fetuses was significantly different from that in controls. The alteration of DNA methylation in brain tissue was more significant than that in other tissues (3.19% vs 3.57 % in controls; $P<0.001$) but there were no significant differences between the different subgroups of patients with NTDs (anencephaly, encephalocoele, spina bifida). In this study, the maternal folate concentration was significantly lower in NTD fetuses and correlated with brain-tissue DNA methylation. *Chen* et al [78] correlated global DNA methylation levels with the complexity of NTDs and *MTHFR* genotype. Global DNA methylation levels were significantly decreased in brain tissue of NTD-affected fetuses (4.12 vs. 4.99% in controls; $P<0.001$). Stratification for the *MTHFR* genotype revealed a skewed distribution of global DNA methylation levels with no differences in methylation status for genotype C/C ($P=0.687$), lower DNA methylation in patients with NTDs and genotype C/T ($P=0.059$) and significantly lower methylation values in patients with

genotype T/T (3.79% vs. 5.23%; P < 0.001). This skewed distribution implied that the T/T genotype contributed to reduced DNA methylation levels in NTD fetuses. The NTD group had a higher proportion of the T/T homozygous mutant but the difference was non-significant (P=0.15).

Impaired expression of **DNA repair genes** leads to chromosome instability and DNA mutations. *Tran et al* [79] combined methylation-specific multiplex ligation-dependent probe amplification (MS-MLPA) and mass spectrometry to investigate the promoter methylation status of seven DNA repair genes (*TP73, MSH6, MGMT, BRCA1, BRCA2, ATM, TP53*). Two genes, *MSH6* and *MGMT*, had a different methylation pattern detected by MS-MLPA but only *MGMT* remained significantly different after adjusting for multiple testing. The mean level of *MGMT* methylation using mass spectrometry was 41.04 % for the NTD case group and 42.71% for the control group (P=0.034) but subgroup analysis showed only significant differences for patients with anencephaly (39.83%). The mean methylation level of the *MGMT* promotor was lower in female patients with NTDs (41.19% vs 44.20%

Table 1: List of human studies focusing on DNA methylation in NTD patients.

Ref	Assay	Subjects	Methylation status	Tissue	Outcome
Liu [72]	- MSP and BSP - MSI	- 17 NTD patients; 7 controls (Imprinted genes) - 22 NTD patients; 7 controls (Mismatch repair genes)	- Imprinted genes (*H19* DMR1 and *IGF2* DMR0) - Mismatch repair genes *(hMLH1* and *hMSH2)*	Brain	Higher DNA methylation of *H19 DMR* in NTD patients (73.3 vs 58.3 % in controls; P<0.05). MSI in 23/50 NTD tissues. Non-significant higher incidence of MSI in patients with *H19 DMR1* hypermethylation.
Wu [73]	- Mass spectrometry - *IGF2* expression in HCT15 cells treated with 5-Aza-CdR	55 NTD patients; 46 controls	- Imprinted genes *(IGF2* DMR0 and DMR2)	Brain, lung, placenta	Hypermethylation of *IGF2* DMR0 in brain tissue of NTD patients (19.3% vs 16.7% in controls; P=0.001). Higher average methylation of *IGF2* DMR0 in lung and placental tissue versus brain tissue. *IGF2* mRNA expression was negatively correlated with methylation of DMR0 (R^2=0.893).
Stolk [74]	- Mass spectrometry	- 48 NTD patients; 62 controls (Dutch study) - 34 NTD patients; 78 controls (Texan study)	- Imprinted genes *(IGF2-DMR, H19, KCNQ10T1);* - Non-imprinted genes (*LEKR/CCNL, MTHFR, VANGL1*)	Peripheral white blood cells	Only for Dutch study cohort: DNA methylation changes for *MTHFR* (-0.33% absolute decrease in patients; P=0.001) and for *LEKR/CCNL* (+1.36% absolute increase in patients; P=0.048), borderline significance for *VANGL* (+0.17% absolute increase in patients; P=0.063).
Wang [75]	- Mass spectrometry - Global DNA Methylation - Folic acid, vitamin B-12, and tHcy in maternal plasma	48 NTD patients; 49 controls	- Global DNA - Transposable elements (LINE-1)	Brain	Lower DNA methylation in NTD patients (5.01% vs 5.95% for controls; P=0.047). Lower LINE-1 methylation in NTD patients (for anencephaly, spina bifida and control samples respectively 52.43%, 57.32%, and 59.03%; P<0.001). Lower plasma vitamin B-12 in NTD patients (P<0.05).
Chang [77]	- HLPC - Global DNA methylation - Maternal serum folate status	45 NTD patients; 45 controls	- Global DNA	Brain, skin, heart, kidney, liver, lung	Lower DNA methylation in brain tissue of NTD patients (3.19% vs 3.57 % in controls; P<0.001). Lower mean maternal folate concentration in NTD fetuses, in correlation with brain tissue methylation status.
Chen [78]	- *MTHFR* genotype - Global DNA methylation	65 NTD patients; 65 controls	- Global DNA	Brain, skin	Lower DNA methylation in brain tissue of NTD patients (4.12% vs 4.99% in controls; P<0.001). Skewed distribution of DNA methylation after stratification for *MTHFR* genotype with significantly lower levels for NTD patients with genotype *T/T* (3.79% vs 5.23% in controls; P < 0.001).
Tran [79]	- MS-MLPA - Mass spectrometry	50 NTD patients; 58 controls	- DNA repair genes (*TP73, MSH6, MGMT, BRCA1, BRCA2, ATM, TP53*)	Brain	Lower DNA methylation of *MGMT* in NTD patients (41.04% vs 42.71%; P=0.034). Lower *MGMT* promotor methylation in female NTDs.
Farkas [80]	- Pyro-sequencing - *RFC1* genotype	68 NTD patients; 38 controls	- Folate transport genes *(FOLR1, PCFT, RFC1)*	Placenta	No significant differences for *FOLR1, PCFT* or *RFC1* methylation, but methylation fractions differed according to *RFC1 80G>A* genotype in NTD patients.
Wang [81]	- Mass spectrometry - *PTCH1* genotype	187 NTD patients; 212 controls	- *SHH* regulator *(PTCH1)*	Brain	Increased risk for spina bifida with the G allele of c.3944C>T (only in females) and the T allele of c.1729-2350G>A. Lower DNA methylation for CpG sites around c.3944C>T GG genotype in patients (75% vs 86% in controls; P=NA).

Abbreviations: Bisulfite sequencing PCR (BSP); Methylation specific-multiplex ligation-dependent probe amplification (MS-MLPA); Methylation Specific PCR (MSP); Microsatellite Instability (MSI); Neural Tube Defect (NTD); Quantitative high-performance liquid chromatography (HLPC); total Homocysteine (tHcy); Whole genome array competitive genomic hybridization (CGH).

in controls, P=0.009). *Liu et al* [72] studied the methylation status of the mismatch repair genes *hMLH1* and *hMSH2* and MSI in NTD tissues. MSI was observed in 23 of the 50 NTD tissues. MSP and BSP were used to determine the methylation patterns of the *hMLH1* and *hMSH2* promoters but these promoters were not significantly hypermethylated in NTDs compared to controls.

Some methylation studies focused on **candidate genes that are already known to be associated with NTD risk**. *Stolk et al* [74] found a significant association for *MTHFR* and *LEKR/CCNL* DNA methylation in a Dutch case-control cohort. However, absolute methylation differences did not exceed 1.36%. *Farkas et al* [80] investigated whether aberrant DNA methylation of folate transport genes in the placenta could compromise folate supplies to the embryo. There were no significant differences in *FOLR1, PCFT* or *RFC1* methylation between placentas from controls and patients with NTDs but there was an inverse relation between DNA methylation in the DMRs of *FOLR1* and *RFC1* and mRNA levels. The mean *RFC1* methylation fraction was lower in NTD patients with *RFC1* 80G>A genotype and high homocysteine levels, suggesting a gene-nutrition interaction between folate intake and *RFC1* genotype, DNA methylation status and mRNA transcription. Sonic hedgehog (*SHH*) signaling plays a crucial role in neurulation. Therefore, *Wang et al* [81] investigated *PTCH1,* a negative regulator of *SHH* signaling. They determined the genotype of 18 SNPs of *PTCH1* and combined these results with their surrounding methylation status. They found an increased risk of spina bifida with the G allele of c.3944C>T (only in females) and the T allele of c.1729-2350G>A. The CpG sites near the c.3944C>T allele were analyzed to better understand the possible roles of this SNP. Patients had lower DNA methylation for CpG sites near the c.3944C>T GG genotype compared to controls (75% vs 86% in controls; P=NA). Therefore, it was suggested that methylation modifications associated with the c.3944C>T polymorphism may be preventive for NTDs.

2.6 Conclusion: can folate affect neural tube closure via changes in DNA methylation?

Nutrition can influence DNA methylation because the mammalian one-carbon metabolism is highly dependent on dietary methyl donors and cofactors. DNA methylation is essential for normal mammalian development and regulation. The long-standing beneficial evidence of folate raises the question whether improved nutrition may further prevent NTDs, not only during embryogenesis but also in the developing nervous system after birth. To date, human studies vary widely in study design, choice of DNA methylation assay and the type of tissues used for DNA extraction. Studies mainly focused on genomic DNA methylation differences and specific methylation differences in imprinted genes, transposable elements and DNA repair enzymes. Findings of global DNA hypomethylation and LINE-1 hypomethylation suggest that disruption of genomic stability may disrupt neural tube closure but current research does not support a linear relation between red blood cell folate and DNA methylation. It is still unclear how specific regions of the genome respond to folate intake. Further studies are required to investigate this relation. Nutri-epigenomics may represent a mechanistic link between nutrition and NTD risk. However, epigenetic marks appear to be controlled by genetic sequence. Hence, research should include genome-wide epigenetic and genetic studies to understand the relative role of genes versus environment in epigenetic variability in patients with NTDs.

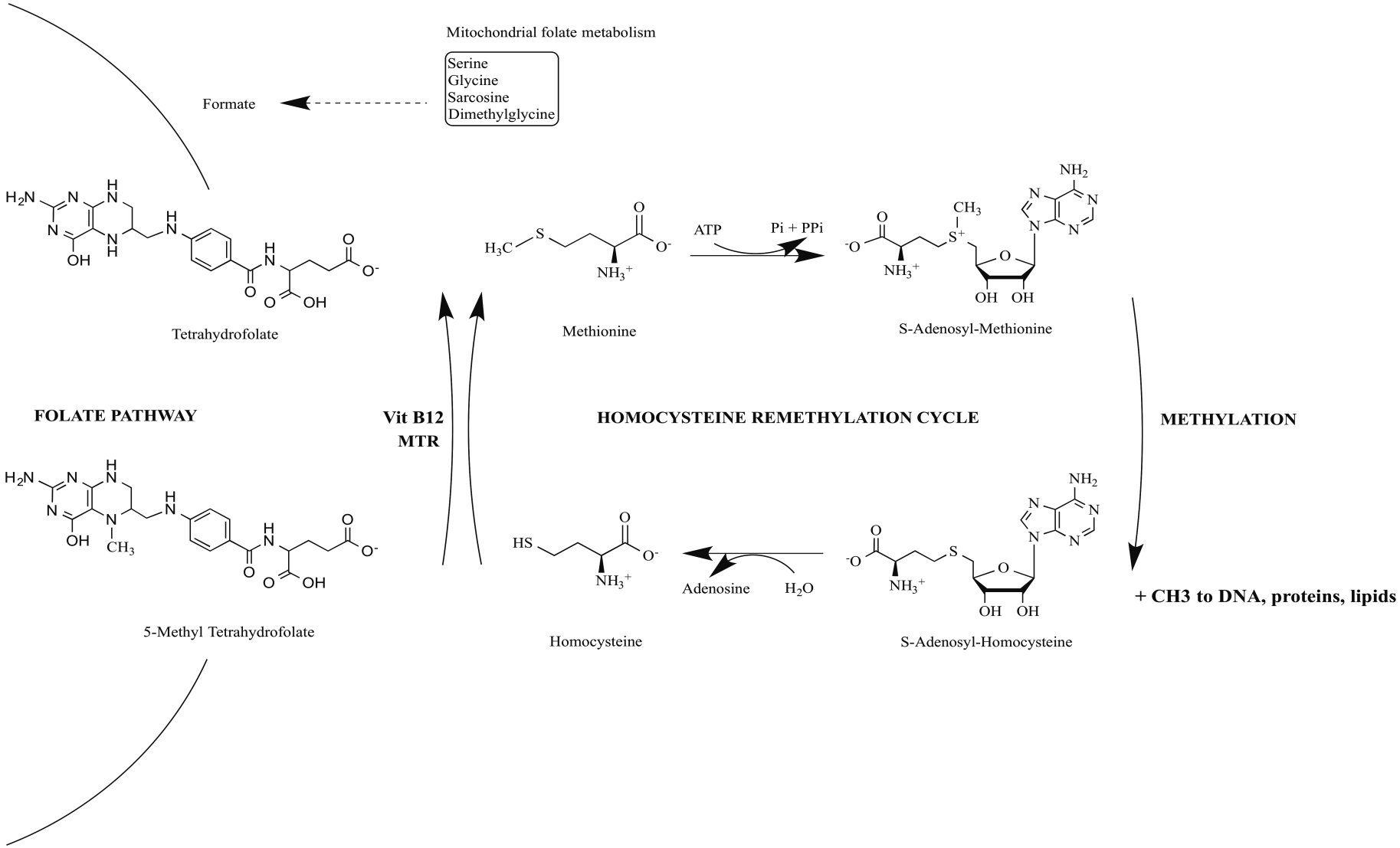

Figure 3. Chemical structures of the main players in the folate dependent homocysteine remethylation cycle. The monoglutamate form 5-methyl tetrahydrofolate is predominant folate in the blood circulation and is taken up into cells by tissue specific folate receptors or carriers. MTR: methionine synthase.

THESIS OBJECTIVES & OVERVIEW

Science never solves a problem without creating ten more.
George Bernard Shaw (1856-1950)

OBJECTIVES & METHODS

The overall aim of this doctoral thesis is to determine gene regions and biological pathways that are more sensitive to changes in DNA methylation during embryogenesis and are associated with neural tube defects (NTDs). In addition to a genome-wide DNA methylation analysis, we performed locus-specific and functional validation studies of candidate genes, as well as functional gene enrichment analyses.

Aim 1: Genome-wide analysis of DNA methylation

Evidence from literature supports the link between an impaired methylation cycle and NTDs. DNA methylation, the most studied form of epigenetic modification, results from the addition of a methyl group to cytosine (5-mC) in the context of CpG dinucleotides. We have applied the Illumina Human Methylation 450K BeadChip (HM450k), using leukocyte DNA from 10 patients with a myelomeningocele (MMC), to identify candidate gene regions that are significantly hypo- or hypermethylated compared to 6 healthy control subjects. The HM450k allows genome-wide methylation analysis: more than 485.000 methylation sites per sample are interrogated at single-nucleotide resolution. It covers 99% of RefSeq genes, 96% of CpG islands (CGI) as well as multiple CGI shores and isolated CpGs. The interrogated cytosines cross promoter regions, 5' and 3' UTRs, gene bodies and intergenic regions. The HM450k represents so far the most standardized methodology to assess DNA methylation at genome-wide level [82,83].

The HM450k array data are analyzed using both a *candidate-gene specific approach* whereby single gene information is extracted from the genome-wide analysis (**Chapter 3** for *HOX* gene cluster as known genes involved in embryogenesis) as well as using a *genome-wide approach* to identify novel genes that are differentially methylated between patients and controls (**Chapter 4**).

Analyzing HM450k data is complex and data filtering, processing and interpretation are not well standardized [83]. In order to acquire knowledge in the technical and analytical aspects of HM450k arrays, I received a Short-Term Scientific Mission grant (supported by COST–BM1209: European Network of congenital imprinting

disorders) to visit the lab of Prof. D. Monk (laboratory of Genomic Imprinting and Cancer at IDIBELL, Barcelona) for training in analyzing HM450k data. During this research stay, I analyzed the HM450k data performed to study overall genome methylation for patients with the imprinting disease pseudohypoparathyroidism (PHP) (**Chapter 5**). Patient samples and their clinical data were already available for this study from the EuroPHP consortium. Next, locus-specific validation studies were performed with the Sequenom EpiTYPER.

Aim 2: Locus-specific validation of candidate gene loci

We performed validation studies for the identified gene loci from the *HOX*-specific (**Chapter 3**) and genome-wide methylation (**Chapter 4**) analysis using the Sequenom EpiTYPER for 83 MMC patients, 12 unaffected healthy siblings, 30 age- and gender matched unrelated young adults without a family history of NTDs and 5 families of patients with MMC. The Sequenom EpiTYPER assay is based on bisulfite-conversion followed by PCR target amplification and a base-specific cleavage process. The resulting cleavage pattern is further analyzed by a mass spectrometry-based method for both qualitative and quantitative methylation information. This methodology allows the simultaneous analysis of a larger sample set of patients with NTDs and informs on both the magnitude and the population variability of the differentially methylated locus of interest.

Aim 3: Functional analysis of candidate genes

Zebrafish are a useful model system for analyzing the effects of gene depletion and overexpression on neural tube development as important similarities in embryonic neurulation between humans and vertebrates have been observed [11]. DNA hyper- or hypomethylation is usually associated with respectively gene silencing and overexpression. Therefore, the effects of candidate genes in zebrafish are studied by the morpholino-induced knock down strategy or via overexpression of mRNA and a detailed morphological analysis of neural tube development during embryogenesis is performed. Whole mount In Situ Hybridization (WISH) using a probe for the paired box gene 2a (pax2a) is used to analyze neural tube development. Functional analysis in zebrafish is used for **Chapters 3** and **4**.

Aim 4: Building biological pathways

In addition to identifying individual genes and their regulatory regions as risk factors for NTDs, the next challenge is to define the developmental requirement for those genes that are obligatory for neurulation and whose disruption or differential expression leads to NTDs. The development of the nervous system is a complex and dynamic process, under influence of many genetic and non-genetic factors, with candidate genes in diverse functional classes. Building well-established cell biological and/or molecular functions into specific signaling pathways is essential to understand their contribution to neurulation and their potential interactions. Reactome and the Ingenuity Pathway Analysis (IPA) programs are used to investigate whether the identified candidate genes are part of a similar biological network. In addition, gene enrichment analysis based on ontologies of gene function is used to identify relevant biological mechanisms. Functional pathway analyses and gene prioritization studies are performed in collaboration with Prof. Y. Moreau for **Chapter 4** (Department of Electrical Engineering ESAT-SCD, University of Leuven, Belgium).

Ethical approval was obtained for this study (S55277).

RESEARCH

The important thing is not to stop questioning.
Curiosity has its own reason for existing.
Albert Einstein (1879-1955)

CHAPTER 3

DNA methylation of Homeobox genes in patients with Spina Bifida

Published paper
Anne Rochtus, Benedetta Izzi, Elise Vangeel, Sophie Louwette, Christine Wittevrongel, Diether Lambrechts, Yves Moreau, Raf Winand, Carla Verpoorten, Katrien Jansen, Chris Van Geet, Kathleen Freson. *DNA methylation analysis of Homeobox genes implicates HOXB7 hypomethylation as risk factor for neural tube defects.*
Epigenetics. 2015;10(1):92-101.

3.1 Abstract

Neural tube defects (NTDs) are common birth defects of complex etiology. Though family- and population-based studies have confirmed a genetic component, the responsible genes for NTDs are still largely unknown. Based on the hypothesis that folic acid prevents NTDs by stimulating methylation reactions, also epigenetic factors as DNA methylation are predicted to be involved in NTDs. Homeobox (*HOX*) genes play a role in spinal cord development and are tightly regulated in a spatiotemporal and collinear manner, partly by epigenetic modifications. We have quantified DNA methylation for the different *HOX* genes by subtracting values from a genome-wide methylation analysis using leukocyte DNA from 10 myelomeningocele (MMC) patients and 6 healthy controls. From the 1575 CpGs profiled for the 4 *HOX* clusters, 26 CpGs were differentially methylated (p-value < 0.05 and β-difference > 0.05) between MMC patients and controls. 77% of these CpGs were located in the *HOXA* and *HOXB* clusters, with the most profound difference for 3 CpGs within the *HOXB7* gene body. A validation case-control study including 83 MMC patients and 30 unrelated healthy controls confirmed a significant association between MMC and *HOXB7* hypomethylation (-14.4%; 95% CI 11.9-16.9%; p-value <0.0001) independent of the *MTFHR 667C>T* genotype. Significant *HOXB7* hypomethylation was also present in 12 unaffected siblings, each related to a MMC patient, suggestive of an epigenetic change induced by the mother. The inclusion of a neural tube formation model using zebrafish showed that Hoxb7a overexpression but not depletion resulted in deformed body axes with dysmorphic neural tube formation. Our results implicate *HOXB7* hypomethylation as risk factor for NTDs and highlight the importance for future genome-wide DNA methylation analyses without preselecting candidate pathways.

3.2 Introduction

Neural tube defects (NTDs), affecting 0.5-2 per 1000 pregnancies, arise as a failure of the neural tube to close in the cranial (anencephaly) or the caudal (myelomeningocele) region [28,84,85]. The nature and severity of NTDs is determined by the stage and axial level at which closure fails. Cranial NTDs are mostly not compatible with life while caudal NTDs give rise to lifelong disabilities. Although more than 250 genes are known to cause NTDs in mice [16,22] and many candidate genes have been studied in patient cohorts, the molecular basis underlying NTDs still remains largely unknown. Folic acid reduced the incidence of NTDs by 50-75% [31]. However, in most NTD-affected pregnancies maternal folic acid levels are within the normal range [86] and despite optimal supplementation a significant proportion of NTDs are even unresponsive to folic acid [31,87]. This would suggest the existence of folic acid resistance in mothers at risk for NTD-affected pregnancies but this hypothesis is not supported by genetic and/or environmental risk factors. Folic acid is central to the one-carbon metabolism that produces pyrimidines and purines for DNA synthesis and for the generation of S-adenosyl-methionine that is a methyl donor for DNA, RNA and protein methylation. The only well-characterized genetic risk factor for NTDs is the *677C>T* variant in the 5,10-methylene tetrahydrofolate reductase gene *(MTHFR)*, causing thermolability of the enzyme and predicted to divert the available methyl groups from the DNA methylation towards the DNA synthesis pathway [31]. Interestingly, the *MTHFR 677C>T* variant is associated with global DNA hypomethylation in both controls and NTDs [31,78], and this seems to be more pronounced under low folic acid conditions [88]. Most DNA methylation studies in patients with NTDs were performed independent of the presence of the *MTHFR 677C>T* variant. Findings of global DNA and *LINE-1* hypomethylation were found in fetal neural tissue DNA from NTD patients, suggesting that disruption of genomic stability may lead to abnormal neural tube closure [75,77].

The methylation hypothesis suggests that folic acid prevents NTDs by enhancing cellular methylation reactions. It is known that a tight regulation of genome-wide erasure of epigenetic footprints with resetting of the methylation signature is critical for normal embryogenesis and therefore, it is believed that DNA methylation changes and genomic instability may disturb neural tube folding [32].

Immediately post fertilization, rapid de-methylation takes place, followed by re-methylation in the blastocyst and early embryo. It is expected that changes in cytosine methylation are not randomly distributed in the genome but are preferentially located at loci that are more sensitive to these processes. Methylome analysis during early embryonic differentiation showed changes in the methylation patterns for developmental regulatory genes, such as Homeobox (*HOX*) genes [89]. The *HOX* gene clusters comprise a family of genes assembled in four clusters (*HOX A, B, C, D* located on chromosomes 7, 17, 12 and 2, respectively). *HOX* genes encode highly conserved transcription factors expressed in the brain and spinal cord that play a central role in establishing the anterior-posterior body axis during embryogenesis (Figure 1) [90,91]. Their expression is tightly regulated in a spatiotemporal and collinear manner, partly by chromatin structure and epigenetic modifications [92-94]. Though genetic studies could not show an association between variants in *HOX* genes and NTDs [90], DNA methylation studies for the *HOX* cluster genes have not yet been performed.

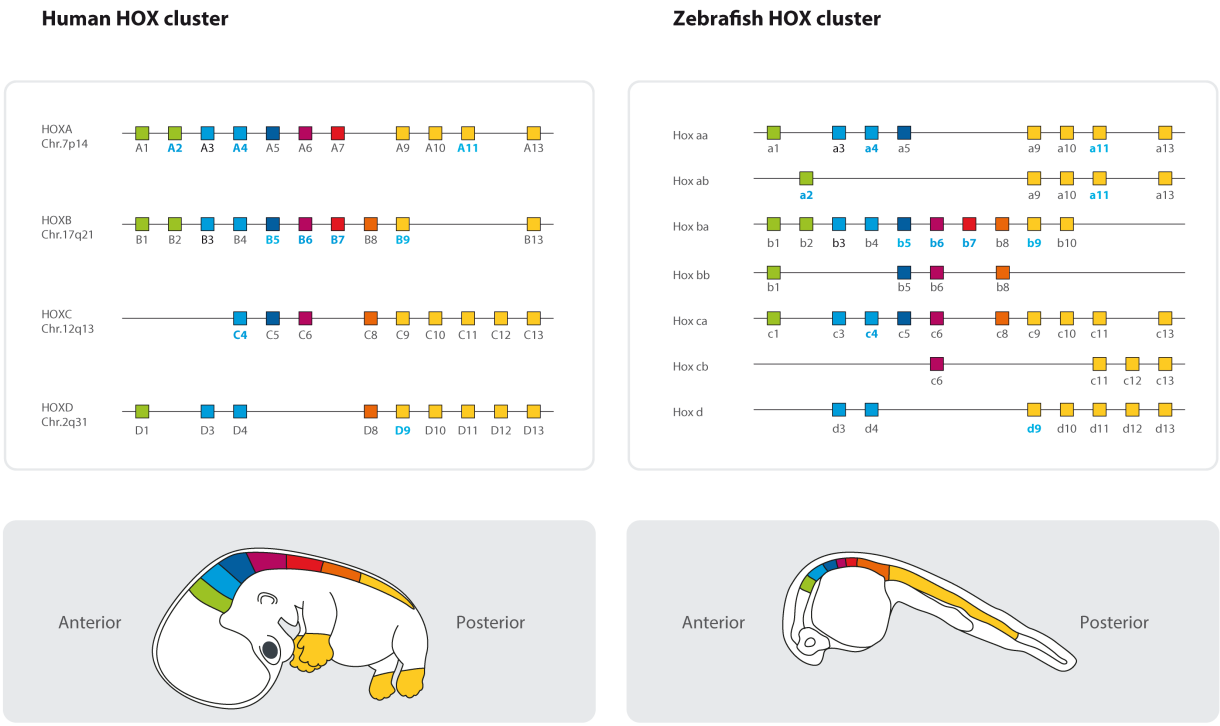

Figure 1: Genomic organization and expression patterns of *HOX* genes for humans and zebrafish. *HOX* genes are evolutionary highly conserved, it appears that an ancestral *HOX* gene cluster was duplicated twice within the 2R genome duplication events, and was important to allow the emergence of vertebrates. Mammals have 39 *HOX* genes distributed in 4 clusters; they pattern the embryo along the rostro-caudal axis. Based on sequence similarities and position within the cluster, genes can be classified in 13 paralog groups (*HOX1-13*). They become activated during early embryogenesis in a time sequence that reflects their physical order within the clusters, referred to as 'temporo-spatial collinearity'. Genes at the 3' end of the clusters are activated first, and

genes located at more 5' genomic positions are activated subsequently. The 3' paralog groups *HOX1-5* have restricted expression borders in general in the hindbrain, while *HOX4-11* genes are detected in the spinal cord. The overall number of hox genes in zebrafish (48) is close to that in mammals (39), despite the existence of seven clusters. This is due to a massive elimination of Hox genes after the additional duplication. Genes indicated in blue refer to the *HOX* genes that are differentially methylated. [Figure adapted with permission from Veraksa A, Del Campo M, McGinnis W (2000) Developmental patterning genes and their conserved functions: from model organisms to humans. Mol Genet Metab 69: 85-100.]

We hypothesize that children born from mothers with folic acid resistance and a disturbed methylation cycle can present with an abnormal DNA methylation profile for *HOX* genes, resulting in increased risk for abnormal embryonic development and NTDs. Therefore, the aim of this study was to investigate DNA methylation of *HOX* genes as mediator of NTD risk using data extracted from a genome-wide DNA methylation analysis study performed for 10 patients with lumbosacral MMC and 6 healthy unrelated controls. A validation study was performed to quantify locus-specific methylation differences in larger cohorts. The functional characterization of the candidate *HOX* gene was finally analyzed using a zebrafish model of neural tube formation.

3.3 Materials and Methods

Ethics statement

Written informed consent to collect blood samples for (epi)genetic studies was obtained from all participants and/or their legal representatives. This study was approved by the Medical Ethics Committee of the University of Leuven (ML9193).

Description of MMC patients, related healthy siblings and unrelated controls

A total of 85 MMC patients and 12 healthy related siblings enrolled in this study are followed at the pediatric neurology department of the University Hospital Leuven (all <18 years). Detailed clinical and general characteristics for all these subjects are reported in Table 1. As sensory and motor functions at and below the level of the spinal cord defect are impaired; paralysis, bowel and bladder dysfunction is present in most of the patients. Folic acid supplementation was recommended, but red blood cell folate was not measured during pregnancy. Table 1 also indicates which MMC patients were included in the 450K array and/or the Sequenom validation study. In addition, we have recruited 30 age- and gender-matched non-related healthy control subjects with no family history of NTDs (15 males and 15 females).

Table 1: Background information of MMC patients included in the HumanMethylation 450K BeadChip and Sequenom EpiTYPER.

Patient	Type MMC	Hy/VP	ACM	Scoliosis	ADL	UI	Ethnicity	Age mother	Patient MTHFR	Patient M/F	Sibling MTHFR	Sibling M/F	Δ Age
1*+	S	yes	1	yes	2	yes	Belgian	36	CC	F			
2*+	LS	yes	2	yes	3	yes	Belgian	29	CT	F			
3*+	LS	yes	2	yes	3	yes	Moroccan	32	CT	M			
4*+	LS	yes	1	yes	3	yes	Indonesian	26	CC	F			
5*+	LS	yes	2	no	2	yes	Belgian		CC	M	CC	F	5
6*+	LS	yes	2	yes	3	yes	Belgian	27	CC	F			
7*+	LS	yes	1	yes	3	yes	Belgian		CC	M			
8*+	S	yes	2	no	1	yes	Belgian	27	CC	F			
9*	S	no	0	no	1	yes	Belgian		TT	M			
10*	LS	yes	2	no	2	yes	Belgian	25	CC	M			
11+	LS	yes	2	yes	3	yes	Belgian	27	CC	M			
12+	LS	yes	2	yes	3	yes	Turkish	28	CC	F			
13+	S	yes	0	no	1	yes	Belgian	33	CT	M			
14+	LS	yes	2	yes	3	yes	Belgian		CC	F			
15+	LS	yes	2	yes	3	yes	Turkish	20	CT	F			
16+	S	yes	2	yes	3	yes	Belgian		TT	M			
17+	LS	yes	2	yes	3	yes	Belgian	25	CT	F			
18+	S	yes	2	yes	2	yes	Belgian	28	CC	M			
19+	LS	yes	2	no	1	yes	Belgian	36	CT	M			
20+	LS	yes	2	yes	1	yes	Belgian		CT	M			
21+	LS	yes	2	yes	3	yes	Belgian	36	CT	F			
22+	TL & LS	yes	2	yes	3	yes	Belgian	23	CC	M			
23+	S	no	0	yes	1	yes	Belgian	30	CT	M			
24+	LS	yes	2	yes	2	yes	Belgian	25	CT	F			
25+	LS	yes	2	no	2	yes	Belgian	34	CC	F			
26+	LS	no	0	no	1	yes	Belgian		CC	F			

27[+]	LS	yes	2	yes	3	yes	Belgian		CT	M	CC	F	-20
28[+]	LS	yes	2	yes	3	yes	Moroccan		CT	F			
29[+]	LS	yes	2	yes	3	yes	Belgian	31	CC	M	CC	M	-19
30[+]	LS	yes	0	no	1	yes	Mongolian		CC	F			
31[+]	LS	no	0	no	1	no	Belgian	20	TT	M	CC	M	-20
32[+]	LS	yes	2	no	1	yes	Belgian	22	CC	M			
33[+]	LS	yes	2	yes	2	yes	Belgian	28	CT	M			
34[+]	LS	yes	2	yes	3	yes	Belgian		CT	F			
35[+]	S	yes	2	no	1	yes	Belgian	33	CT	M			
36[+]	LS	yes	2	no	3	yes	Belgian	27	CC	M			
37[+]	LS	yes	NA	yes	2	yes	Belgian	26	CT	F			
38[+]	LS	yes	2	yes	2	yes	Belgian		CT	F			
39[+]	LS	yes	2	yes	3	yes	Belgian	28	CT	F			
40[+]	LS	yes	2	no	1	yes	Belgian	32	CC	M			
41[+]	LS	no	NA	no	3	yes	Belgian	36	CC	M	CT	M	-26
42[+]	L	yes	2	yes	3	yes	Ukrainian	20	CC	F			
43[+]	LS	yes	2	no	1	yes	Belgian	25	CC	F	TT	M	20
44[+]	LS	yes	2	yes	3	yes	Belgian		CC	M			
45[+]	LS	yes	2	yes	3	yes	Belgian	29	CT	F			
46[+]	LS	yes	2	yes	3	yes	Belgian		CC	F			
47[+]	S	yes	2	no	1	yes	Moroccan	31	CT	F			
48[+]	LS	yes	2	yes	2	yes	Belgian	27	CT	F			
49[+]	S	yes	2	yes	3	yes	Belgian	34	CC	F			
50[+]	S	no	NA	no	1	yes	Belgian	36	CT	F	CC	F	17
51[+]	LS	yes	2	no	3	yes	Belgian	30	CC	F			
52[+]	LS	yes	2	no	1	yes	Moroccan	24	CC	F			
53[+]	S	yes	2	no	1	yes	Belgian	28	CC	F			
54[+]	S	no	NA	no	1	yes	Belgian		CT	F			
55[+]	LS	yes	2	no	2	yes	Bosnian	31	CT	F	CC	M	53
56[+]	S	no	0	no	1	yes	Belgian	30	CC	F			
57[+]	LS	yes	2	no	1	yes	Belgian	24	CC	F			
58[+]	S	no	2	no		yes	Moroccan	26	CC	F			
59[+]	LS	yes	2	yes	3	yes	Belgian	27	CC	F			
60[+]	LS	yes	2	no	1	yes	Turkish	35	CT	F	CC	F	-101
61[+]	LS	yes	2	yes	3	yes	Belgian		CT	F			
62[+]	LS	yes	2	no	1	yes	Turkish	29	CT	F			
63[+]	LS	yes	2	yes	3	yes	Belgian	35	CT	F			
64[+]	L & CP	yes	2	no	2	yes	Belgian	40	CT	F	CT	F	-27
65[+]	LS	yes	2	yes	2	yes	Belgian		CT	F			
66[+]	LS	yes	2	yes	2	yes	Belgian	24	CT	F			
67[+]	LS	yes	2	yes	2	yes	Belgian		CT	F			
68[+]	S	yes	2	no	1	no	Belgian		CT	M			
69[+]	LS	yes	2	yes	3	yes	Belgian	24	CT	M			
70[+]	LS	yes	2	yes	3	yes	Belgian	29	CC	M			
71[+]	LS	yes	2	yes	3	yes	Belgian	33	CC	F			
72[+]	LS	yes	2	yes	2	yes	Belgian	29	CC	M			
73[+]	LS	yes	2	yes	3	yes	Belgian	29	CT	F	CT	F	-24
74[+]	LS	yes	2	yes	2	yes	Belgian		CT	M			
75[+]	LS	yes	2	no	1	yes	Belgian		CC	F			
76[+]	LS	yes	2	yes	2	yes	Belgian	31	CT	F			
77[+]	LS	yes	2	yes	3	yes	Belgian	26	CC	M			
78[+]	LS	yes	2	yes	3	yes	Belgian	30	CT	M			
79[+]	S	no	0	no	1	yes	Belgian		CT	M			
80[+]	LS	yes	2	no	1	yes	Belgian	30	CC	F			
81[+]	LS	yes	NA	no	2	yes	Turkish		CT	M			
82[+]	TL	yes	2	yes	3	yes	Belgian		TT	F			
83[+]	TL	yes	2	yes	1	yes	Belgian	24	TT	F			
84[+]	TL	yes	1	yes	3	yes	Belgian	37	CC	F			
85[+]	TL	yes	2	no	1	no	Belgian		TT	F			

*Inclusion in HumanMethylation 450K BeadChip (10 MMC patients) and [+]Sequenom EpiTYPER (83 MMC patients); MMC: myelomeningocele; M: male; F: female; S: Sacral; LS: Lumbosacral; TL: Thoracolumbal; CP: Cheilopalatoschisis; Hy/VP: presence of hydrocephaly and ventriculoperitoneal drain; ACM: Arnold Chiari Malformation: 1 = type 1, 2 = type 2; NA: Not Available; ADL: Activities of daily life: 1 = ambulatory, 2 = household ambulatory with wheelchair for longer distances, 3 = wheelchair dependent; UI: urinary incontinence; *MTHFR 677C>T* genotype (*CC/CT/TT*) in 85 MMC patients: 47% *CC* - 53% *CT/TT* versus 40% *CC* - 60% *CT/TT* in 30 healthy unrelated controls (P-value = ns).

Genome-wide DNA methylation analysis using the HM450k

Genome-wide DNA methylation analysis was assessed using Illumina Infinium HumanMethylation 450K BeadChip (Illumina, Inc., California, USA) that provides a genome-wide coverage of CpG sites (99% of RefSeq genes, covering the promoter region, 5'UTR, first exon, gene body and 3'UTR, Figure 2) [95]. Bisulfite conversion of leukocyte DNA (1 µg) was performed using the EZ DNA methylation kit (Zymo Research, Irvine CA, USA). Control nested PCR reactions were done on both unconverted and converted DNA to verify DNA conversion. Arrays were processed according to the manufacturer's protocol. Samples were randomly distributed to control for batch effects. Before analyzing the data, possible sources of technical bias were excluded. Probes were excluded from further analysis if >95% of samples had a detection value >0.01 [83]. The software GenomeStudio (Illumina) was used to convert on-chip fluorescent methylation values into numerical values (β-value). Methylation, described as a β-value, is a continuous variable ranging between 0 (no methylation) and 1 (full methylation) for each CpG site. From this genome-wide analysis, we extracted the methylation levels for the different CpGs that cover all regions within the *HOX* clusters (for overview see Table 2). We discarded the following probes (608 in total): i) probes with absent signals in one or more of the DNA samples analyzed, ii) non-CpG probes, iii) probes containing SNPs and iv) leukocyte-specific probes [83]. The signal processing was conducted using the Illumina Methylation Analyzer (IMA) package implicated in the open source statistical environment R [96]. Two filters were applied to identify differentially methylated CpGs between MMC patients and controls: i) absolute β-value difference >0.05 and ii) p-value <0.05 as calculated with the Wilcoxon rank-sum test.

Table 2: Number of probes for the 4 *HOX* clusters included in the HM450k.

Cluster	Gene	UCSC RefSeq	Gene region including	Total	Filtered
A	*HOX A1*	Chr7:27132614-27135625	Chr7:27131625-27240499	481	298
	HOX A13	Chr7:27236499-27239725			
B	*HOX B1*	Chr17:46606807-46608272	Chr17:46602807-46810111	409	236
	HOX B13	Chr17:46802127-46806111			
C	*HOX C4*	Chr12:54410636-54449814	Chr12:54328576-54453814	360	232
	HOX C13	Chr12:54332576-54340328			
D	*HOX D1*	Chr2:177053307-177055635	Chr2:176953532-177059635	325	201
	HOX D13	Chr2:176957532-176960666			
				1575	967

Nucleotide positions accord to the NCBI build 37/hg19.

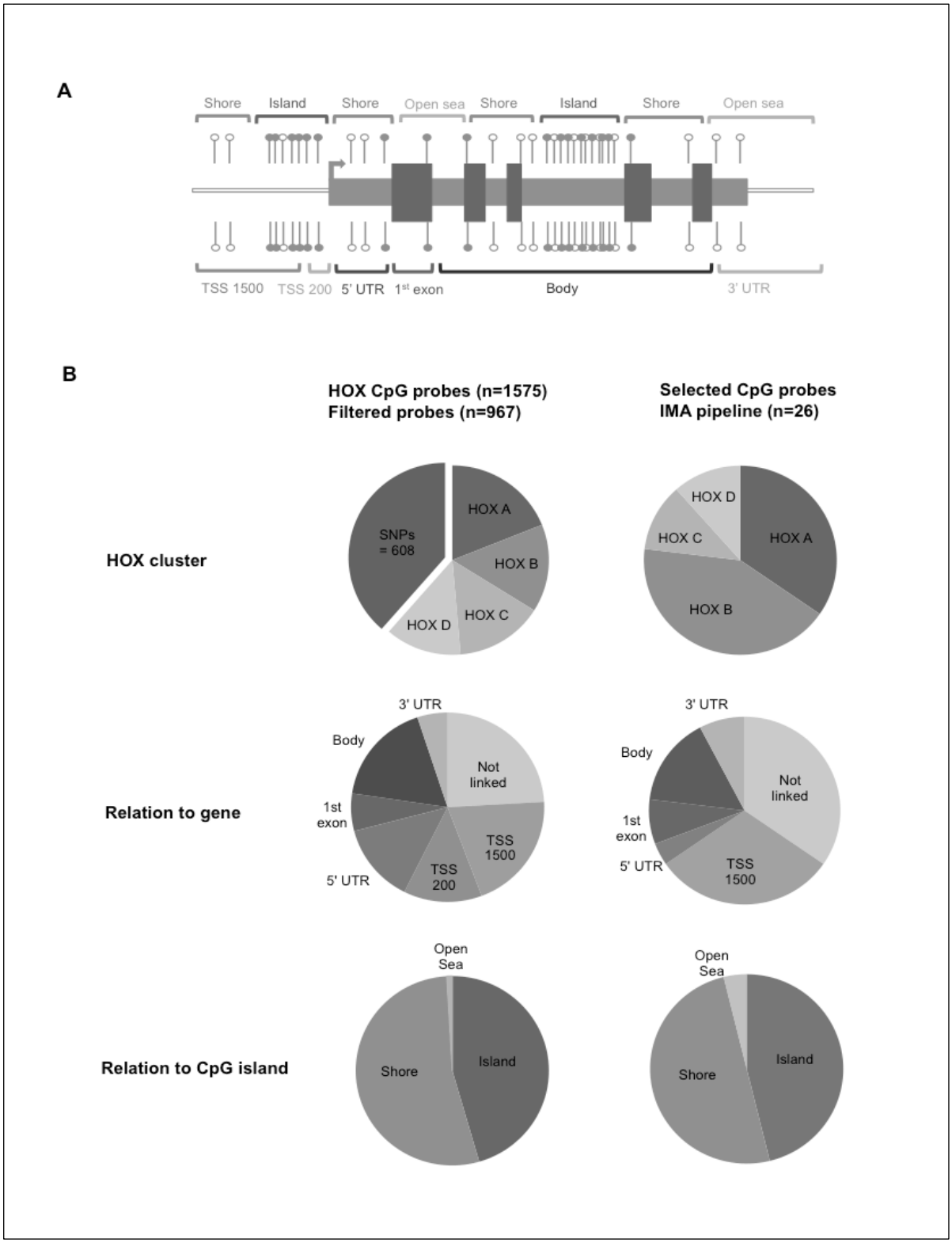

Figure 2. Genomic context of CpG methylation by HumanMethylation 450k Beadchip.
A. Schematic diagram of CpGs depicts their genomic context relative to the nearest CpG island (top) or gene (bottom). Island context is defined as being within an "island" (dark grey), in a 4kb "shore" (grey) flanking the island, or in an "open sea" (light grey) more than 4kb from an island. Gene context is defined relative to the nearest open reading frame: within 1500 (TSS1500) or 200 bp (TSS200) of a transcription start site, in the 5' UTR, the 1st exon of a transcript, in the body of gene or the 3' UTR. B. Pie charts show the distribution of the CpGs examined based upon their genomic context for all probes retained from the array (left column) and for all the differentially methylated probes (right column). Distribution within the *HOX* clusters and gene and island context after analysis with the IMA R package is presented.

Methylation of CpGs within the HOXB7 gene body using the Sequenom EpiTYPER

Leukocyte DNA (1 µg) was subjected to bisulfite treatment using the MethylDetector™ bisulfite modification kit (Active Motif, Carlsbad CA, USA) as we described [97,98]. The Sequenom MassARRAY (Sequenom, San Diego, CA, USA) was used for quantitative DNA methylation analysis of the CpG island within the *HOXB7* gene body using conditions described. [97] Long cycling incubation was applied to further optimize the conversion reaction. [99] Primers were designed using the Sequenom EpiDesigner BETA software (www.epidesigner.com), taking into account amplicon coverage, number of CpGs, fragment size and number of nucleotide repeats in the primer sequence. The primers were: 5'-aggaagagagGTGTTGGGATTATAGGTTTGAGTTT-3' and 5'-cagtaatacgactcactatagggagaaggctACTAAACTTCTCTTCCTCTCCCTTTC-3'. This 395 bp long amplicon covers 26 CpGs but the EpiTYPER analysis only detected 10 separate analytical units that comprise single, duplicate or triplicate CpGs as shown in Figure 3A. The Illumina probe cg07547765 is similar as CpG6. The 2 other Illumina probes cg11041817 and cg22622477 are located within the studied CpG Sequenom amplicon but were not detected by the EpiTYPER. PCR steps were performed in triplicate for each DNA sample and a standard deviation between replicates was mostly <10%. When triplicate measurements had a SD >10% or when only one of the triplicates was available, data for that sample were excluded. The mean of 3 values was used for further analyses. The EpiTYPER analysis method reports CpG methylation values as percentage. Statistical analyses to quantify DNA methylation differences were performed using the Prism 6 software (GraphPad Software Inc., San Diego, CA, USA). A two-tailed T-test was used to assess differences in mean DNA methylation levels between cohorts for the overall *HOXB7* amplicon considered as methylation average and for each CpG unit within this amplicon separately.

MTHRF 677C>T genotyping

Leukocyte DNA from MMC patients, related healthy siblings and unrelated healthy controls was screened for the presence of the *MTHFR 677C>T* variant by PCR and restriction digestion as described [100].

Functional in silico analysis of HOXB7 methylation versus expression

A correlation between *HOXB7* CpG promoter methylation and gene expression was studied by data mining using the open source database MENT (Methylation and Expression database of Normal and Tumor tissues) [101]. The database only included Illumina 27K BeadChip CpG probes (cg09357097 and cg06493080 as shown in Figure 4A) that are located in the *HOXB7* promoter and not in the gene body.

Hoxb7a overexpression and depletion in zebrafish

Wild-type AB zebrafish strains were maintained according to standard protocols [102]. Embryos were produced by natural mating and collected and fixed at different stages based on standard morphological criteria [103]. To produce Hoxb7a mRNA, the full coding Hoxb7a transcript (NM_001115091.2) was PCR amplified and cloned in the pGEM T Easy vector (Promega, Madison, WI, USA). Forward and reverse primers were 5'-ATGAGTTCATTGTATTATGCGA-3' and 5'-GTAGTTTATACATCTATATTAA-3'. Next, capped and polyadenylated Hoxb7a mRNAs were synthesized using mMESSAGE mMACHINE® High Yield Capped RNA Transcription Kit and Poly(A) Tailing Kit (both from Ambion, Austin, TX, USA) according to the manufacturer's protocol. The synthesized mRNA was diluted in phenol red to different concentrations as indicated in the figure legends. Morpholino (MO) injection was performed with a splice Hoxb7a-MO (5'-AGCACCTGTGAAAAGCGCAGAATGA-3'). This MO was designed against Chr17: 46,685,144-46,685,550. Off-target effects were assessed by injecting with a standard control MO against beta-globin (5'-CCT CTT ACC TCA GTT ACA ATT TAT A 3'). MOs were designed by Gene Tools, LLC (Philomath, OR, USA). All injected embryos were life-screened at 24, 48 and 72 hours post-fertilization (hpf) using a Zeiss Lumar V12 (Carl Zeiss Microscopy, Thornwood, NY, USA) and images were captured with a Leica DFC310 FX digital color camera (Leica Microsystems, Wetzlar, Germany). Overexpression and depletion experiments were performed in duplicate. Ethical approval was obtained for these studies.

Pax2a whole mount in situ hybridization

Whole mount In Situ Hybridization (WISH) with a probe for the paired box gene 2a (pax2a) was performed 24h after injection of MOs or Hoxb7a mRNA. Pax2a cDNA obtained from Dr. W. Driever (University of Freiburg, Germany) was cloned in the pGEM-3zf+ for the synthesis of a digoxygenin (DIG) labeled antisense RNA probe as described [104]. The Pax2a probe was subsequently used to analyze the influence of Hoxb7a overexpression and inhibition on spinal cord and notochord formation using standard morphological criteria [103]. WISH experiments were performed in duplicate. Embryos were screened using a Zeiss Lumar V12 (Carl Zeiss Microscopy, Thornwood, NY, USA) and images were captured with a Leica DFC310 FX digital color camera (Leica Microsystems, Wetzlar, Germany).

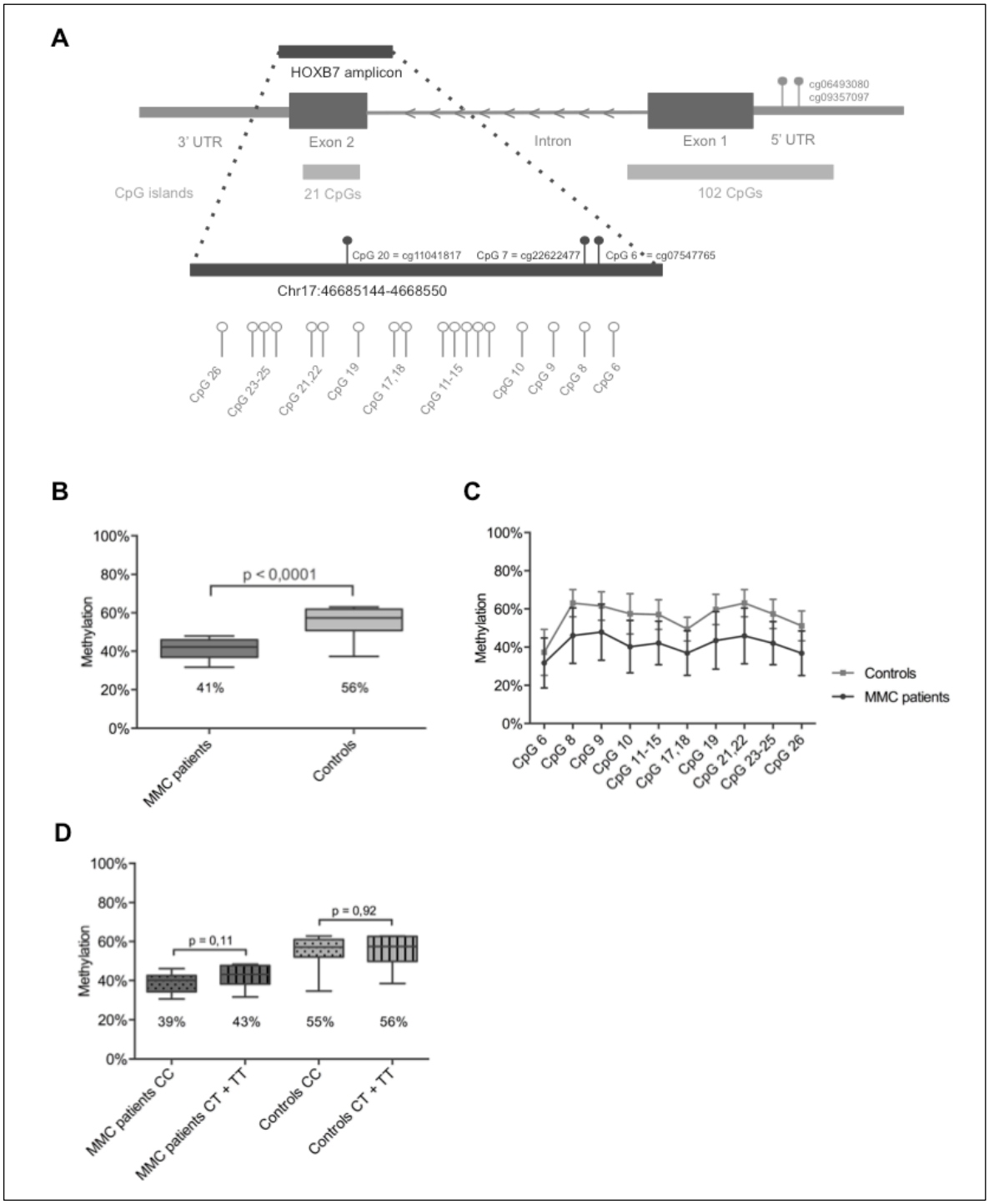

Figure 3. *HOXB7* methylation studies by Sequenom EpiTYPER in MMC patients. A: Localization of the studied amplicon (Chr17:46,685,144-46,685,550) within *HOXB7* Exon 2. The amplicon covers 26 single CpGs and our assay provides data 10 analytical CpG units. Nucleotide positions accord to the NCBI build 37/hg19. The CpG units studied by the HM450k (cg11041817, cg22622477 and cg07547765) and the *in silico* analysis (cg06493080, cg09357097) are also indicated. B: Boxplot representing the methylation pattern of MMC patients and controls with box = 25th and 75th percentiles; bars = min and max values. The mean methylation level of each group is shown below the plot. C: Methylation pattern for each CpG unit within the amplicon. Wilcoxon Rank-Sum test was performed. D. Boxplot representing the methylation pattern of MMC patients and controls divided according to *MTHFR 677C>T* genotype with box = 25th and 75th percentiles; bars = min and max values. The mean methylation level of each group is shown below the plot.

3.4 Results

DNA methylation analysis of the different HOX genes in MMC case-control study

Methylation values for all CpGs located within the 4 *HOX* clusters were extracted from data obtained from a 450K array-based genome-wide methylation analysis, using leukocyte DNA from 10 MMC cases and 6 unrelated age- and gender-matched healthy controls. Detailed clinical characteristics of these MMC patients are reported in Table 1. Pie charts were made to show the equal distribution of the filtered CpG probes (n=967) based on i) location within the 4 different *HOX* clusters, ii) location with respect to gene transcripts and iii) location with respect to the CpG Island (Figure 2). From the 967 filtered CpGs profiled on the HM450k (Table 2), only 26 CpGs were found to be differentially methylated between MMC patients and controls (Table 3). Interestingly, 25 of these 26 CpGs were hypomethylated for the MMC patients and 20 of the 26 CpGs were located within the *HOXA* or *HOXB* clusters. Only for the *HOXB7* gene, 3 different CpG probes (cg11041817, cg22622477 and cg07547765) were significantly hypomethylated in MMC patients (β-differences of -0.29; -0.16 and -0.26, respectively with all p-values of 0.007). These 3 probes are located within a single CpG island at chr17:46,685,244-46,685,449 within the *HOXB7* gene body (Figure 3A).

HOXB7 methylation analysis in MMC case-control study

A validation study using larger cohorts (83 MMC patients described in Table 1) was performed with the Sequenom EpiTYPER technology to quantify methylation of the above selected CpG island located in the *HOXB7* gene body. A Sequenom amplicon was developed that covers 26 CpGs (Figure 3A) including the 3 significant CpGs detected in the 450K array. Within this amplicon, the EpiTYPER detected 10 analytical CpG units for which CpG6 is similar to cg07547765. DNA methylation values for the amplicon for 83 MMC patients and 30 unrelated healthy controls were normally distributed (Shapiro-Wilk test, P>0.05). A significant *HOXB7* hypomethylation (p-value < 0,0001) was detected for MMC patients versus controls with mean methylation values of 41% (95% CI: 38-45%) versus 56% (95% CI: 50-61%), respectively (Figure 3B). The mean level of methylation for each CpG unit within the amplicon was also significantly different between MMC patients and controls (Figure 3C). To exclude an effect of changes in methylation due to

differences in ethnicity, the *HOXB7* methylation pattern between 70 Belgian MMC patients was compared to 10 Non-Caucasian MMC patients without significant differences.

Table 3: Methylation of the *HOX* genes using the HumanMethylation 450K BeadChip and analysis.

Cluster	Gene	Chr	Illumina ID	P-value	β-diff	Ctrls (n=6)		MMC (n=10)	
				< 0.05	> 0.05	Mean	SD	Mean	SD
A: Chr.7p14	*HOXA2*	7	cg06055873	0.016	-0.06	0.32	0.03	0.26	0.04
	HOXA2	7	cg19432993	0.031	-0.12	0.69	0.05	0.57	0.12
	HOXA2	7	cg06166490	0.016	-0.12	0.70	0.06	0.58	0.11
	HOXA2	7	cg04027736	0.022	-0.11	0.61	0.06	0.50	0.11
	HOXA2	7	cg00445443	0.042	-0.10	0.41	0.08	0.31	0.11
		7	cg15037137	0.007	-0.05	0.85	0.02	0.80	0.07
	HOXA4	7	cg25952581	0.042	-0.09	0.45	0.06	0.37	0.11
	HOXA4	7	cg17591595	0.042	-0.08	0.73	0.05	0.65	0.09
	HOXA11	7	cg24709033	0.011	-0.06	0.27	0.03	0.21	0.04
B: Chr.17q21	*HOXB5*	17	cg01405107	0.042	0.09	0.49	0.05	0.58	0.08
	HOXB6	17	cg09983216	0.016	-0.13	0.55	0.08	0.42	0.10
	HOXB7	**17**	**cg11041817**	**0.007**	**-0.29**	**0.70**	**0.08**	**0.41**	**0.20**
	HOXB7	**17**	**cg22622477**	**0.007**	**-0.16**	**0.36**	**0.06**	**0.20**	**0.09**
	HOXB7	**17**	**cg07547765**	**0.007**	**-0.26**	**0.71**	**0.10**	**0.44**	**0.18**
		17	cg19051015	0.022	-0.09	0.72	0.05	0.63	0.07
	HOXB9	17	cg15117739	0.007	-0.10	0.68	0.04	0.57	0.07
	HOXB9	17	cg12057127	0.042	-0.06	0.72	0.01	0.67	0.07
		17	cg20454400	0.031	-0.06	0.37	0.04	0.31	0.05
		17	cg16654603	0.011	-0.09	0.67	0.02	0.58	0.08
		17	cg02052915	0.016	-0.05	0.36	0.03	0.31	0.04
C: Chr.12q13		12	cg08299265	0.016	-0.06	0.39	0.04	0.33	0.03
		12	cg26643142	0.031	-0.06	0.35	0.03	0.30	0.05
	HOXC4	12	cg18473521	0.011	-0.12	0.43	0.08	0.31	0.07
D: Chr.2q31	*HOXD9*	2	cg04730882	0.005	-0.07	0.35	0.03	0.28	0.05
		2	cg07783843	0.011	-0.06	0.24	0.02	0.18	0.04
		2	cg05525812	0.007	-0.07	0.25	0.02	0.18	0.05

Nucleotide positions accord to NCBI build 37/hg19. Selection is performed along both β-value > 0.05 difference and p-value < 0.05; calculated with Wilcoxon Rank-Sum test. The 3 probes in **bold** are located within the same CpG island at Chr17:46,685,244-46,685,449 within the *HOXB7* gene body. This region was selected for the validation study using Sequenom EpiTYPER. β-diff: β-difference; Chr: chromosome; Ctrls: controls; MMC: myelomeningocele.

As findings of global DNA hypomethylation and *LINE*-1 hypomethylation suggest that disruption of genomic stability may disrupt neural tube closure and the *MTHFR 677C>T* variant is associated with global DNA hypomethylation, we determined the *MTHFR 677C>T* variant for MMC patients and healthy controls (Table 1). Interestingly, an intrinsic defect in the folic acid pathway related to *MTHFR* activity

seems not to be involved as no association was found between *MTHFR 677 CC* versus *CT+TT* carriers and *HOXB7* methylation (Figure 3D).

HOXB7 methylation analysis in unaffected siblings of MMC patients

For 12 out of 83 MMC patients, DNA was also collected from their healthy siblings (Table 1). Remarkably, the mean methylation level of the *HOXB7* amplicon was not different between MMC patients and their unaffected siblings with values of 37% (95% CI: 33-40%) versus 40% (95% CI: 37-42%) (Figure 4A). Multiple T-testing for each CpG within the *HOXB7* amplicon also showed no significant differences between patients and healthy siblings (Figure 4B).

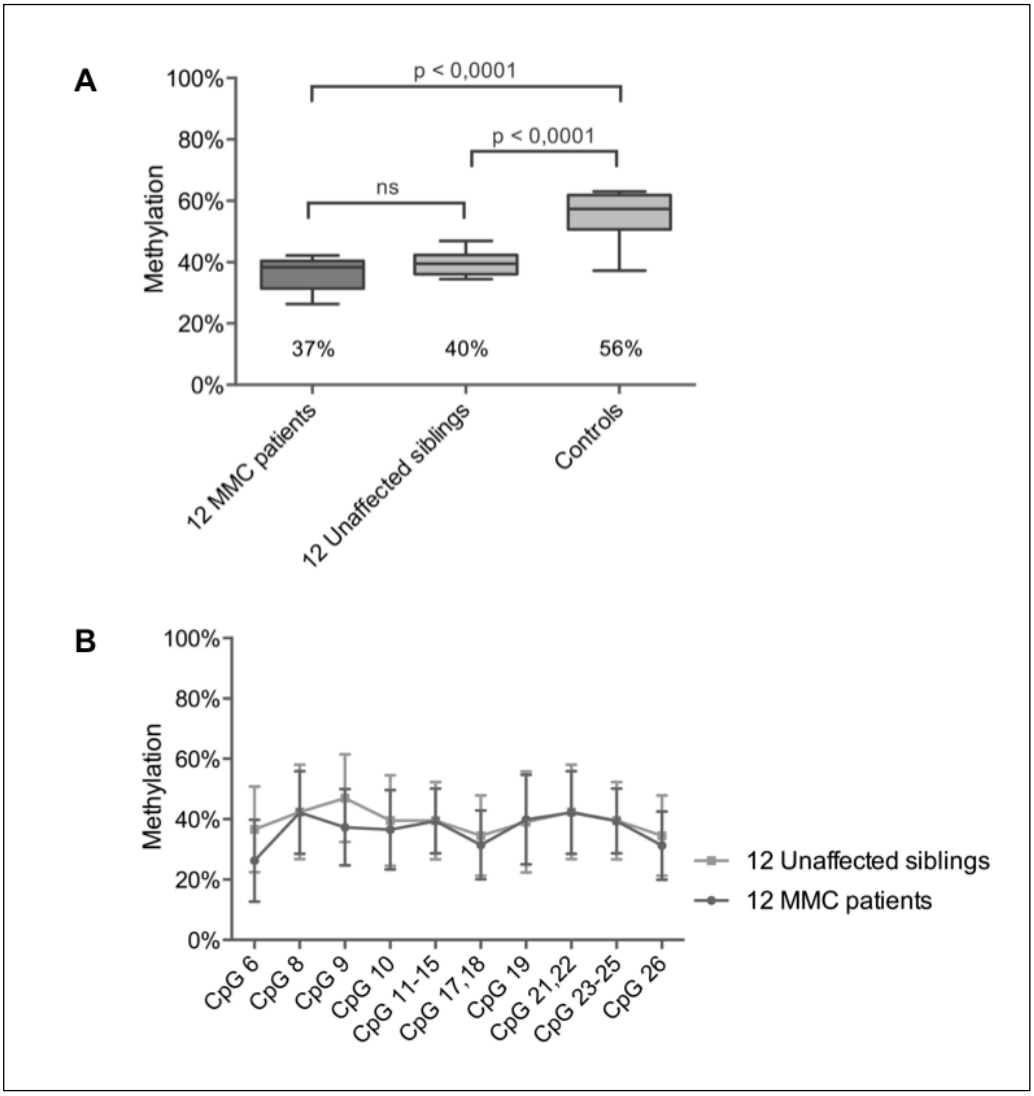

Figure 4. *HOXB7* methylation studies by Sequenom EpiTYPER in pairs of unaffected siblings versus MMC patients. A: Boxplot representing the methylation pattern of affected siblings and unaffected siblings with box = 25th and 75th percentiles; bars = min and max values. The mean methylation level of each group is shown below the plot. B: Methylation pattern for each CpG unit within the amplicon. Wilcoxon Rank-Sum test was performed.

HOXB7 methylation versus expression

Since leukocyte RNA was not collected for our cohorts, we used the MENT database to estimate a correlation between *HOXB7* methylation and gene expression. The 2 CpGs (cg09357097 and cg06493080) located in the *HOXB7* promoter (Figure 3A) showed no correlation with gene expression in normal brain and blood tissues. However, there is evidence that lower *HOXB7* methylation values in brain tightly regulate higher and stable gene expession levels compared to the higher methylation levels in blood that are associated with a variable gene expression (Figure 5). Interestingly, cg06493080 showed a strong negative correlation with gene expression in different cancer tissues, especially for brain (correlation -0.15, P-value 0.008).

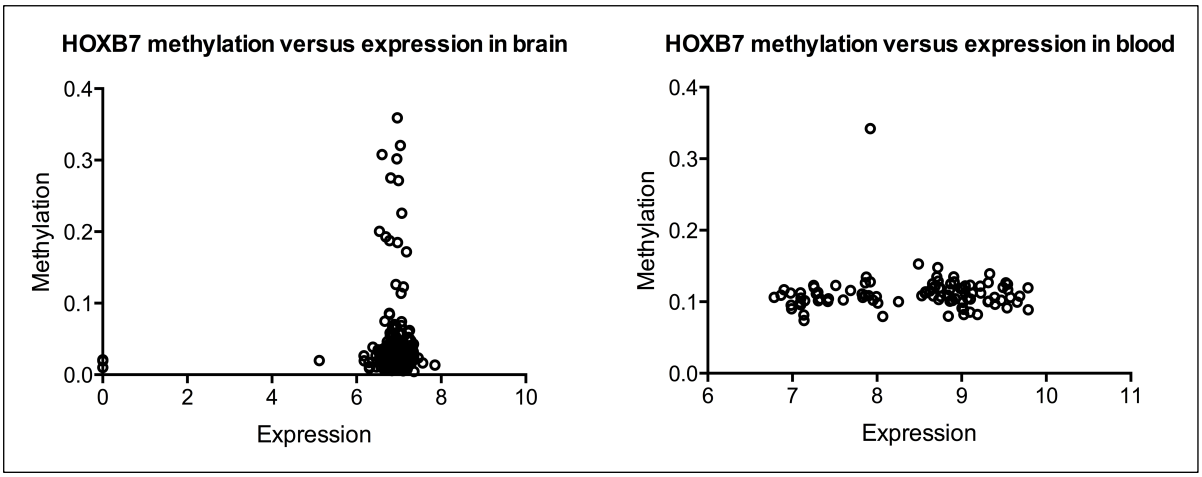

Figure 5. *HOXB7* cg06493080 methylation versus expression in normal tissue extracted from brain and blood. *HOXB7* methylation versus expression in A: brain and B: blood. A low degree of methylation and high expression is observed for brain tissue. In blood *HOXB7* has a higher methylation compared to brain tissue and the expression pattern is highly variable for similar methylation levels. Data are extracted from the MENT database (Methylation and Expression database of Normal and Tumor tissues (http://mgrc.kribb.re.kr:8080/MENT/). Cg06493080 is located in the promotor region of *HOXB7* on position Chr17:46688310. Datasets GSE15745 (brain) and GSE26212 (blood) contain respectively 492 and 96 samples.

Hoxb7a overexpression and depletion in zebrafish

Functional genetics was performed in zebrafish to study alterations in Hoxb7a expression during embryogenesis and neural tube formation. The regulation of the *HOX* clusters is highly conserved between humans and zebrafish (Figure 1). Hoxb7a has an anterior expression limit adjacent to the somite 3-4 boundary at the 20 somite stage [105]. We analyzed embryos with Hoxb7a depletion and overexpression using microinjection of a splice morpholino (MO) and synthetic Hoxb7a mRNA, respectively. MO-induced Hoxb7a depletion resulted in hypopigmentation and developmental delay with dysmorphy in 83-94 % of the embryos at 24 hours post fertilization (hpf) (Figure 6). However, pax2a staining to visualize neural tube formation at 24 hpf was not different between Hoxb7a- or control-MO injected embryos, even for the severely affected Hoxb7a depleted embryos (Figure 6). Embryos injected with different concentrations of Hoxb7a mRNA also present with severe to mild malformations in about 48-71 % of the embryos at 24 hpf (Figure 7B). These embryos had shorter anterior/posterior axes as well as crooked or bent tails (Figure 7A). Interestingly, pax2a staining after overexpression of Hoxb7a for different concentrations showed a neural tube was that was absent or completely disorganized (Figure 7C).

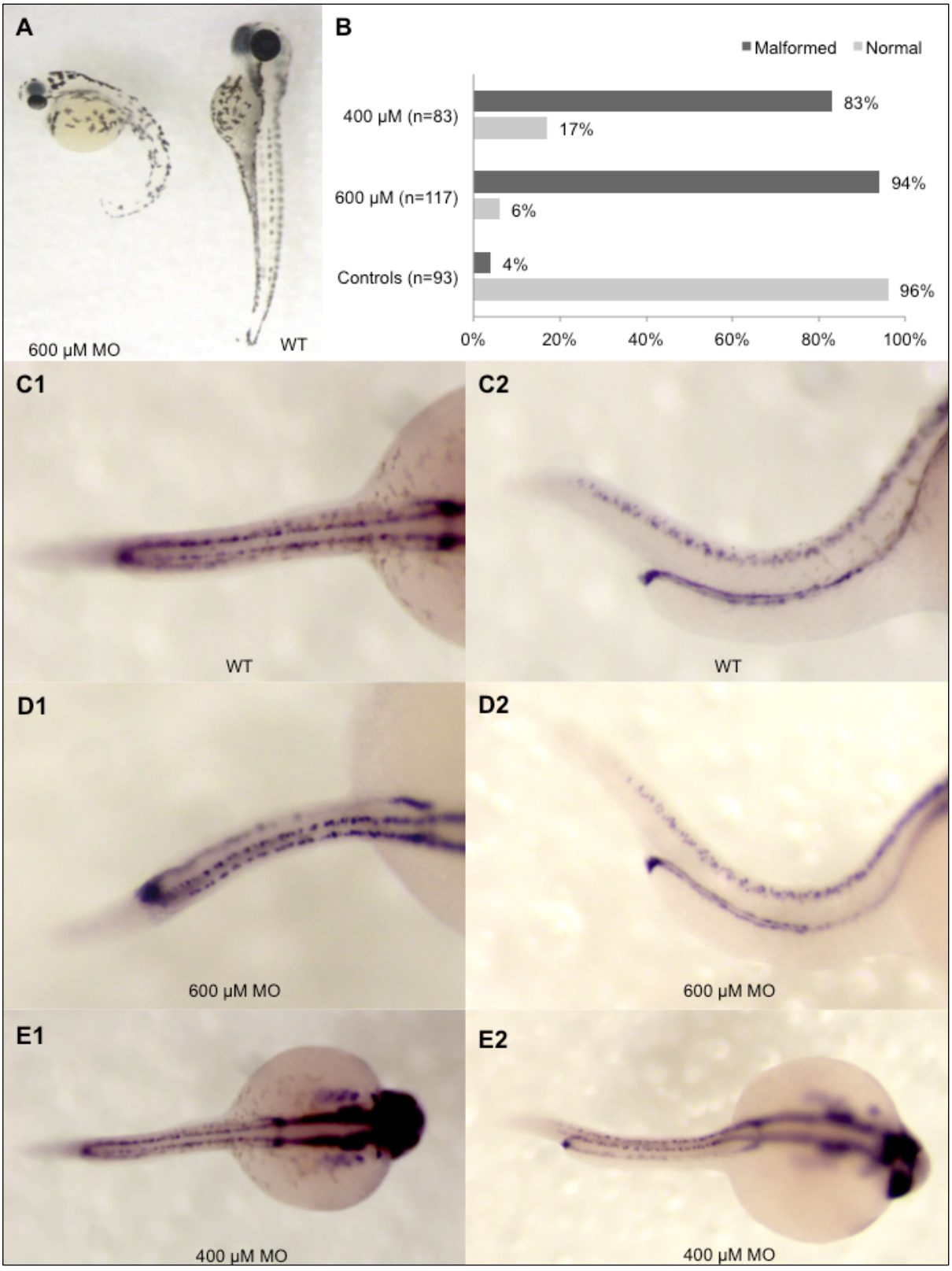

Figure 6. Phenotype analysis of Hoxb7a depletion in zebrafish embryos. A: Phenotype analysis at 72hpf of 600 µM Hoxb7a MO injected zebrafish resulted in a developmental delay with hypopigmentation, shortening and bending of the tail. B: Phenotype analysis after pax2a staining at 24 hpf resulted in about 88% embryos with a developmental delay. C1-2: Pax2a WISH at 24hpf in control AB zebrafish; D1-2: Pax2a staining in 24hpf zebrafish after microinjection of 600 µM Hoxb7a MO is normal; E1-2: Pax2a staining in 24hpf zebrafish after microinjection of 400 µM Hoxb7a MO is normal.

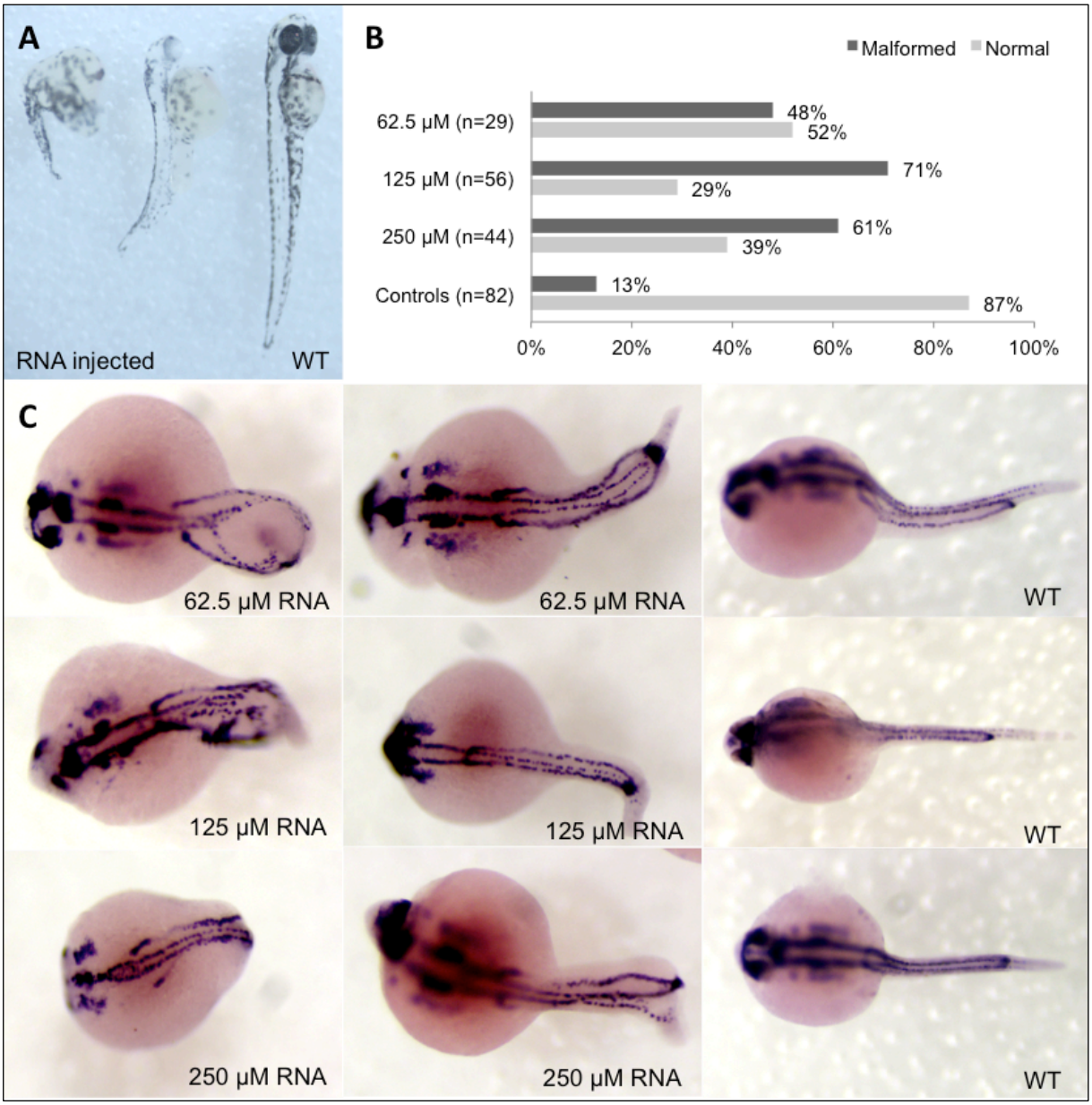

Figure 7. Phenotype analysis of Hoxb7a-overexpression in zebrafish embryos. A: Phenotype analysis at 72 hpf of Hoxb7a mRNA injected zebrafish resulted in significant hypopigmentation and malformation in 66% of the injected zebrafish. These embryos had shorter anterior/posterior axes as well as crooked or bent tails. B: Phenotype analysis after pax2a at 24 hpf resulted in about 63% embryos with a mild or severe affected phenotype after Hoxb7a overexpression compared to 13% in injected controls. C: Pax2a staining after microinjection of different concentrations of mRNA. From left to right severe, mild affected and wild type (WT) embryos at 24 hpf. WT zebrafish show expression in the hindbrain, hindbrain-midbrain boundary, neural tube, mesoderm, optic stalk, otic vesicle and pronephric duct. Microinjection 62.5 µM mRNA, 125 µM mRNA and 250 µM mRNA resulted in respectively 48%, 71% and 61% malformed zebrafish. There was no correlation between mRNA dosage and severity of malformation.

3.5 Discussion

As *HOX* genes play key roles in neural tube closure and many studies have shown that folic acid prevents NTDs by stimulating cellular methylation reactions, we extracted methylation data for the different *HOX* genes from a genome-wide DNA methylation analysis performed for 10 MMC patients and 6 unrelated healthy controls. Interestingly, 25 of the 26 CpGs were hypomethylated for the MMC patients with the *HOXB7* gene body as most significant locus. Interestingly, *HOXB7* hypomethylation was not only confirmed in a larger MMC cohort but was also detected in 12 healthy siblings each related to a MMC patient. These results are suggestive for a maternal effect that contributes to *HOXB7* hypomethylation. Additional healthy siblings must be recruited but gender, age, *MTHFR 677C>T* genotype or MMC being the firstborn or not, seem no predictive risk factors for NTDs based on data for these sibling pairs (Table 1). *HOXB7* hypomethylation by itself is likely not to be causative for NTDs but rather be part of a complex combination of environmental and (epi)genetic risk factors. We found no association between *MTHFR CC* versus *CT+TT* carriers and *HOXB7* methylation suggesting that an intrinsic defect in the folic acid pathway related to *MTHFR* activity is not involved. Though we had no measurements of maternal folic acid levels or uptake, it is known that folic acid levels in most affected pregnancies are within the normal range [86] and despite optimal supplementation a significant proportion of NTDs are unresponsive to folic acid [31,87]. We therefore hypothesize that these mothers have folic acid resistance leading to a disturbed methylation cycle with alterations in DNA methylation and an increased risk for abnormal embryonic development. Additional studies must be undertaken to study the association between maternal folic acid intake and *HOXB7* methylation in DNA from the mother and her offspring.

HOX genes encode for evolutionary highly conserved transcription factors expressed in the central nervous system (Figure 1). They are tightly regulated in a spatiotemporal and collinear manner [92-94], patterning the embryo along the rostro-caudal axis. The *HOXA* and *HOXB* clusters have a closer phylogenetic relationship and hence share more functionality than with either the *HOXC* or *HOXD* cluster [106]. Their cooperative functioning is necessary for the generation of the cranial neural crest and craniofacial diversity [107-109]. The spinal cord is a caudal

structure, but the neural cells from which it derives initially express rostral, forebrain-like characteristics. The caudal character emerges soon after neural induction, through different extrinsic signals [110,111]. According to our study, differential *HOX* gene methylation in MMC patients occurs in both anterior and posterior *HOX* genes. Moreover, failure in establishing correct *HOX* gene methylation in the *HOXA* and *HOXB* clusters may result in disturbances in neural cell identity that ultimately leads to neural malformations. *HOX* gene clusters are evolutionary highly conserved between human and zebrafish and a neural tube formation zebrafish model was previously used to study *VANGL1* [43]. *HOX7* has two paralog members in humans and only one in zebrafish (Figure S1) but the zebrafish Hoxb7a gene shares 60% homology with the human *HOXB7* sequence. As *HOXB7* hypomethylation is suggestive for *HOXB7* overexpression, Hoxb7a overexpression experiments were performed in zebrafish. Overexpression of Hoxb7a in zebrafish resulted in developmental abnormalities and pax2a staining showed abnormal neural tube formation in about 60% of the embryos.

In the present study, we were of course not able to use patients DNA samples from brain or spinal cord tissue. Concordant DNA methylation profiles in brain and blood samples from the same individuals suggest that blood might hold promise as surrogate for brain tissue to detect DNA methylation [112-114]. Genome-wide methylation arrays revealed similar methylation patterns for the *HOX* genes in breast cancers and white blood cells, which suggests that methylation is more likely to be a normal developmental and tissue-specific process that does not directly relate to the malignant mechanism [115]. Interestingly, functional *in silico* analysis using the MENT database showed no correlation with gene expression in normal brain and blood tissues for the methylation of two *HOXB7* promoter CpGs but there is evidence that lower *HOXB7* methylation values in brain tighly regulate higher and stable gene expession levels compared to the higher methylation levels in blood that are associated with a variable *HOXB7* gene expression. These data would suggest that *HOXB7* hypomethylation is associated with higher gene expression. A limitation of our study was the lack of *HOXB7* gene expression studies using leukocyte RNA from MMC cases and unrelated healthy controls but RNA samples were not collected. Additional studies are needed to correlate the methylation levels of the *HOXB7* gene

body CpGs with *HOXB7* gene or protein expression values. Furthermore, it would be interesting to compare our findings in leukocytes with neural tissue.

3.6 Conclusion

This is the first study that uses genome-wide DNA methylation data for the locus-specific analysis of the different *HOX* genes in patients with NTDs. We found evidence that *HOXB7* hypomethylation is a potential risk factor for MMC but also that the underlying methylation defect is present in both affected and non-affected offspring. This could confirm the hypothesis that children born from mothers with folic acid resistance and a disturbed methylation cycle, can present with alterations in DNA methylation with high risk for abnormal embryonic development. Investigating the complex etiology of NTDs requires consideration of more DNA methylation studies; therefore genome-wide DNA methylation analysis without focusing on candidate pathways could reveal more epigenomic changes associated with NTDs. The challenge ahead is to determine which DNA regions are more sensitive to methylation changes during embryogenesis and lead to NTDs.

CHAPTER 4

Genome-wide DNA methylation in patients with Spina Bifida

In Review
Anne Rochtus, Raf Winand, Griet Laenen, Elise Vangeel, Benedetta Izzi, Christine Wittevrongel, Yves Moreau, Carla Verpoorten, Katrien Jansen, Chris Van Geet, Kathleen Freson. *Methylome analysis for spina bifida shows SOX18 hypomethylation as risk factor with evidence for a complex (epi)genetic interplay to affect neural tube development.*

4.1 Abstract

Background: Neural tube defects (NTDs) are severe congenital malformations that arise from failure of neurulation during early embryonic development. The molecular basis underlying most human NTDs remains still largely unknown. Based on the hypothesis that folic acid prevents NTDs by stimulating methylation reactions, DNA methylation changes could play a role in NTDs. Indeed, we performed a methylome analysis for patients with myelomeningocele (MMC) and using a candidate CpG analysis for *HOX* genes, a significant association between *HOXB7* hypomethylation and MMC was found.

Methods: In the current study, we analysed leukocyte methylome data of 10 patients with MMC and 6 controls using IMA and WateRmelon R-packages and performed validation studies using larger MMC and control cohorts with Sequenom EpiTYPER.

Results: The methylome analysis showed 75 CpGs in 45 genes that are significantly differentially methylated in MMC patients. CpG-specific methylation differences could be replicated for the top 6 candidate genes *ABAT, CNTNAP1, SLC1A6, SNED1, SOX18* and *TEPP*, though *SOX18* was the only locus with an overall methylation difference (p-value = 0.0003). Chemically-induced DNA demethylation in HEK cells resulted in *SOX18* hypomethylation and increased expression. Injection of *sox18* mRNA in zebrafish resulted in NTDs that could not be rescued by addition of folic acid. Quantification of DNA methylation for the *SOX18* locus was also determined for 5 families where parents had normal methylation values compared to significant lower values for both the MMC as their non-affected child. Interestingly, *SOX18* methylation studies for a boy with MMC and a paternally inherited chromosomal deletion that includes *BMP4* showed extremely low methylation values that are also present in his healthy mother while his father had normal values.

Conclusion: This is the first genome-wide methylation study in leukocytes for patients with NTDs. We report *SOX18* as a novel MMC risk gene but our findings also suggest that *SOX18* hypomethylation must interplay with environmental and (epi)genetic factors to cause NTDs. Further studies are needed that combine methylome data with next generation sequencing approaches to support such additive effect of (epi)genetics as cause for spina bifida.

4.2 Introduction

Neural tube defects (NTDs) are severe congenital malformations with a frequency of 1-2 per 1000 pregnancies [28]. Despite its high prevalence and severe consequences, the underlying molecular basis of most human NTDs remains largely unknown. Folic acid supplementation is known to reduce the incidence of NTDs, though its mode of action for NTD prevention is poorly understood. The only well-characterized genetic risk factor for human NTDs is the 677C>T change in the 5,10-methylene tetrahydrofolate reductase (*MTHFR*) gene. This variant is known to lead to hyperhomocysteinemia and global DNA hypomethylation [31,55,56]. This association led to the hypothesis that folic acid prevents NTDs by stimulating DNA methylation. Therefore, changes in DNA methylation are predicted to be involved in NTDs [31,40]. Different research groups have quantified global (e.g. via LINE-1 elements) or locus-specific (e.g. imprinted genes, transposable elements, DNA repair enzymes) DNA methylation for patients with NTDs using DNA from diverse types of tissues [40]. Methylation studies of imprinted genes showed significant hypermethylation of the *IGF2* and *H19* differentially methylated regions (DMRs) using brain tissue of NTD patients [72,73]. Some methylation studies focused on DNA methylation of DNA repair genes but only for *MGMT* a slightly lower DNA methylation in brain was found for NTD patients [79]. Investigation of DNA methylation of the candidate genes folate receptor α (*FOLR1*), proton-coupled folate transporter (*PCFT*) and reduced folate carrier 1 (*RFC1*) genes did not show significantly differences between patients and controls.though some minor differences were observed according to *RFC1* 80G>A genotype [80]. This suggests a gene-nutrition interaction between folate intake and the *RFC1* genotype in NTD-affected births. The most robust finding of all DNA methylation studies for NTDs was found for LINE-1 and global DNA methylation. Lower levels of LINE-1 and global DNA methylation were found for NTD patients and the hypomethylation was more pronounced for cranial compared to caudal NTDs [75]. We previously performed a genome-wide DNA methylation study using the HumanMethylation 450K BeadChip (HM450k) and leukocyte DNA from 10 patients with myelomeningocele (MMC) and 6 unrelated healthy controls. DNA methylation profiles for the Homeobox (*HOX)* genes were subtracted from the overall methylome data as these genes are known to play a central role in neural tube development and are tightly regulated by epigenetic modifications [116]. We found evidence that *HOXB7* hypomethylation is a potential

risk factor for MMC. Interestingly, a study by Kok et al. found that DNA methylation of *HOXB7* in particular but also the majority of the other *HOX* genes tend to be increased after folic acid and vitamin B12 supplementation [117]. A recent meta-analysis investigated the impact of maternal plasma folate during pregnancy on DNA methylation in cord blood [118]. They found that multiple developmental processes are influenced by maternal folate, including neural tube development.

For this study, we analysed the data of the genome-wide DNA methylation study without focusing on candidate genes or pathways to discover novel methylation changes associated with MMC. The analysis was performed using Illumina Methylation Analyzer (IMA) [96] and WateRmelon [119] R-packages. Findings were confirmed using a locus-specific validation study with the Sequenom EpiTYPER and in larger MMC and control cohorts. The most significant overall hypomethylation was found for the *SOX18* locus in MMC patients. Furthermore, *SOX18* expression studies were performed in chemically-induced hypomethylated DNA from HEK cells and neural tube development was studied in *sox18* mRNA injected zebrafish embryos. Additionally, we quantified *SOX18* methylation in 5 families that include parents, the MMC patient and its non-affected sibling and in 1 family with a MMC patient that has a paternally inherited *BMP4* deletion.

4.3 Materials and methods

Ethics statement

Written informed consent to collect blood samples for (epi)genetic studies was obtained from all participants and/or their legal representatives. This study was approved by the Medical Ethics Committee of the University of Leuven (study ML9193).

Description of MMC patients, related healthy siblings and unrelated healthy controls

A total of 85 MMC patients, 12 healthy related siblings and 30 age- and gender matched non-related healthy control subjects enrolled in this study. The MMC patients are followed at the pediatric neurology department of the University Hospital Leuven (all <18 years). Detailed clinical and general characteristics for all these subjects are previously reported in Table 1 of Chapter 3 [116]. As sensory and motor functions at and below the level of the spinal cord defect are impaired; paralysis, bowel and bladder dysfunction is present in most of the patients. Folic acid supplementation was recommended, but red blood cell folate was not measured during pregnancy. For the family study we included the parents of 5 sibling pairs (pairs 5,27,29,41,60 from Table 1 in Chapter 3 [116]).

Description of case of Caucasian boy with BMP4 deletion

The male patient was born at full term to a G2P1 Caucasian mother by a lower segment caesarean section after an uncomplicated pregnancy with normal prenatal ultrasounds. At birth, he presented an open lumbosacral myelomeningocoele and bilateral talipes equinovarus. The anterior fontanelle was full and bulging. Bilateral lower limb weakness was evident, and initially he did not have neurogenic bladder or bowel dysfunction. Cranial ultrasound revealed hydrocephaly and Arnold-Chiari II malformation. External ventriculoperitoneal drainage and surgical repair of the spinal defect were performed at the day of birth. Renal ultrasound showed a multicystic dysplastic kidney on the right side.

Comparative genomic hybridization using an 180k oligo array platform (180K Cytosure ISCA v2, OGT, Oxford, UK) showed a 1.665 kb deletion on chromosome 14q22.1q22.2 (14:53,267 987-54,933 219; NCBI/hg19, February 2009) and a

microdeletion on chromosome 2p11.2 (2:83,380 184-83,915 440; NCBI/hg19, February 2009). The deleted region on chromosome 14 spans the genes *FERMT2, DDHD1, BMP4, DKN3* and *CNIH* (Figure 1), the microdeletion on chromosome 2 does not cover any known gene. The father of the patient has postaxial polydactyly, severe myopia and pro-optosis. He carries both deletions. The mother of the patient has a 45X/46XX mosaicism. She consumed periconceptional synthetic folic acid supplementation. The DECIPHER ID of the patient is 288171 (hhtps://decipher.sanger.ac.uk).

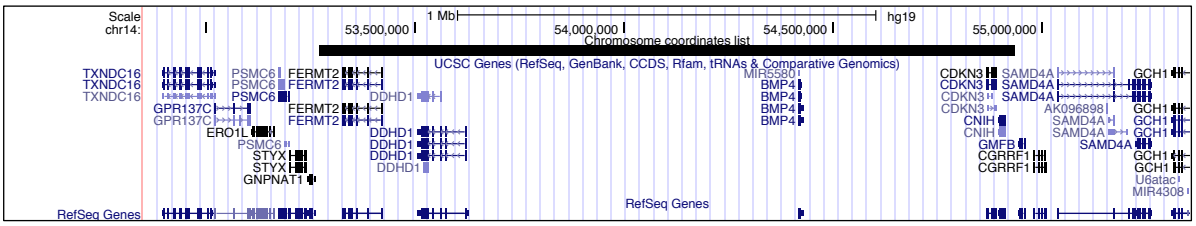

Figure 1. Genetic deletion on Chr 14q22 of Caucasian boy with lumbosacral myelomeningocele. Bar indicates 1.665 kb deletion on chromosome 14q22.1q22.2 (53,267,987-54,933,219) encompassing the genes *FERMT2, DDHD1, BMP4, DKN3* and *CNIH*. Nucleotide positions accord to NCBI build 37/hg19.

MTHRF 677C>T genotyping

Leukocyte DNA from MMC patients, related healthy siblings and unrelated healthy controls was screened for the presence of the *MTHFR 677C>T* variant by PCR and restriction digestion as described [100]. The *MTHFR* genotype of the 85 MMC patients and 12 unaffected siblings is previously reported in [116]. Genotyping for the 10 parents of the family study revealed six parents (3M/3F) with a *CT* genotype and four parents (2M/2F) with a *CC* genotype.

Genome-wide DNA methylation analysis using the HM450K

Leukocyte DNA (1 µg) was subjected to bisulfite treatment using the EZ DNA methylation kit (Zymo Research, Irvine CA, USA). Subsequently, genome-wide DNA methylation was assessed using Illumina Infinium HumanMethylation 450K BeadChip (Illumina, Inc., California, USA). The HM450k experiment and data preprocessing were performed as described previously [116]. The analysis was conducted using both the Illumina Methylation Analyzer (IMA) package implicated in the open source statistical environment R [96] and the WateRmelon R-package [119]. The following three filters were applied on the data for the two pipelines to identify the most significant differentially methylated regions between MMC patients

and controls: i) absolute β-value difference > 0.10; ii) P-value < 0.01 and iii) presence of multiple CpGs per locus. The data discussed in this publication have been deposited in NCBI's Gene Expression Omnibus [120] and are accessible through GEO Series accession number GSE81846.

Functional enrichment analysis

Based on the results from the genome-wide DNA methylation analysis a list of CpGs corresponding to differentially methylated CpG sites was generated and tested for enrichment of known gene ontology pathways. This is performed by means of a hypergeometric test and an FDR-based multiple testing correction of the obtained P-values. The cut-off threshold was set at P<0.001. The enrichment analysis was visualized using the open-source plugin Enrichment Map [121] in Cytoscape 3.2.1.

Methylation of CpGs for 6 genes using the Sequenom EpiTYPER

Leukocyte DNA (1 µg) was subjected to bisulfite treatment using the MethylDetector^{TM} bisulfite modification kit (Active Motif, Carlsbad CA, USA). Subsequently, DNA methylation analysis of the top 6 differentially methylated genes was analyzed by Sequenom EpiTYPER (Sequenom, San Diego, CA, USA) as we described in previous research [97,98,116]. The primers are described in Table 1. Statistical analyses to quantify DNA methylation differences were performed using the Prism 6 software (GraphPad Software Inc., San Diego, CA, USA). Not all DNA methylation values are normally distributed (D'Agostino and Pearson normality test). A two-tailed t-test with Welch's correction was used to assess differences in mean DNA methylation levels between cohorts for the amplicons considered as methylation average and for each CpG unit within this amplicon separately.

Table 1: Primers for the validation studies with Sequenom EpiTYPER.

Gene	Primers	Size	No of CpGs	Cove-rage	Amplicon
ABAT_L	aggaagagagTTTAGAATGGAGGTTGTAGGAGAGA	304	12	12	Chr16: 8806432 - 8806735
ABAT_R	cagtaatacgactcactatagggagaaggctCTTCCAAATTCCCAATCTATAACAT				
CNTNAP1_L	aggaagagagAAAATTTTATTTGGTATTTGGGAAA	384	29	29	Chr17: 40838821-40839204
CNTNAP1_R	cagtaatacgactcactatagggagaaggctCCCTCCCAACTTAAACATCTAACTA				
SLC1A6_L	aggaagagagATGGGAGTATTTTATTTGTGGGAAT	435	13	13	Chr19: 15121145-15121580
SLC1A6_R	cagtaatacgactcactatagggagaaggctAAAAACACACAACTCTTTCCTAACCTA				
SNED1_L	aggaagagagTGAAGTTTATTTTTAGAAGAGTAAGGTAA	470	30	29	Chr2: 241989125-241989592
SNED1_R	cagtaatacgactcactatagggagaaggctTCCAAACAAAATATCAAAATAACCC				
SOX18_L	aggaagagagTGTTTTGTTTAGAGGAGAGTAGTTTGA	284	29	19	Chr20: 62679321-62679605
SOX18_R	cagtaatacgactcactatagggagaaggctACAAATAACCCAAAAACCCAAAA				
TEPP_L	aggaagagagTTTTAGTTAAATTTGGTGGGATGTG	460	27	25	Chr16: 58019630-58020090
TEPP_R	cagtaatacgactcactatagggagaaggctAAACACCTTACCCTCCCTAACAAC				

Primers used for the validation studies with Sequenom EpiTYPER. Nucleotide positions accord to NCBI build 37/hg19. Chr: chromosome; No of CpGs: number of CpG sites in the amplicon; coverage: number of CpG sites that are analysed with Sequenom EpiTYPER.

Gene overexpression in zebrafish

Wild-type AB zebrafish strains were maintained according to standard protocols [102]. Embryos were produced by natural mating and collected and fixed at different stages based on standard morphological criteria [103]. Zebrafish embryos were injected with abat, slc1a6 and sox18 mRNA. The production of mRNA was performed as previously reported [116]. Details of transcripts and primers are described in Table 2. Off-target effects were assessed by injecting with a standard control MO against beta-globin (5'-CCT CTT ACC TCA GTT ACA ATT TAT A 3'). All injected embryos were life-screened at 24 hours post-fertilization (hpf) using a Zeiss Lumar V12 (Carl Zeiss Microscopy, Thornwood, NY, USA) and images were captured with a Leica DFC310 FX digital color camera (Leica Microsystems, Wetzlar, Germany). Experiments were performed in triplicate. Ethical approval was obtained for these studies.

Table 2: Primers for the functional validation studies in zebrafish.

Gene	Primers	Refseq	Ensembl
Abat	5'-CTG TCT GTG TCT CGG TGA GTG CTA CAC ATG-3' 5'-AGG CCA GAC ACT ACT CTA TTT ATG CTC-3'	NM_201498.2	ENSDARG00000006031
Sox18	5'-CGT GTT GGT CTT GCT GGA ATG AAT-3' 5'-TTA TCC TGT AAT GCA GGC GCT GTA ATA GA-3'	XM_001337666.1	ENSDARG00000058598

Nucleotide positions accord to NCBI build 37/hg19.

Pax2a whole mount in situ hybridization

Whole mount In Situ Hybridization (WISH) for the paired box gene 2a (pax2a) was performed with digoxigenin-labeled antisense riboprobes as previously described [104,116]. The influence of gene overexpression on spinal cord and notochord formation was studied using standard morphological criteria [103]. WISH experiments were performed in duplicate.

Gene expression analysis in HEK293 cells

The human embryonic kidney (HEK) cell line were cultured under standard conditions or pretreated with 5 µM 5-aza-2'-deoxycytidine (Sigma Aldrich, Belgium) for demethylation studies. All cells were maintained at 37°C in a humidified environment with 5% CO_2.

Leukocyte DNA (1 µg) was extracted and subjected to bisulfite treatment using the MethylDetector^{TM} bisulfite modification kit (Active Motif, Carlsbad CA, USA) as we described [97,98]. The primers from the validation study were used for amplification of the amplicons (Table 1). Subsequently, Sanger sequencing was performed and the methylation ratio were compared before and after 5-aza-2'-deoxycytidine treatment.

Total RNA was extracted from cells using TRIzol (Invitrogen) reagent, according to the manufacturer's protocol. cDNA was synthesized using reverse transcriptase (Invitrogen, Ghent, Belgium). Human gene expression was measured using Sybr Green PCR. qRT-PCR reactions were analysed using an ABI 7000 real-time PCR machine (Life Technologies). Expression was quantified via the ΔΔCt method [122] and expressed in arbitrary units. Primer sequences are listed in Table 3.

Table 3: Primers for the real-time quantitative PCR.

Gene	Refseq	Sequence
ABAT	Hs.PT.58.21416182	5'- TTT CGG AAG CTG AGA GAC ATC -3'
		5'- GCT GAA GGT CAT CAC GTC TG -3'
SOX18	NM_018419	5'- GTGGCACTGGCCAAACT-3'
		5'- GTGTTACCTCTCATTGTCTCCAG -3'
SLC1A6	Hs.PT.58.50488526.g	5'- CCT TCT AGT GTT CCC AGT TTC TAC -3'
		5'-CAT CTC ATC AGA TCT AAG TGT CTA GAG-
CNTNAP1	Hs.PT.58.25634554	5'- GTA CCA GCT AAC CAC TCG AC -3'
		5'- GAG AAC TTC TGC TCT GTC AGT G -3'
TEPP	Hs.PT.58.19812321.g	5'- GTA CTT GAA GCC CGA CGT G -3'
		5'- ACT GTA GCT GGA GCC GAA -3'
SNED1	Hs.PT.58.26360591	5'- CTA CCG AGT TCA CCA AGA CAT -3'
		5'- GTG GAG TGT AAC AAG AAC GTC T -3'

Nucleotide positions accord to NCBI build 37/hg19.

4.4 Results

DNA methylation of LINE elements and folic acid regulatory genes

Findings of global DNA and LINE-1 hypomethylation in patients with NTDs [69,75] suggest that genomic instability might interfere with neural tube closure. We extracted the methylation values for all LINE-1 and LINE-2 probes from our HM450k study. About 20158 CpG probes correspond to 1498690 LINE-1 and LINE-2 elements. The mean methylation of these LINE probes was not significantly different between MMC patients and controls (mean β-value was 77,6% versus 77,7%; respectively) though unsupervised hierarchical clustering analysis grouped almost all MMC patients separately from the controls (Figure 2).

We next extracted methylation values for 43 genes (including 698 CpG probes) involved in the folic acid and the one carbon metabolism [26]. There are no methylation differences for the folic acid genes between MMC patients and controls (Figure 3). According to unsupervised hierarchical clustering analysis, samples are clustered irrespective of the subgroup.

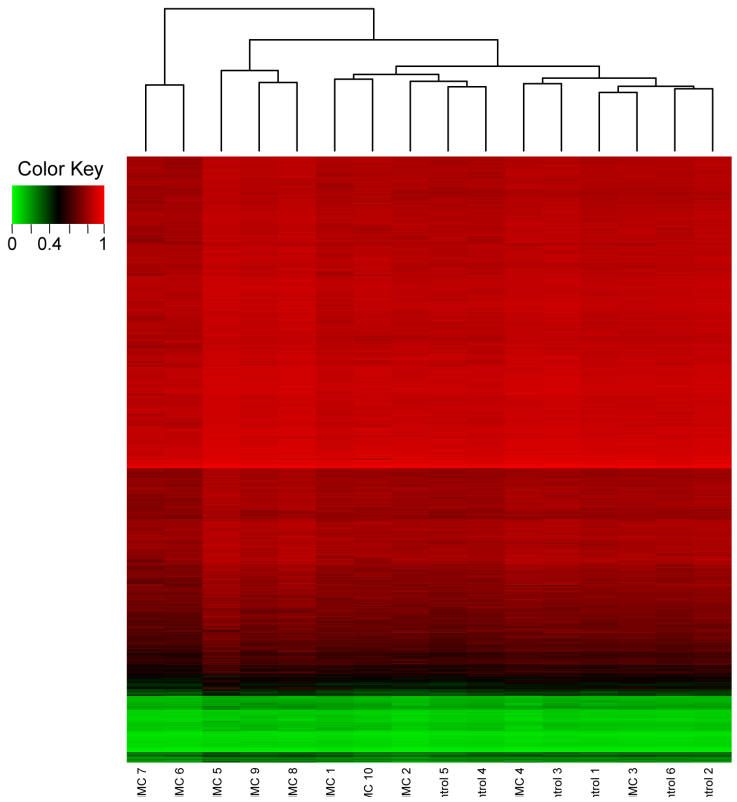

Figure 2. Whole genome methylation in MMC patients vs. controls. Unsupervised hierarchical clustering analysis of the subgroups. Methylation values for LINE-1 and LINE-2 repetitive elements are extracted from data obtained with the HM450k. Heatmaps represent 3575 randomly selected CpGs (1% total CpGs). Green and red represent 0 and 1 methylation, respectively. MMC: myelomeningocele.

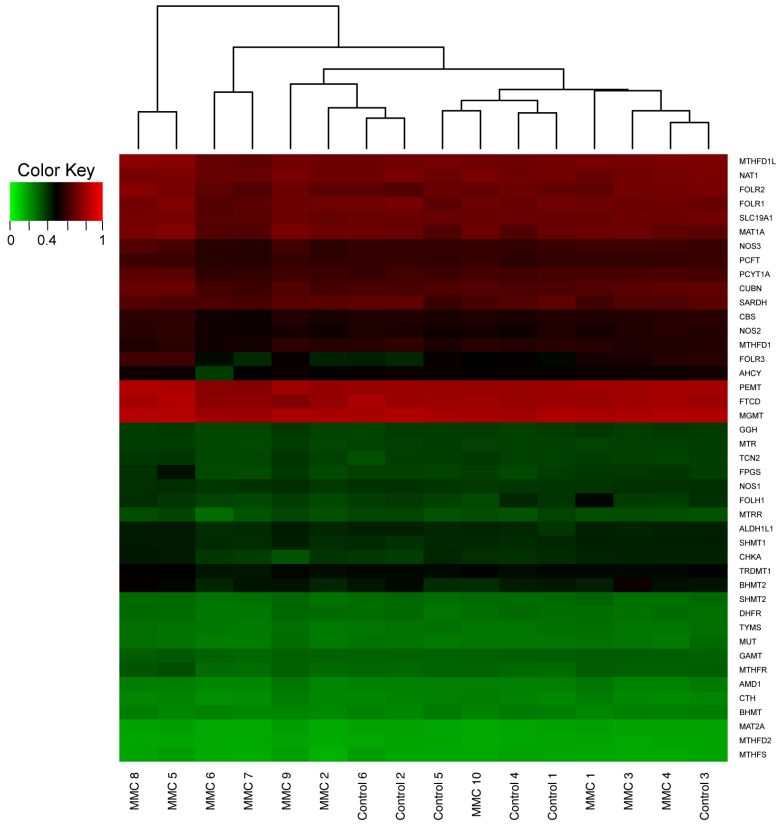

Figure 3. Heatmap showing methylation of genes involved in the folate and one carbon metabolism in MMC patients. Methylation values of the genes are extracted from data obtained with the HM450k. Green and red represent 0 and 1 methylation, respectively. MMC: myelomeningocele.

Methylome analysis for gene identification

The HM450k data were analysed and the 6 highest ranked genes were *ABAT, CNTNAP1, SLC1A6, SNED1, SOX18,* and *TEPP* (Table 4). Ranking genes based on having a β-value > 0.10 and p-value < 0.01 resulted in a total of 45 genes that include 75 CpG sites (Table 5) with a significant differential methylation value in MMC patients. Among these 75 CpGs, 54 CpGs (72%) are associated with decreased methylation in MMC patients. To evaluate if certain biological functions would be enriched in this gene list, we performed a functional enrichment analysis, that showed an overrepresentation of gene ontology classes mainly related to cytoplasm, transcription, neuron projection, synaptic processes, cell projection and some minor others (Figure 4). Interestingly, the genes seem to act together through various pathways, as they are often involved in divergent gene ontology categories. The gene ontology enrichment analysis favours the hypothesis that NTDs are the result of a complex multifactorial combination.

Table 4: Top 6 differentially methylated genes investigated by HM450k and selected for validation with Sequenom EpiTYPER.

Gene	Illumina ID	WateRmelon		IMA R-package		Gene group
		P-value	β-diff	P-value	β-diff	
ABAT Chr16p13	cg01881182	0,0017	-0,20	0,0047	-0,15	5' UTR
	cg16586594	0,0005	-0,18	0,0005	-0,19	5' UTR
	cg08834902	0,0047	-0,23	0,0047	-0,16	5' UTR
SLC1A6 Chr19p13	cg12695707	0,0002	-0,27	0,0005	-0,16	TSS1500
	cg09470638	0,0010	-0,25	0,0048	-0,14	TSS200
	cg02489552	0,0002	-0,14	0,0002	-0,21	TSS200
SOX18 Chr20q13	cg02231404	0,0010	-0,20	0,0010	-0,21	Body
	cg22138735	0,0005	-0,17	0,0005	-0,17	Body
TEPP Chr16q21	cg04370442	0,0047	-0,15	0,0075	-0,16	Body
	cg12499872	0,0005	-0,31	0,0005	-0,15	Body
CNTNAP1 Chr17q21	cg16308533	0,0005	-0,17	0,0010	-0,19	Body
	cg11629889	0,0002	-0,14	0,0010	-0,16	Body
SNED1 Chr2q37	cg23491743	0,0017	-0,16	0,0030	-0,17	Body
	cg25241559	0,0005	-0,15	0,0005	-0,17	Body

Nucleotide positions accord to NCBI build 37/hg19. β-diff: β-difference; Chr: chromosome; MMC: myelomeningocele. These 6 genes were selected for the validation study using Sequenom EpiTYPER.

Table 5: Top 75 differentially methylated CpGs investigated by HM450k and top 45 genes selected for functional gene enrichment.

				WateRmelon		IMA R-package		MMC (n=10)		Controls (n=6)		Gene group
Gene	Chr	mapinfo	Illumina ID	P-value	β-diff	P-value	β-diff	Mean	SD	Mean	SD	
CAPZB	1	19732786	cg16694480	0,0047	-0,24	0,0047	-0,16	0,51	0,08	0,67	0,05	Body
HEYL	1	40098811	cg12634306	0,0030	-0,21	0,0075	-0,22	0,44	0,16	0,66	0,03	Body
ROR1	1	64602654	cg07797372	0,0010	0,14	0,0010	0,12	0,61	0,05	0,49	0,05	Body
MTMR11	1	149908313	cg13476072	0,0010	0,16	0,0005	0,10	0,81	0,03	0,70	0,06	Body
PEAR1	1	156883745	cg13224583	0,0017	-0,26	0,0017	-0,20	0,51	0,16	0,72	0,03	Body
ENAH	1	225838196	cg13305444	0,0010	-0,12	0,0017	-0,10	0,71	0,06	0,82	0,03	Body
GALNT2	1	230415343	cg00589617	0,0047	-0,32	0,0030	-0,23	0,62	0,18	0,85	0,07	3'UTR
	2	795935	cg21032567	0,0017	-0,11	0,0030	-0,12	0,72	0,07	0,84	0,03	
	2	9324127	cg06153448	0,0010	0,20	0,0030	0,14	0,63	0,05	0,48	0,10	
UCN	2	27530884	cg06536868	0,0005	-0,13	0,0030	-0,12	0,46	0,09	0,59	0,03	5'UTR
	2	45397874	cg20201270	0,0005	0,15	0,0030	0,12	0,43	0,11	0,31	0,03	
	2	131094827	cg01331772	0,0017	-0,35	0,0017	-0,32	0,37	0,18	0,69	0,08	
	2	202929157	cg10590964	0,0030	0,19	0,0030	0,12	0,80	0,06	0,68	0,03	
NRP2	2	206628625	cg05348875	0,0075	-0,26	0,0075	-0,17	0,58	0,13	0,75	0,09	Body
PLCD4	2	219472607	cg17980119	0,0030	-0,17	0,0030	-0,11	0,57	0,10	0,68	0,03	TSS200
ECEL1P2	2	233251770	cg13138089	0,0017	-0,15	0,0017	-0,15	0,55	0,20	0,70	0,02	TSS200
SNED1	2	241989271	cg23491743	0,0017	-0,16	0,0030	-0,17	0,67	0,15	0,84	0,04	Body
SNED1	2	241989379	cg25241559	0,0005	-0,15	0,0005	-0,17	0,70	0,17	0,87	0,01	Body
CC2D2A	4	15480643	cg18797590	0,0075	0,12	0,0075	0,11	0,77	0,07	0,66	0,03	Body
LDB2	4	16575323	cg08262002	0,0017	0,18	0,0030	0,11	0,77	0,07	0,66	0,06	Body
CYP4V2	4	187126073	cg09526685	0,0047	-0,22	0,0047	-0,12	0,77	0,09	0,89	0,03	Body
FLJ44606	5	126409061	cg18710053	0,0002	-0,12	0,0002	-0,12	0,23	0,05	0,35	0,03	5'UTR
CCNI2	5	132083532	cg08957484	0,0017	-0,12	0,0030	-0,13	0,18	0,09	0,31	0,03	1stExon
KCTD16	5	143847362	cg18991165	0,0017	0,17	0,0017	0,11	0,91	0,02	0,81	0,06	Body
	6	33128923	cg16604233	0,0002	0,16	0,0002	0,15	0,73	0,06	0,58	0,04	
	6	75459158	cg22322277	0,0075	0,16	0,0075	0,11	0,67	0,07	0,56	0,07	
	6	158097037	cg10525394	0,0002	-0,16	0,0002	-0,12	0,64	0,07	0,76	0,03	
PNLDC1	6	160241556	cg15829665	0,0030	-0,15	0,0075	-0,11	0,47	0,10	0,57	0,04	3'UTR
PARK2	6	161836525	cg10735454	0,0005	-0,19	0,0002	-0,14	0,43	0,06	0,57	0,04	Body
	7	117323381	cg26310285	0,0002	0,16	0,0002	0,11	0,72	0,04	0,62	0,05	
	7	120414717	cg18264932	0,0075	-0,15	0,0075	-0,12	0,66	0,12	0,79	0,03	
STMN4	8	27115956	cg11688949	0,0030	-0,14	0,0010	-0,14	0,43	0,11	0,57	0,02	TSS200
C9orf167	9	140175679	cg13416866	0,0017	-0,15	0,0017	-0,16	0,39	0,10	0,54	0,04	3'UTR
PRKG1	10	53287690	cg08751451	0,0075	0,20	0,0075	0,15	0,81	0,05	0,67	0,13	Body
C10orf120	10	124459681	cg15840151	0,0010	-0,17	0,0010	-0,10	0,58	0,07	0,68	0,05	TSS1500
YPEL4	11	57417949	cg03773647	0,0005	-0,16	0,0002	-0,10	0,55	0,08	0,66	0,01	TSS1500
SHANK2	11	70484490	cg00447817	0,0017	-0,13	0,0017	-0,13	0,68	0,06	0,81	0,05	Body
SHANK2	11	70560211	cg07192048	0,0030	-0,25	0,0030	-0,21	0,41	0,09	0,62	0,10	Body
SHANK2	11	70673256	cg04262428	0,0017	0,11	0,0005	0,10	0,28	0,04	0,18	0,03	Body
SHANK2	11	70760166	cg25885280	0,0047	-0,13	0,0075	-0,11	0,53	0,06	0,64	0,05	Body
ODZ4	11	78761473	cg20831648	0,0047	-0,12	0,0047	-0,10	0,66	0,08	0,76	0,04	Body
	11	116328665	cg11921539	0,0028	-0,12	0,0002	-0,11	0,46	0,07	0,57	0,01	

	11	119662882	cg09938664	0,0002	-0,11	0,0002	-0,11	0,40	0,04	0,51	0,03	
PRDM10	11	129793108	cg16983588	0,0005	0,26	0,0005	0,17	0,64	0,09	0,47	0,04	Body
NTF3	12	5543269	cg27423216	0,0002	-0,25	0,0002	-0,26	0,40	0,12	0,66	0,04	Body
FBRSL1	12	133135463	cg20454518	0,0010	-0,10	0,0017	-0,11	0,32	0,04	0,43	0,05	Body
	13	27498239	cg23681440	0,0002	0,13	0,0002	0,14	0,58	0,05	0,44	0,03	
C13orf33	13	31481184	cg13251181	0,0030	0,13	0,0075	0,14	0,58	0,10	0,44	0,02	Body
	13	33455187	cg10288525	0,0040	0,21	0,0017	0,13	0,80	0,07	0,67	0,04	
BMP4	14	54419614	cg08046044	0,0005	-0,12	0,0010	-0,12	0,18	0,05	0,30	0,03	5'UTR
	14	101175970	cg18089426	0,0010	0,14	0,0017	0,14	0,73	0,09	0,59	0,06	
ARNT2	15	80853140	cg13148921	0,0005	-0,23	0,0017	-0,21	0,39	0,11	0,60	0,13	Body
CPEB1	15	83317526	cg17453840	0,0030	-0,13	0,0075	-0,14	0,70	0,16	0,84	0,03	TSS1500
FLYWCH1	16	2975552	cg01215511	0,0047	-0,23	0,0047	-0,16	0,64	0,16	0,80	0,03	5'UTR
ABAT	16	8806531	cg01881182	0,0017	-0,20	0,0047	-0,15	0,42	0,07	0,57	0,08	5'UTR
ABAT	16	8806569	cg16586594	0,0005	-0,18	0,0005	-0,19	0,34	0,08	0,53	0,08	5'UTR
ABAT	16	8806690	cg08834902	0,0047	-0,23	0,0047	-0,16	0,53	0,10	0,70	0,06	5'UTR
TEPP	16	58019866	cg04370442	0,0047	-0,15	0,0075	-0,16	0,71	0,21	0,88	0,02	Body
TEPP	16	58019893	cg12499872	0,0005	-0,31	0,0005	-0,15	0,73	0,17	0,88	0,01	Body
KCNAB3	17	7832680	cg15951188	0,0047	-0,18	0,0047	-0,19	0,58	0,14	0,77	0,05	1stExon
CNTNAP1	17	40838983	cg16308533	0,0005	-0,17	0,0010	-0,19	0,66	0,15	0,86	0,04	Body
CNTNAP1	17	40839022	cg11629889	0,0002	-0,14	0,0010	-0,16	0,71	0,13	0,88	0,03	Body
QRICH2	17	74270190	cg09812376	0,0056	0,19	0,0047	0,20	0,51	0,10	0,31	0,13	3'UTR
	19	7934807	cg23995446	0,0075	0,12	0,0047	0,11	0,23	0,11	0,11	0,03	
SLC1A6	19	15121333	cg12695707	0,0002	-0,27	0,0005	-0,16	0,65	0,08	0,81	0,06	TSS1500
SLC1A6	19	15121509	cg09470638	0,0010	-0,25	0,0048	-0,14	0,67	0,11	0,81	0,04	TSS200
SLC1A6	19	15121531	cg02489552	0,0002	-0,14	0,0002	-0,21	0,47	0,13	0,68	0,08	TSS200
LRFN1	19	39799037	cg26910511	0,0047	-0,14	0,0030	-0,16	0,69	0,14	0,85	0,05	Body
R3HDML	20	42965025	cg25779645	0,0075	-0,16	0,0075	-0,10	0,55	0,08	0,65	0,03	TSS1500
SOX18	20	62679635	cg02231404	0,0010	-0,20	0,0010	-0,21	0,32	0,12	0,53	0,04	Body
SOX18	20	62679713	cg22138735	0,0005	-0,17	0,0005	-0,17	0,15	0,06	0,33	0,06	Body
	22	19141030	cg14372705	0,0017	0,21	0,0017	0,14	0,64	0,09	0,50	0,04	
	22	28074071	cg16331674	0,0030	-0,25	0,0017	-0,11	0,76	0,10	0,87	0,01	
	22	28074146	cg16084133	0,0010	-0,17	0,0005	-0,15	0,68	0,12	0,84	0,02	
SELM	22	31500896	cg21361322	0,0047	-0,39	0,0047	-0,13	0,77	0,13	0,90	0,01	3'UTR

Nucleotide positions accord to NCBI build 37/hg19. Selection is performed after analysis with two pipelines and application of two selection criteria: i) absolute β-value difference > 0.10 and ii) P-value < 0.01. β-diff: β-difference; Chr: chromosome; MMC: myelomeningocele; SD: standard deviation. These 45 genes were selected for the functional gene enrichment analysis.

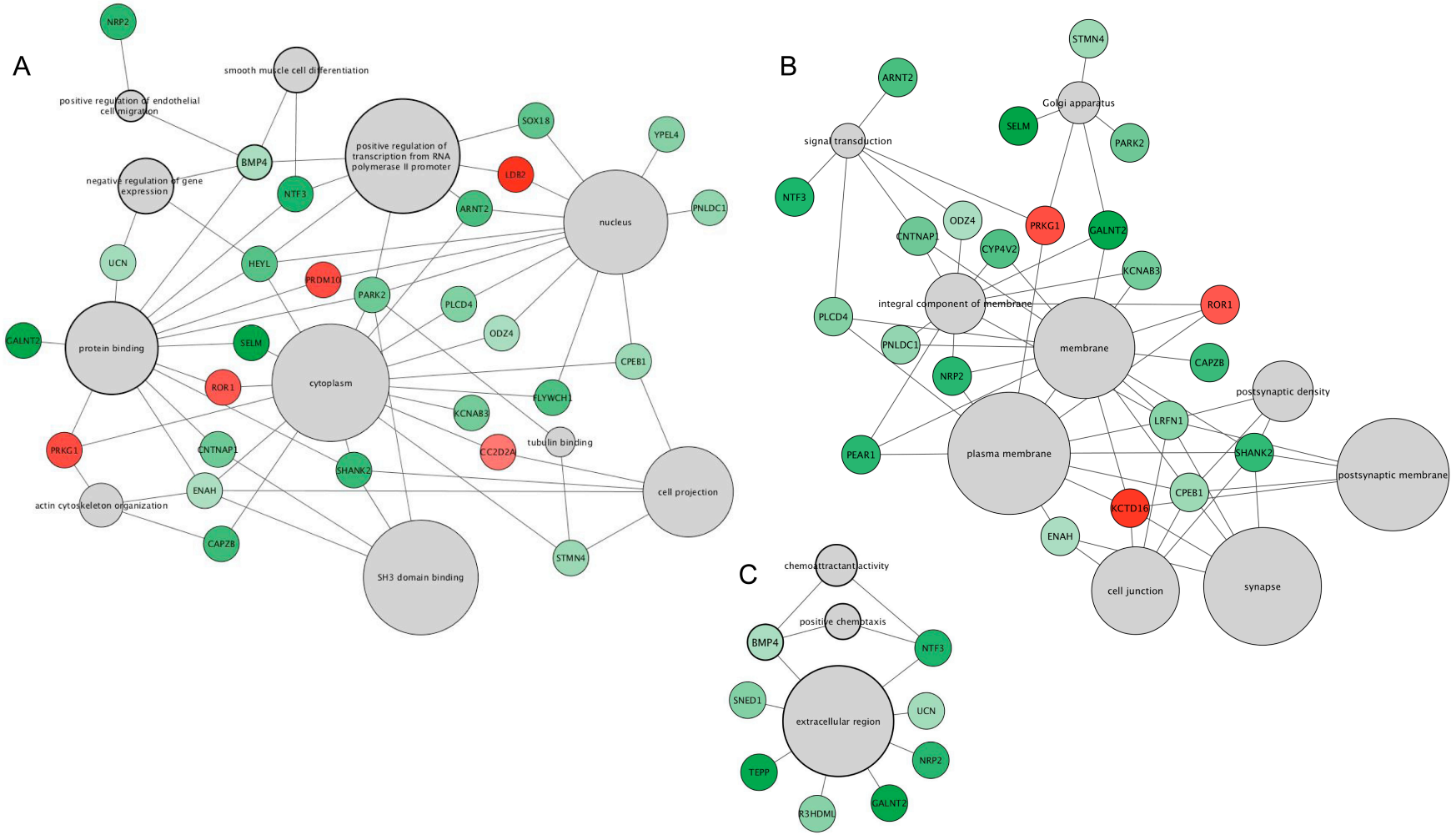

Figure 4. Gene ontology enrichment map based on top differentially methylated genes in MMC patients. The map displays three clusters of functionally related gene-sets in MMC patients vs. controls (A, B and C). Gray nodes represent GO classes and the size of each node is correlated with its significance (adjusted P-value). Green and red nodes represent hypomethylated and hypermethylated genes, respectively. The intensity of the color is correlated with β-difference. Dark circles represent GO classes that include BMP4.

Validation study in larger MMC and control cohorts

A validation study was performed with the Sequenom EpiTYPER to quantify DNA methylation for loci that contain the CpGs of the 6 highest ranked genes. The validation was performed for 83 MMC patients (fully described in Table 1 of Chapter 3 and previously in [116]) and 30 unrelated healthy controls. All gene loci include some specific significantly hypomethylated CpGs in MMC patients compared to controls (Figure 5; left panels). However, only for the *SOX18* locus, a significant overall hypomethylation was found for MMC patients versus controls (-14%; 95% CI [-8%, -20%], P-value = 0.0003) (Figure 5; right panels). For the other 5 genes *ABAT, CNTNAP1, SLC1A6, SNED1,* and *TEPP*, the overall methylation of the studied locus was not significantly different between MMC patients and controls.

As differences in global DNA hypomethylation have previously been described in patients with NTDs in association with the *MTHFR 677C>T* variant, we genotyped this variant for our cohorts. Similar to our previous findings for the *HOXB7* locus [116], we did not find an association between *MTHFR 677 CC* versus *CT+TT* carriers and changes in *SOX18* methylation values (data not shown).

Figure 5. Validation of the top 6 differentially methylated genes by Sequenom EpiTYPER in MMC patients versus controls. Left: methylation pattern for each CpG unit within the amplicons. Multiple t-test was performed for each CpG. P-value: *<0.05. Right: boxplot representing methylation pattern with box = 25th and 75th percentiles; bars = min and max values. The mean methylation level of each group is shown above the plot. The validation study is performed for 83 MMC patients and 30 controls. * CpGs were first identified by HM450k.

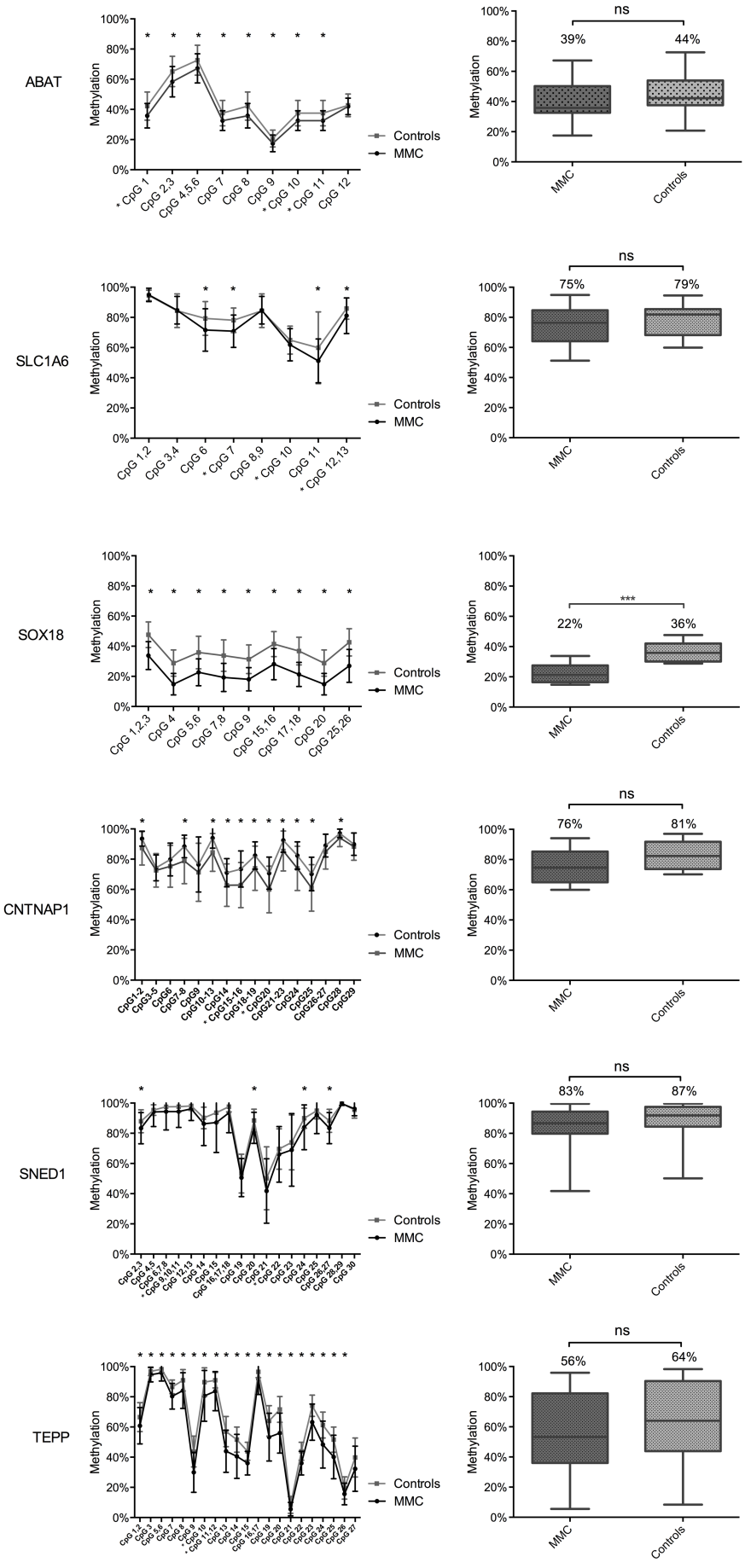
ABAT
SLC1A6
SOX18
CNTNAP1
SNED1
TEPP
Methylation
Controls
MMC
ns
***
39%
44%
75%
79%
22%
36%
76%
81%
83%
87%
56%
64%

Chemically-induced demethylation versus gene expression analysis

Demethylation studies were performed in HEK cells that were treated for 72 hours with 5 µM 5-aza-2'-deoxycytidine (AZA). Bisulfite sequencing using primers similar to the Sequenom EpiTYPER study confirmed CpG demethylation for all CpGs within the top 6 ranked genes (*ABAT, CNTNAP1, SLC1A6, SNED1, SOX18,* and *TEPP*) after AZA treatment but again with the most pronounced difference detected for the *SOX18* locus (Figure 6A). Gene expression was measured for *ABAT, CNTNAP1, SLC1A6, SNED1, SOX18,* and *TEPP* using qRT-PCR but only *TEPP* and *SOX18* expression was significantly increased after AZA treatment (Figure 6B).

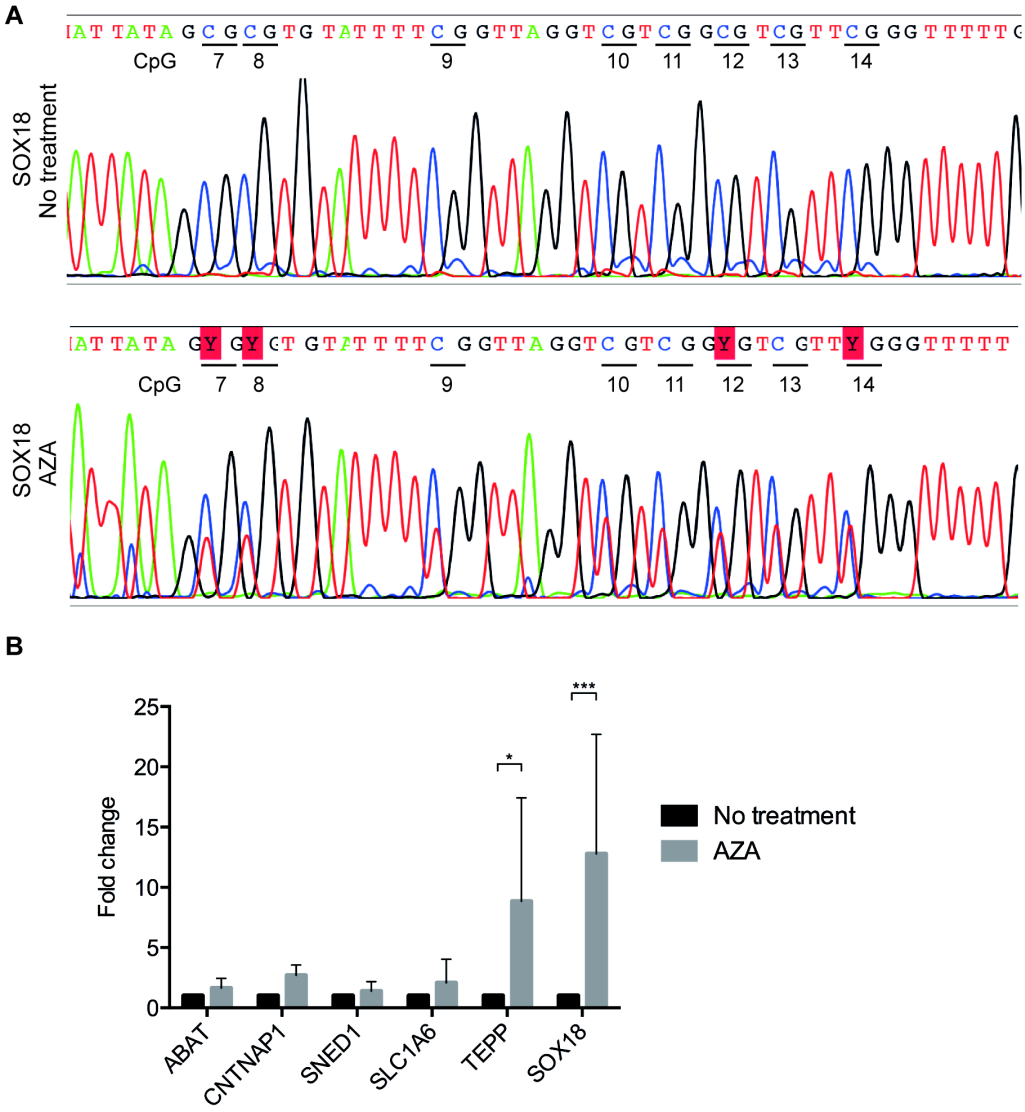

Figure 6. Demethylation studies and gene expression analysis. Demethylation studies were performed using 5 µM 5-aza-2'-deoxycytidine in HEK cell line. A) Sanger sequencing showing demethylation of *SOX18* after 5-aza-2'-deoxycytidine treatment. The CpGs from the *SOX18* amplicon are annotated below the sequence. B) Gene expression analysis of top 6 genes using qRT-PCR. Standard: standard culture conditions; AZA: 5-aza-2'-deoxycytidine. P-value: *<0.05, ***<0.001.

Gene expression studies in Zebrafish

Functional genetic studies were performed in zebrafish to study alterations of *sox18* and *abat* expression during embryogenesis and neural tube formation. Both genes are highly conserved between humans and zebrafish (68% for *sox18* and 70% for *abat*). We analysed embryos that express high levels of *sox18* and *abat* after microinjection of synthetic mRNA. Detailed morphological analysis of neural tube formation during embryogenesis was performed using whole mount in situ hybridization (WISH) with a probe for the paired box gene 2a (*pax2a*) gene. Embryos injected with *abat* and *sox18* mRNA developed with mild (for *abat*) to severe (for *sox18*) malformations in about 50% (for *abat*) to 74% (for *sox18*) of the embryos at 24 hours post fertilization (hpf) (Figure 7). Embryos that express high levels of *abat* present with mainly abnormal neural tube structures (Figure 7A) while embryos with high *sox18* levels are more severely affected having a general developmental delay that includes neural tube malformation (Figure 7B). We also investigated if addition of 0,1 mM folic acid to the egg water would rescue the phenotype [123] but no significant differences would be observed (Figure 7C).

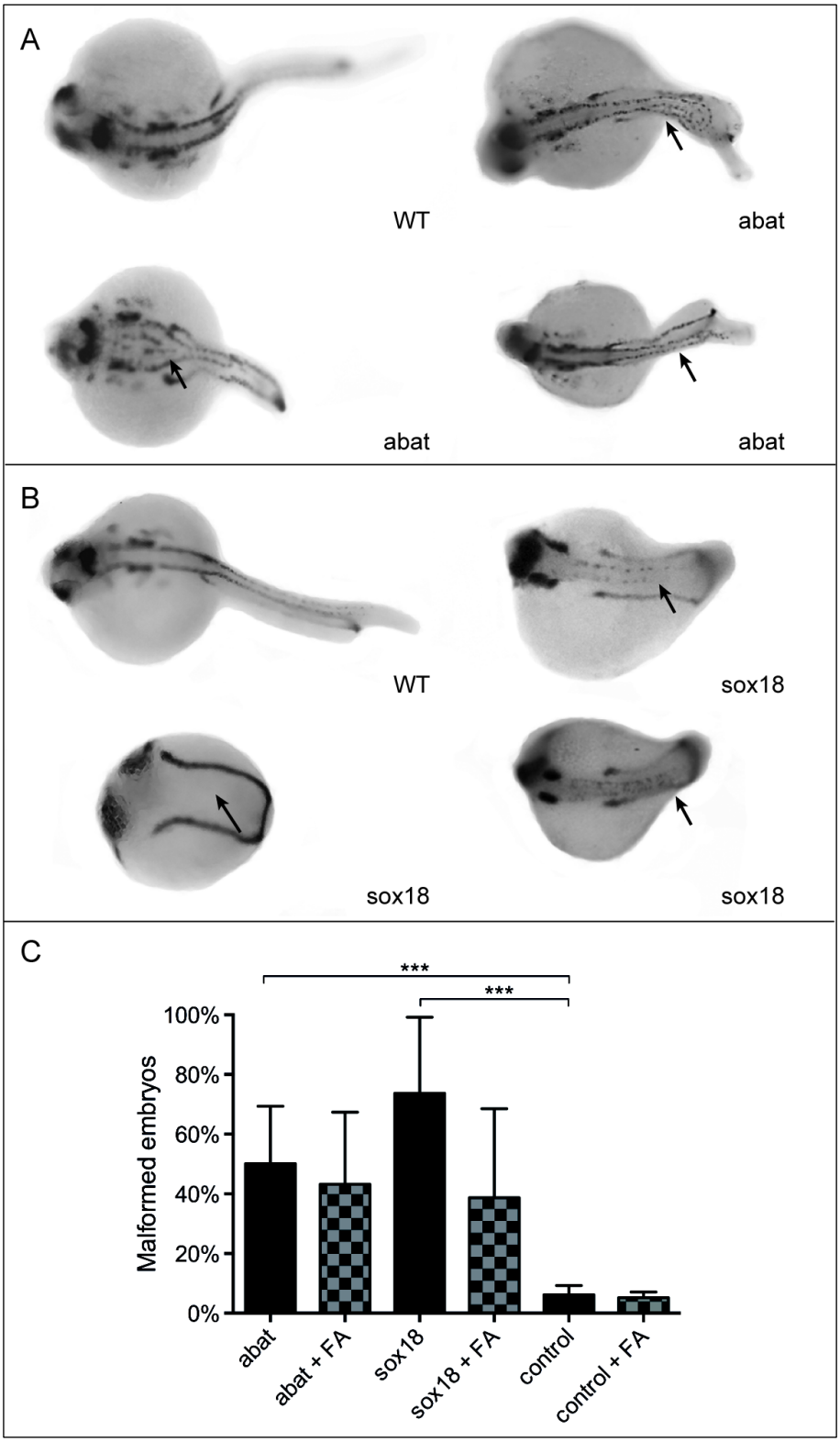

Figure 7. Phenotype analysis of gene overexpression in zebrafish embryos. A) and B) Pax2a staining after microinjection of Abat mRNA (A) and Sox18 mRNA (B). Wild type (WT) zebrafish show expression in the hindbrain, hindbrain-midbrain boundary, neural tube, mesoderm, optic stalk, otic vesicle, and pronephric duct. Spinal cord malformation is indicated with an arrow. C) Phenotype analysis after Pax2a staining at 24 hpf resulted in respectively 50% and 74% embryos with an affected phenotype after Abat and Sox18 overexpression. Folic acid supplementation after gene overexpression did not significantly influence the phenotype. P-value: ***<0.001.

SOX18 methylation studies in 5 MMC patients and their non-affected siblings and parents

To study the inheritance of the *SOX18* methylation changes, we quantified *SOX18* methylation for 5 MMC patients and their non-affected siblings and parents with the Sequenom EpiTYPER (Figure 8A). Interestingly, not only the MMC patients but also their non-affected healthy siblings presented with similar levels of *SOX18* hypomethylation whereas their parents had methylation values comparable to these of the unrelated control cohort (Figure 8A). There were no significant DNA methylation differences between the 5 MMC patients, their siblings and the overall MMC cohort. The quantification of DNA methylation for the separate CpGs revealed higher methylation values for the parents compared to the MMC patient and its healthy sibling for all CpGs (Figure 8B). These data would implicate that *SOX18* hypomethylation is not sufficient to cause a NTD.

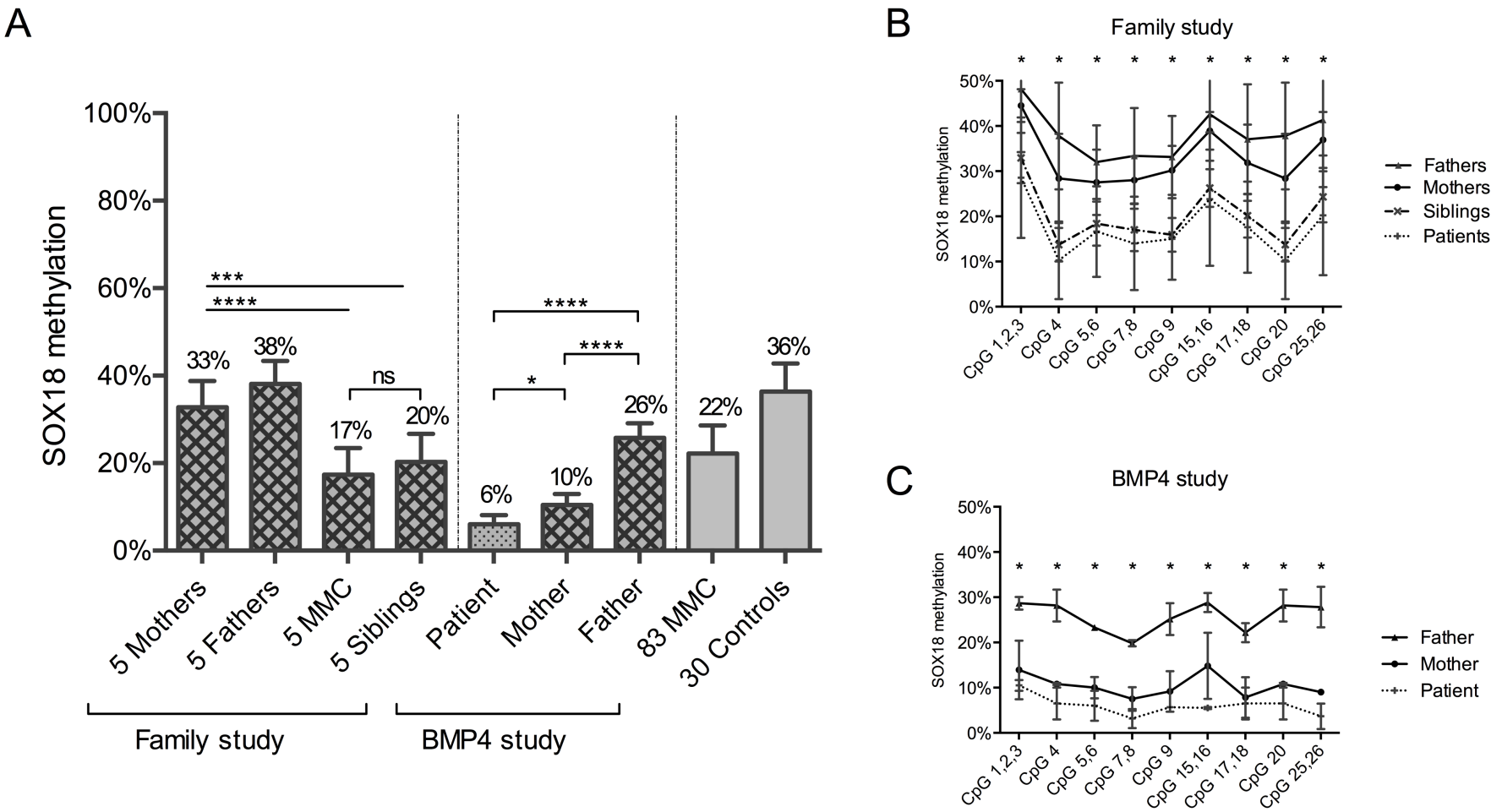

Figure 8. *SOX18* methylation for the family study and the *BMP4* study by Sequenom EpiTYPER. A) Mean methylation and standard deviation of *SOX18* methylation for the family study and the BMP4 study. The mean methylation level of each group is shown above the plot. P-value: *<0.05, **<0.01, ***<0.001,****<0.0001. B) Methylation pattern for each CpG unit within the *SOX18* amplicon for the family study. Multiple t-test was performed for each CpG. P-value: *<0.05. C) Methylation pattern for each CpG unit within the *SOX18* amplicon for the *BMP4* study. Multiple t-test was performed for each CpG. P-value: *<0.05. The family study consists of MMC patients, their unaffected siblings and their parents (n = 5 for each group). The *BMP4* study describes the family of a patient with a *BMP4* deletion. The father is carrier of the *BMP4* deletion.

SOX18 methylation studies in the parents of a MMC patient with a paternally inherited BMP4 deletion

To investigate the influence of an underlying genetic factor, *SOX18* DNA methylation was quantified in a boy with lumbosacral MMC and his parents. The boy has paternally inherited microdeletions that comprise 14q22.1q22.2 (14:53,267,987-54,933,219;NCBI/hg19, February 2009) and 2p11.2 (2:83,380 184-83,915 440;NCBI/hg19, February 2009). 14q22.1q22.2 covers the genes *FERMT2, DDHD1, BMP4, DKN3* and *CNIH* (Figure 1) while the other deletion in the 2p11.2 region does not include genes. The father has postaxial polydactyly, severe myopia and pro-optosis but no spina bifida. His clinical phenotype is compatible with a *BMP4* deletion syndrome. Interestingly, *BMP4* is one of the 45 genes that showed DNA methylation changes in our HM450k analysis (Table 5) and is also present in the functional enrichment network very closely connected to *SOX18* (Figure 4). The *BMP4* deletion patient but also his mother presented with significantly lower methylation values compared to the father and the group of unrelated healthy controls (Figure 8A). Both overall as well as the CpG-specific methylation covering the *SOX18* locus were significantly different between the patient and his mother (Figure 8A and 8B).

4.5 Discussion

Current research supports the hypothesis that abnormal DNA methylation contributes to NTDs [32,40]. However, rather than DNA hypomethylation of individual candidate loci, a complex combination of environmental and (epi)genetic factors are likely causative for NTDs [124,125]. Analysis of HM450k methylation data for 10 MMC patients and 6 unrelated healthy controls showed no statistically significant difference in global DNA methylation as determined via the LINE-1 and LINE-2 methylation. However, unsupervised hierarchical clustering analysis showed that MMC patients are more closely related to one another compared to unrelated healthy controls. The DNA methylation values extracted for candidate genes related to folic acid and the one carbon metabolism revealed no significant differences between MMC patients and controls. Therefore, we next analysed the HM450k data using a genome-wide approach. As divergence between the two Infinium assays generates two different types of data [126], different correction and normalization methods are suggested to make the datasets comparable. Therefore, we have used the two analysis pipelines (WateRmelon and IMA) and these resulted in the identification of significant hypomethylation for the genes *ABAT, CNTNAP1, SLC1A6, SNED1, SOX18 and TEPP.* Further validation by Sequenom EpiTYPER confirmed CpG-specific DNA hypomethylation for these genes. However, only the *SOX18* locus showed highly significant overall hypomethylation for MMC patients. Recessive and dominant mutations in *SOX18* in humans are known to cause hypotrichosis-lymphedema-telangiectasia syndrome with a combination of hair and cardiovascular anomalies, including symptoms of lymphatic dysfunction [127]. More recently, *SOX18* has also been identified as a novel target of the Hedgehog signalling pathway, which plays an important role in neural tube development [128]. Most studies available to date have focused on the role of *SOX18* depletion or loss of function mutants while our study points to a potential role of *SOX18* hypomethylation leading to increased *SOX18* expression. Knowledge on the biology of *SOX18* overexpression is sparse but evidence for a role in neural tube formation is at least supported by our zebrafish studies that showed strongly malformed tails with abnormal neural tube development in embryos with high levels of *sox18* after injection of its mRNA.

As periconceptional folate is important for NTD prevention, we compared our findings with a large dataset that examined the association between maternal plasma folate during pregnancy and genome-wide DNA methylation in newborn cord blood [118]. Interestingly, one of the top differentially methylated CpGs of this study (cg12695707 within the *SLC1A6* gene locus) was also detected as a hypomethylated CpG in our study (Table 4). Therefore, *SLC1A6* seems to be sensitive to maternal plasma folate in both healthy controls as in MMC patients. In addition, multiple developmental processes seem to be influenced by maternal folate, including neural tube development. Recently, we described the importance of *HOX* gene methylation in neurulation [116], which is also influenced by maternal plasma folate [117]. In addition, we checked if our candidate genes are also represented in another large-scale meta-analysis that investigated the influence of maternal smoking on DNA methylation in newborns [129]. Five of our 75 candidate loci with abnormal methylation being *BMP4, ENAH, GALNT2, NRP2* and one CpG in a locus without an annotated gene seem to be highly significantly influenced by maternal smoking. Bone morphogenetic protein 4 *(BMP4)* is of special interest as it is involved in craniofacial development and an important candidate gene for cleft palate defects [130]. However, *BMP4* has not yet been implicated directly in lumbosacral MMC. Based on the meta-analysis, *BMP4* is associated with increased methylation after maternal smoking [129].

In addition to dietary and environmental factors, DNA sequence variability influences DNA methylation. The influence of DNA sequence variability on DNA methylation is estimated to differ between 22-80% [131]. In order to investigate how genetic factors might influence DNA methylation, we first genotyped the *MTHFR 677C>T* variant as this variant is known to lead to hyperhomocysteinemia and global DNA hypomethylation especially under low folate conditions [88]. We did not find an additive effect of the *MTHFR* variant on *SOX18* methylation. To investigate whether candidate genes from literature might be differentially methylated, we compared the findings of our top 45 significantly differentially methylated genes with the gene list from a recent NTD wiki database that provides an online up-to-date list of genes implicated in neural tube closure (http://ntdwiki.wikispaces.com). Only one gene of our top genes, *ENAH,* was present in the candidate gene list. However, the interplay between genetics and epigenetics in driving a disease phenotype is not well

understood and is completely unknown for NTD etiology. As we hypothesized that there may be a maternal factor that contributes to a disturbed DNA methylation cycle, we performed *SOX18* methylation studies for 5 families including the MMC patient and their non-affected parents and sibling. Both parents had methylation levels comparable to these of the control cohort while the MMC patients and their healthy siblings had significantly lower *SOX18* methylation. These findings are suggestive of an epigenetic change induced by the mother. In addition, we report here the first MMC case with a combined genetic and epigenetic defect involving a paternally inherited chromosomal deletion that includes *BMP4* and a maternally inherited defect in *SOX18* methylation. The MMC child, born from Caucasian non-related parents, was diagnosed with a lumbosacral NTD and carries a paternally inherited 14q22.1-2 deletion that involves *FERMT2, DDHD1, BMP4, DKN3* and *CNIH*. *BMP4* deletions have been associated with variable defects of the eyes, palate, limbs and brain and with developmental and growth delay but not with NTDs [132,133]. Mutations in *DDHD1* are found in patients with hereditary spastic paraplegia [134], *CDKN3* is linked with different cancers while for *FERMT2* and *CNIH* no human diseases have been described. The father with the same chromosomal deletion has postaxial polydactyly, severe myopia and pro-optosis but no NTD. Interestingly, *SOX18* methylation studies in the parents and patient showed pronounced hypomethylation in the mother and patient. Though further biological studies are needed to support any functional interplay between *BMP4* and *SOX18*,, this pedigree illustrates the inheritance of genetic and epigenetic factors that could cause a NTD. It is worth to notice that both *SOX18* [135-137] and *BMP4* [138,139] have been described as regulators of angiogenesis and this could explain an old concept that there might be a vascular basis for NTDs [140]. The vascular hypothesis states that NTDs result from a disturbance in the timely development of the vasculature. A constant nutrition supply is essential for normal embryonic development. The transition from an avascular to a vascular organism is normally accomplished during the fourth postconceptional week. The neural system has a very prolific growth during the prevascular stage and is therefore the first to outgrow its nutrient supply. As both *SOX18* and *BMP4* are implicated in the establishment of a vascular network, there might be a vascular basis for NTDs [136,137].

An important shortcoming of our study is the fact that we only had access to leukocyte DNA for assessment of methylation. We do not know whether differential methylation of the same gene set would be observed in brain or spinal cord tissue of MMC patients. But concordant methylation alterations in brain and blood suggest that blood methylation might be representative for brain methylation [112,113,141,142]. It is known that DNA methylation in blood is significantly more variable than DNA methylation in brain tissues [141]. Horvath et al. [142] and Farré et al. [141] identified an epigenetic signature of age that is not related to cell type composition and that does not require a correction for cellular heterogeneity. This is an interesting finding, as until now there was still no clear evidence that epigenetic marks of different cell types respond in a similar way to environmental influences. The sample size of our genome-wide study was small, but the reproducibility of significant hypomethylation of the top CpGs in a much larger cohort suggests that the application of two pipelines to analyse the HM450k dataset was a good strategy.

4.6 Conclusion

This is the first study that investigates genome-wide DNA methylation in leukocytes in patients with NTDs. We report *SOX18* as novel risk gene for NTDs but our findings also suggest that *SOX18* hypomethylation and increased expression must interplay with other environmental and (epi)genetic factors that are causative for NTDs. Therefore further studies should focus on a gene discovery design for MMC that includes both DNA methylation and next generation sequencing approaches. It is possible that gene variants in combination with changes in methylation are more prone to result in a multifactorial disease as spina bifida.

CHAPTER 5

Genome-wide DNA methylation in patients with Pseudohypoparathyroidism

Published paper
Anne Rochtus, Alejandro Martin-Trujillo, Benedetta Izzi, Francesca M Elli, Intza Garin, Agnes Linglart, Giovanna Mantovani, Guiomar Perez de Nanclares, Suzanne Thiele, Brigitte Decallonne, Chris Van Geet, David Monk, Kathleen Freson. *Genome-wide DNA methylation analysis of pseudohypoparathyroidism patiens with GNAS imprinting defects.*
Clinical Epigenetics. Jan 26 2016; 8:10.

Context of the study

Analyzing HM450k data is complex and data processing and interpretation need to be given particular consideration and care [83]. In order to acquire knowledge in the technical and analytical aspects of the HM450k arrays, I received a Short-Term Scientific Mission grant (within the framework of the COST–BM1209 project: European Network of congenital imprinting disorders) to visit the lab of Prof. D. Monk in the laboratory of Genomic Imprinting and Cancer at IDIBELL in Barcelona, Spain. During this research visit, I analyzed the data of the HM450k BeadChip performed to study the imprinting disease pseudohypoparathyroidism. Patient samples and their clinical data were already available for this study and the array processing of the HM450k was performed by the Genome Centre (Bart's and the London School of Medicine and Dentistry, Londen, UK). I also did locus-specific validation studies with the Sequenom EpiTYPER for this study. Obtained expertise in data analysis and filtering was used for this doctoral thesis.

5.1 Abstract

Background: Pseudohypoparathyroidism (PHP) is caused by (epi)genetic defects in the imprinted *GNAS* cluster. Current classification of PHP patients is hampered by clinical and molecular diagnostic overlap. The European Consortium for the study of PHP designed a genome-wide methylation study to improve molecular diagnosis.

Methods: The HumanMethylation 450K BeadChip was used to analyze genome-wide methylation in 24 PHP patients with parathyroid hormone resistance and 20 age- and gender-matched controls. Patients were previously diagnosed with *GNAS*-specific differentially methylated regions (DMRs) and include 6 patients with known *STX16* deletion ($PHP^{\Delta stx16}$) and 18 without deletion (PHP^{neg}).

Results: The array demonstrated that PHP patients do not show DNA methylation differences at the whole genome level. Unsupervised clustering of *GNAS*-specific DMRs divides $PHP^{\Delta stx16}$ versus PHP^{neg} patients. Interestingly, in contrast to the notion that all PHP patients share methylation defects in the *A/B* DMR while only $PHP^{\Delta stx16}$ patients have normal *NESP, GNAS-AS1 and XL* methylation, we found a novel DMR (named *GNAS-AS2)* in the *GNAS-AS1* region that is significantly different in both $PHP^{\Delta stx16}$ and PHP^{neg}, as validated by Sequenom EpiTYPER in a larger PHP cohort. The analysis of 58 DMRs revealed that 8/18 PHP^{neg} and 1/6 $PHP^{\Delta stx16}$ patients have multi-locus methylation defects. Validation was performed for *FANCC* and *SVOPL* DMRs.

Conclusions: This is the first genome-wide methylation study for PHP patients that confirmed that *GNAS* is the most significant DMR, and the presence of *STX16* deletion divides PHP patients in 2 groups. Moreover, a novel *GNAS-AS2* DMR affects all PHP patients and PHP patients seem sensitive to multi-locus methylation defects.

5.2 Introduction

Genomic imprinting is a parent-of-origin dependent gene expression that is essential for mammalian development. A mechanism underlying allele-specific expression is DNA methylation. The addition of a methyl group to DNA cytosine nucleotides at CpG sites can occur in an allele-specific manner, and allele-specific methylation in imprint control regions (referred to as differentially methylated regions, DMR) is associated with parent-of-origin dependent gene expression. Imprinting disorders are a group of rare diseases affecting growth, development and metabolism, that are associated with (epi)genetic disruption of imprinting genes [66]. Pseudohypoparathyroidism (PHP) is a rare endocrine disorder that can be caused by genetic or epigenetic alterations in the imprinted cluster *GNAS* localized on chromosome 20q13.3 [143]. The human *GNAS* locus harbors four DMRs encompassing the promoters of four alternative transcripts: exon A/B (*GNAS-A/B*: TSS DMR = ***A/B***), GNAS antisense (*GNAS-AS1*: TSS DMR = ***AS1***), extra-large stimulatory G protein (*GNAS-XL*: Ex1 DMR = ***XL***) and neuroendocrine secretory protein 55 (*GNAS-NESP*: TSS DMR = ***NESP***) (Figure 1A) [144]. PHP type I (PHP1A and PHP1B) patients are characterized by end-organ resistance to the action of the parathyroid hormone (PTH), which leads to hypocalcemia, hyperphosphatemia and elevated levels of PTH in absence of vitamin D deficiency. They often also have thyroid stimulating hormone (TSH) resistance [143,144]. PHP1A patients have in addition to hormone resistance clinical features collectively referred to as Albright's Hereditary Osteodystrophy (AHO) that include brachydactyly, short stature and round face; they may also present with obesity, subcutaneous ossifications, mental retardation and behavior problems [145,146]. PHP1A is caused by heterozygous maternally inherited inactivating mutations in the coding sequence of Gsα (exons 1 to 13 of *GNAS*) [143,144,147]. On the other hand, paternally inherited inactivating mutations lead to pseudopseudohypoparathyroidism (PPHP), characterized by AHO features but without hormone resistance [143,144,147]. Most patients affected with the PHP1B form of the disease exhibit mainly PTH resistance and subclinical TSH resistance and do not have AHO features. In some cases however, typical brachydactyly, severe obesity [148] and congenital hypothyroidism [149,150] have been described in PHP1B patients highlighting the overlap between PHP1A and PHP1B. All PHP1B patients have methylation abnormalities in the *GNAS* cluster with loss of imprinting at the *A/B* DMR [147]. The familial form of PHP1B (often referred to

as autosomal dominant AD-PHP1B) is typically associated with microdeletions in the *STX16* region located upstream of the *GNAS* cluster [151-154] and less frequently with deletion removing the *NESP* DMR [155]. On the other hand, sporadic PHP1B patients have broad *GNAS* methylation defects that involve all four *GNAS* DMRs without a known underlying genetic cause [143,144,147].

However, from recent data, it becomes clear this original PHP classification is no longer accurate for the following four reasons: i) broad *GNAS* methylation defects were also found for PHP1B patients with an AHO phenotype [148,156-158], (ii) the degree of the methylation defect seems not to correlate with the disease severity [159], iii) reduced Gsα activity is no longer exclusive for PHP1A with inactivating mutations but recently also was described for PHP patients with epigenetic defects [160,161] and iv) partial *GNAS* methylation defects have been described [162]. Moreover, as shown for other imprinting disorders, such as Silver-Russell or Beckwith-Wiedemann syndrome, also some PHP1B patients were shown to have multi-locus imprinting defects as studied by a targeted approach that comprised known imprinted loci [163-165]. Therefore, there is a strong need to improve the current classification of PHP patients that might be feasible based on more detailed (epi)genetic or clinical data using larger patient cohorts analyzed with more powerful techniques. The European Consortium for the study of PHP (EuroPHP) designed the present genome-wide methylation study to gain insight in epigenetic profiles that might improve an epigenetic-based classification. We have analyzed the methylomes of 24 previously diagnosed PHP patients with *GNAS* epigenetic defects recruited from 5 European centers. This sample set includes 6 patients with the *STX16* 3-kb recurrent microdeletion ($PHP^{\Delta stx16}$) [152] and 18 without any identified deletion within the *GNAS* locus (PHP^{neg}). The following analyses were performed i) changes in DNA methylation at the genome-wide level, ii) unsupervised cluster analysis for the *GNAS* locus and comparisons with previous *GNAS* methylation data used for PHP diagnosis and iii) detailed DNA quantification analysis for other imprinted DMRs. DNA methylation data were validated with the Sequenom EpiTYPER for additional PHP patients with PTH resistance and proven epigenetic defects.

A.

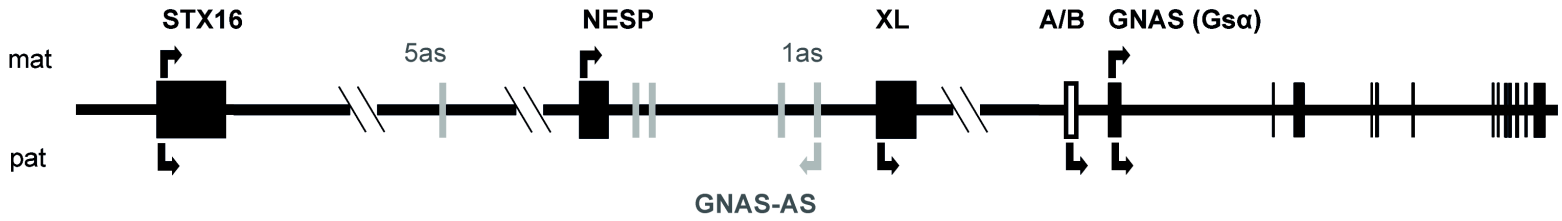

B.

	This study		LAB 1	LAB 2	LAB 3	LAB 4	LAB 5	LAB 5
	450K BeadChip	*Sequenom EpiTYPER*	*Sequenom EpiTYPER*	*Pyrosequencing*	*MLPA*	*Pyrosequencing*	*MLPA*	*Pyrosequencing*
NESP	Chr20:57414039-57418612	/	Chr20:57415104-57415451	/	Chr20:57415673-57415972	Chr20:57415718-57415832	Chr20:57414760-5741592	Chr20:57415470-57415853
GNAS-AS	Chr20:57425649-57428033 (GNAS-AS1)	Chr20:57427572-57428023 (GNAS-AS2)	/	/	Chr20:57426653-57426945	Chr20:57426696-57426916	Chr20:57425849-57426057	Chr20:57426730-57426801
XL	Chr20:57428905-57431463	/	Chr20:57430892-57431270	/	Chr20:57429173-57429469	Chr20:57429167-57429304	Chr20:57429259-57430253	Chr20:57429113-57430411
A/B	Chr20:57463265-57465201	/	Chr20:57464928-57465295	Chr20:57464773-57464823	Chr20:57463553-57463848	Chr20:57463531-57463749	Chr20:57463711-57464627	Chr20:57463686-57464627

C.

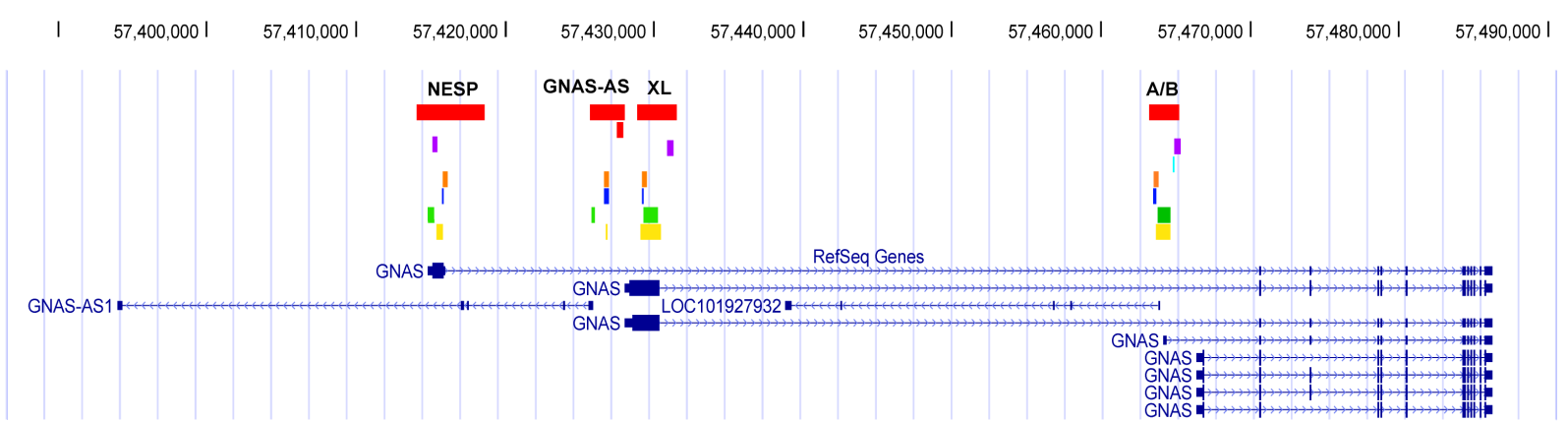

Figure 1. Human *GNAS* cluster. A. Schematic diagram of the human *GNAS* cluster with DMRs *A/B*, *XL*, *GNAS-AS and NESP* and the upstream *STX16* gene region. The arrows show initiation and direction of transcription for maternal (mat) and paternal (pat) derived transcripts. **B.** Overview of the different *GNAS* methylation studies that were performed for 24 PHP patients in this study using the HM450k and Sequenom EpiYTPER and previously, by 5 different European centers using the specified techniques and loci. **C.** Detailed schematic representation of the 4 *GNAS*-DMRs investigated by the different European laboratories and the consortium. Nucleotide positions are indicated according to NCBI build 37/hg19.

Table 1: Clinical and molecular characteristics of the PHP patients enrolled in the genome-wide DNA methylation study.

1. Clinical characteristics									2. Initial diagnostic screening							3. HM450k				
Patient	Gender	PTH-res	TSH-res	Ca↓	P↑	OS	BD	Additional features	STX16	LAB	Label	NESP	AS	XL	A/B	NESP	AS1	AS2	XL	A/B
1	F	yes	yes	yes	yes	no	no	Two café-au-lait spots, autoimmune thyroiditis		4	Full PHP1B - broad	94	7	27	3	90**	10**	8**	34*	13**
2*	M	yes	yes	yes	yes	no	no			3	Full PHP1B - broad	80	7	8	2	89**	10**	8**	6**	12**
3	M	yes		yes	yes	no	no	Von Willebrand disease		5	Full PHP1B - broad	88	4	6	0	88**	10**	8**	7**	13**
4*	M	yes	no	yes	yes	no	no			1	Full PHP1B - broad	92		8	7	89**	10**	8**	7**	13**
5*	M	yes	no	yes	yes	no	no			3	Full PHP1B - broad	82	7	8	2	89**	9**	8**	7**	12**
6	F	yes	no	yes	yes	no	no			1	Full PHP1B - broad	92		10	9	89**	9**	7**	5**	12**
7	M	yes	no	yes	yes	no	no	Bilateral cryptorchidism, osteopenia of hands, behaviour problems		4	Full PHP1B - broad	95	5	4	3	89**	9**	8**	5**	12**
8*	F	yes		yes	no	no	yes			5	Full PHP1B - broad	90	3	4	0	89**	10**	8**	6**	12**
9	F	yes	yes	yes	no		no	Enchondromatosis		5	Partial PHP1B -broad	83	23	34	33	63	27	23	24*	35
10	F	yes	no	yes	yes	no	yes	Exostosis		4	Partial PHP1B -broad	84	20	24	13	75*	22*	16**	33*	31
11	F	yes								5	Partial PHP1B -broad	80	10	27	14	78*	23*	19*	34*	28
12*	M	yes	yes	yes	no	no	no	Severe hypertension with organ damage, hypercalciuria		3	Full PHP1B - broad	77	8	8	3	75*	12**	8**	7**	17**
13*	F	yes	yes	yes	yes	no	yes			3	Partial PHP1A -broad	76	8	7	5	73*	15**	9**	5**	21*
14*	M	yes	yes	yes	no	no	no			3	Partial PHP1B -broad	80	10	19	29	76*	19**	13**	30*	21*
15	F	yes	yes	yes	yes	yes	no	Langerhans cell histiocytosis, neonatal hydrocephaly, sessile exostosis		4	Partial PHP1A -broad	86	18	18	7	81**	18**	15**	32*	21*
16	F	yes	yes	yes	yes	no	no	Fahr's syndrome (calcifications of basal ganglia), autoimmune thyroiditis		4	Partial PHP1B -broad	91	12	30	7	85**	17**	16**	43	21*
17	F	yes	no	yes	no	no	no		ΔSTX16	3	PHP1B - A/B only	42	36	44	6	46	36	16**	45	14**
18*	F	yes	yes	no	no				ΔSTX16	2	PHP1B - A/B only	-	-	-	4	50	37	14**	47	14**
19	M	yes	yes	yes	yes	yes	no	Calcifications of basal ganglia	ΔSTX16	4	PHP1B - A/B only	49	42	52	3	50	41	18**	48	15**
20	F	yes	no	yes	yes	no	yes		ΔSTX16	1	PHP1B - A/B only	39	-	36	10	50	40	16**	50	15**
21	M	yes	yes	no	yes				ΔSTX16	2	PHP1B - A/B only	-	-	-	4	52	41	16**	51	13**
22	M	yes	no	yes	no	no	no		ΔSTX16	1	PHP1B - A/B only	29	-	38	14	53	42	14**	51	14**
23*	F	yes	no	yes	yes	no	no			3	Partial PHP1B -broad	54	26	30	7	55	36	26	40	41
24	M	yes	no	yes	yes	no	no	Severe osteopenia without ossifications		5	Partial PHP1B -broad	70	35	46	44	57	39	34	41	43
																50 ± 7	46 ± 7	39 ± 7	50 ± 4	51 ± 9

Table 1: Clinical and molecular characteristics of the PHP patients enrolled in the genome-wide DNA methylation study. From left to right: 1) clinical characteristics; 2) mean methylation values of *GNAS* studies that were performed previously by 5 different European centers as described in figure 1; 3) mean methylation values of *GNAS* investigated with HM450k. Ordering of the patients according to unsupervised hierarchical clustering of *GNAS* methylation investigated with HM450k. Patients* have methylation changes at imprinted genes other than *GNAS*. Methylation values are presented as %. BD: brachydactyly; Ca: calcium; F: female; LAB: laboratory of initial diagnostic screening, annotation as shown in figure 1; M: male; OS: heterotopic ossifications; P: phosphate; PTH-res: Parathyroid hormone resistance; TSH-res: Thyroid-stimulating hormone resistance; ΔSTX16: patients with underlying *STX16* deletion. * methylation < or > than 3SD outside the mean of the controls; ** methylation < or > than 3SD outside the mean of the controls and < 0.20 or > 0.80 absolute methylation. Mean ± SD of the 20 controls from the HM450k array is shown below the HM450k columns.

5.3 Materials and methods

Patient samples

A total of 61 PHP patients were enrolled by 5 different endocrinology centers from the European PHP Consortium. The molecular diagnosis for PHP was performed by each center using the methylation detection assay for the *GNAS* DMRs as previously described with methodologies and the location of the studied amplicons in Figure 1 and Table 1 [162]. All PHP patients included in this study have PTH resistance and were labeled with PHP1A if an obvious AHO phenotype was present (only brachydactyly and subcutaneous ossifications were noticed, Table 1). Based on the genetic screening for *STX16* deletions and *GNAS* methylation screening, laboratories were asked to label the patients with: i) *STX16* deletion present or not, ii) AB-only or broad methylation defect and iii) full or partial methylation defect [162]. This resulted in the use of the following labels (Table 1): PHP1B - A/B only, full PHP1B - broad, partial PHP1B - broad and partial PHP1A - broad. These terms are based on the original classification used for patients with PHP type I.

Table 1 presents the patients for the genome-wide study and Table 2 the patients for the replication studies. The order of the patients in Table 1 was determined by unsupervised cluster analysis of genome-wide data for only the *GNAS* locus. The total number of PHP patients that were enrolled for the HumanMethylation 450K (HM450k) array and Sequenom studies are specified in Table 2. Shortly, the genome-wide DNA methylation study was performed for 24 PHP patients and 20 age- and gender-matched healthy controls (Table 1). Validation of *NESP-AS2* was performed for 42 PHP patients and 20 controls. Validation of the methylation levels of *FANCC, SVOPL* and *WDR27* was performed in 26 PHP patients and 12 controls.

Table 2: Number of PHP patients enrolled in the genome-wide and Sequenom EpiTYPER validation studies.

	HM450k	Sequenom EpiTYPER			
Patients		WDR27	SVOPL	FANCC	NESP-AS
STX16 del	6	5 (3)	5 (3)	5 (3)	20 (3)
no-STX16 del	18	21 (3)	21 (3)	21 (3)	22 (3)
all	24	26 (6)	26 (6)	26 (6)	42 (6)
Controls	20	12 (2)	12 (2)	12 (2)	20 (10)

Patients are divided in two groups based on the presence or absence of STX16 deletion. Patients included in both the genome-wide study and the locus-specific validation study with Sequenom EpiTYPER are indicated between brackets.

Informed consent for methylation and genetic studies was obtained from all participants and/or their legal representatives after approval of these studies by local Ethical Committees.

Genome-wide methylation profiling using the HM450k array

Genomic DNA was extracted from leukocytes using standard techniques and bisulfite converted using the EZ DNA methylation kit (Zymo Research, Irvine CA) as previously described [116]. The array was performed by the Genome Centre (Bart's and the London School of Medicine and Dentistry, Londen, UK) on the HumanMethylation 450K BeadChip (Illumina) using manufacturer's reagents and protocols. An identical control sample was assigned to each batch and samples were distributed randomly to control for batch effects. The correlation for the internal quality control was high (> 0.99). The methylation level (β-value) was calculated using the Methylation Module of BeadStudio software.

HM450k data filtering and genome-wide analysis

After normalization of the data using GenomeStudio software, data were analyzed using a pipeline developed within the R statistical analysis environment (http://www.r-project.org, Bioconductor, Seattle, USA). Before analyzing the data, we excluded possible sources of technical bias. Probes with a high detection value (p>0.01) in more than 10% of the samples (644 probes) and probes containing any missing values (13194 probes) were removed, as well as non-CpG and gender matched probes. Finally, we excluded probes as they contained SNPs present in >1% of the population and leukocyte-specific probes [166,167]. In total, we analyzed

355105 probes for all DNA samples (73% of probes). No statistical batch control was required as all the cases and controls had been processed in the same time and correlation for the quality control was high (> 0.99). The mean methylation and standard deviation were determined for the control population and individual samples. We did not detect any differentially methylated DMRs between the 20 control samples. DNA samples from imprinting syndrome patients were considered epimutated if the methylation value for an imprinted DMR differed was outside 3 standard deviations from the 20 control samples. Cluster analysis was performed within the R statistical analysis environment.

HM450k data filtering for analysis of imprinted genes

We analyzed 58 imprinted DMRs that also included the DMRs of the *GNAS* cluster (Table 3). The list was based on the known imprinted DMRs from the consensus list from the European Network of Human Congenital Imprinting Disorders (http://www.imprinting-disorders.eu). In addition, we included novel human imprinted DMRs from recent research that combined whole-genome bisulfite sequencing with HM450k to generate methylation profiles [168] as well as four novel candidate DMRs (*GLP2R, JAKMIP1, LOC100130522/PARD6G-AS1, SVOPL*) from research using genome-wide methylation profiling with HM450k in patients with multilocus methylation defects [169]. These regions have not yet been further characterised to determine SNP vs parental-origin methylation and tissue profile. Some DMRs of the list are secondary DMRs (i.e. *DIRAS3*:Ex2-DMR, all the *SNRPN* DMRs).

Table 3: Location of 58 human imprinted DMRs investigated in this study.

Imprinted DMR	Chr	Start	End	Methylation origin	Germline derived	Associated disease
PPIEL:Ex1-DMR	1	40024626	40025540	M	Oocyte gDMR	MLID
DIRAS3:Ex2-DMR	1	68512505	68513486	M	Oocyte gDMR	MLID
DIRAS3:TSS-DMR	1	68515433	68517545	M	Oocyte gDMR	MLID
GPR1-AS:TSS-DMR	2	207066967	207069445	M	Oocyte gDMR	
ZDBF2/GPR1:IG-DMR	2	207114583	207136544	P	Sperm gDMR-secondary DMR	
JAKMIP1	4	6107021	6107339			
NAP1L5:TSS-DMR	4	89618184	89619237	M	Oocyte gDMR	MLID
VTRNA2-1:DMR	5	135414802	135416645	M	Oocyte gDMR	
FAM50B:TSS-DMR	6	3849082	3850359	M	Oocyte gDMR	MLID
PLAGL1:alt-TSS-DMR	6	144328078	144329888	M	Oocyte gDMR	TNDM; MLID

IGF2R:Int2-DMR	6	160426558	160427561	M	Oocyte gDMR	MLID
WDR27:Int13-DMR	6	170054504	170055618	M	Oocyte gDMR	MLID
GRB10:alt-TSS-DMR	7	50848726	50851312	M	Oocyte gDMR	MLID
PEG10:TSS-DMR	7	94285537	94287960	M	Oocyte gDMR	MLID
MEST:alt-TSS-DMR	7	130130122	130134388	M	Oocyte gDMR	MLID
SVOPL	7	138348774	138349443			
HTR5A:TSS-DMR	7	154862719	154863382	M	Oocyte gDMR	
ERLIN2:Int6-DMR	8	37604992	37606088	M	Oocyte gDMR	MLID
PEG13:TSS-DMR	8	141108147	141111081	M	Oocyte gDMR	MLID
FANCC:Int1-DMR	9	98075400	98075744	M	Oocyte gDMR	MLID
INPP5F:Int2-DMR	10	121578046	121578727	M	Oocyte gDMR	
H19/IGF2:IG-DMR	11	2018812	2024740	P	Sperm gDMR	SRS/BWS
IGF2:Ex9-DMR	11	2153991	2155112	P	No-secondary DMR	SRS/BWS
IGF2:alt-TSS-DMR	11	2168333	2169768	P	Sperm gDMR	SRS/BWS
KCNQ1OT1:TSS-DMR	11	2719948	2722259	M	Oocyte gDMR	BWS (rare Sotos syndrome)
RB1:Int2-DMR	13	48892341	48895763	M	Oocyte gDMR	
MEG3/DLK1:IG-DMR	14	101275427	101278058	P	Sperm gDMR	TS14/KOS14
MEG3:TSS-DMR	14	101290524	101293978	P	No-secondary DMR	TS14/KOS14
MEG8:Int2-DMR	14	101370741	101371419	M	No-secondary DMR	
miR 4508/	15	23807086	23807592			
MKRN3:TSS-DMR	15	23807086	23812495	M	Oocyte gDMR-secondary DMR	
MAGEL2:TSS-DMR	15	23892425	23894029	M	No-secondary DMR	
NDN:TSS-DMR	15	23931451	23932759	M	No-secondary DMR	
***SNRPN* intragenic CpG32**	15	24346736	24347142			
***SNRPN* intragenic CpG29**	15	24671872	24672679			
***SNRPN* intragenic CpG30**	15	24722753	24723071			
***SNRPN* intragenic CpG40**	15	25017924	25018886			
SNRPN:alt-TSS-DMR	15	25068564	25069481	M	No-secondary DMR	
SNRPN_2	15	25093008	25093829			
SNRPN_3	15	25123027	25123905			
SNURF:TSS-DMR	15	25200004	25201976	M	Oocyte gDMR	PWS/AS
IGF1R:Int2-DMR	15	99408496	99409650	M	Oocyte gDMR	
ZNF597:3' DMR	16	3481801	3482388	M	Oocyte gDMR	
ZNF597:TSS-DMR	16	3492828	3494463	P	No-secondary DMR	
GLP2R	17	9729250	9729424			
LOC100130522/PARD6G-AS1	18	77905355	77905947			
ZNF331:alt-TSS-DMR1	19	54040510	54042212	M	Oocyte gDMR	MLID
ZNF331:alt-TSS-DMR2	19	54057086	54058425	M	Oocyte gDMR	
PEG3:TSS-DMR	19	57348493	57353271	M	Oocyte gDMR	MLID
MCTS2P:TSS-DMR	20	30134663	30135933	M	Oocyte gDMR	MLID
NNAT:TSS-DMR	20	36148604	36150528	M	Oocyte gDMR	
L3MBTL1:alt-TSS-DMR	20	42142365	42144040	M	Oocyte gDMR	MLID
GNAS-NESP:TSS-DMR	20	57414039	57418612	P	No-secondary DMR	PHP
GNAS-AS1:TSS-DMR	20	57425649	57428033	M	Oocyte gDMR	PHP

GNAS-XL:Ex1-DMR	20	57428905	57431463	M	Oocyte gDMR	PHP
GNAS A/B:TSS-DMR	20	57463265	57465201	M	No-secondary DMR	PHP
WRB:alt-TSS-DMR	21	40757510	40758276	M	Oocyte gDMR	MLID
NHP2L1:alt-TSS-DMR	22	42077774	42078873	M	Oocyte gDMR	MLID

Nucleotide positions accord to NCBI build 37/hg19. The list is based on both known and novel imprinted DMRs. Novel imprinted DMRs are indicated in **bold**. DMR: differentially methylated region; M: maternally derived methylation; P: paternally derived methylation; gDMR: germline DMR; PHP = Pseudohypoparathyroidism; SRS: Silver Russell syndrome; BWS: Beckwith Wiedemann syndrome; AS: Angelman syndrome; PWS: Prader Willi syndrome; MLID: Multi-locus imprinting disturbance; TS14: Temple syndrome; KOS14: Kagami-Ogata syndrome; TNDM: Transient Neonatal Diabetes.

Validation of NESP-AS2 and FANCC, SVOPL, WDR27 methylation using the Sequenom EpiTYPER

Leukocyte DNA (1 µg) was subjected to bisulfite treatment using the MethylDetector^{TM} bisulfite modification kit (Active Motif, Carlsbad CA, USA) as we described [97,98,116,162,168]. The Sequenom MassARRAY (Sequenom, San Diego, CA, USA) was used for quantitative DNA methylation analysis of the CpGs within the amplicons of *FANCC, SVOPL* and *WDR27* using conditions described. Long cycling incubation was applied to further optimize the conversion reaction [99]. Primers were designed using the Sequenom EpiDesigner BETA software (www.epidesigner.com), taking into account amplicon coverage, number of CpGs, fragment size and number of nucleotide repeats in the primer sequence. PCR steps were performed in triplicate for each DNA sample and a standard deviation between replicates was mostly <10%. When triplicate measurements had a SD >10% or when only one of the triplicates was available, data for that sample were excluded. The mean of 3 values was used for further analyses. The EpiTYPER analysis method reports CpG methylation values as percentage. Statistical analyses to quantify DNA methylation differences were performed using the Prism 6 software (GraphPad Software Inc., San Diego). DNA samples from PHP patients were considered epimutated if the methylation value for an imprinted DMR was outside two and three standard deviations determined from the control samples. A two-tailed T-test was used to assess differences in mean DNA methylation levels between cohorts for the overall amplicon considered as methylation average and for each CpG unit within this amplicon separately.

GNAS molecular analysis

Genomic DNA was isolated from leukocytes. Genotype for the GNAS exon 5 SNP (rs7121) at codon 131 was determined by PCR with the forward primer 5'-ttggtagcgccctcccaggc-3' and the reverse primer 5'- catgttcctatatggacactg-3'. After denaturation at 95°C, 40 cycles of DNA amplification were performed using Taq PCR Mastermix at 95°C for 30 s, 58°C for 60 s, and 72°C for 60 s. The PCR products were digested using the restriction enzyme FokI and analyzed on a 2% agarose gel. Only samples heterozygous at FokI polymorphism were selected. One patient and one control were heterozygous. Total RNA was extracted from platelets using TRIzol (Invitrogen) reagent, according to the manufacturer's protocol. The *GNAS* gene was amplified from platelet RNA to check expression of *XL*.

5.4 Results

Genome-wide DNA methylation analysis for PHP patients

The Illumina Infinium HumanMethylation 450K BeadChip (HM450k) was used to determine genome-wide DNA methylation profiles in 24 PHP patients and 20 age- and gender-matched healthy controls. Table 1 presents the clinical characteristics of the PHP patients that all have PTH resistance and hypocalcemia. Mild AHO features were only present in patients 8, 10, 13, 15 and 20. All 24 PHP patients were previously diagnosed with a *GNAS* epigenetic defect using different methodologies (Figure 1B/C) and methylation values for the different *GNAS* DMRs obtained by these assays are shown in Table 1. We have included 6 PHP patients with a deletion of the *STX16* region upstream of *GNAS* and hypomethylation of the *A/B* DMR only (referred to as $PHP^{\Delta stx16}$) and 18 PHP patients without the deletion and full or partial methylation defects in *A/B, XL, AS1* and *NESP* DMRs (referred to as PHP^{neg}) (Table 1). Hierarchical cluster analysis of all CpGs according to the different subtypes $PHP^{\Delta stx16}$, PHP^{neg} or control (Figure 2A) and unsupervised hierarchical clustering analysis of the data (Figure 2B) showed that the samples are clustered irrespective of the subgroup, suggesting that there are no subgroup differences at whole genome level. To further exclude a global methylation defect in PHP patients, we also analyzed the methylation of DNA repetitive elements (*LINE-1* and *LINE-2*) that again showed no differences between patients and controls (data not shown).

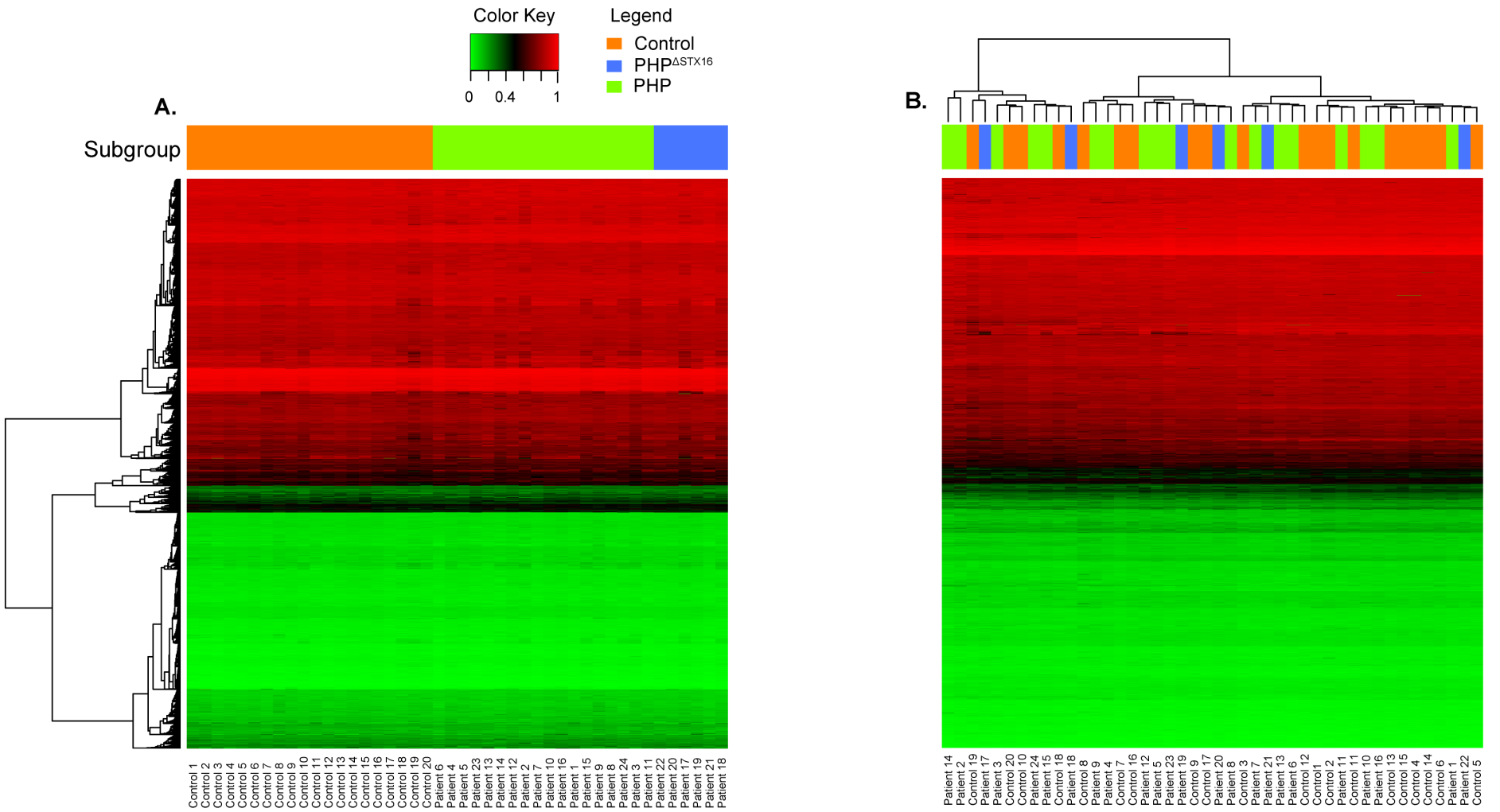

Figure 2. Whole genome methylation in PHP patients vs. controls. Methylation values are extracted from data obtained with the HM450k. A) Clustering according to different subgroups. B) Unsupervised hierarchical clustering analysis of the subgroups. Control: controls; $PHP^{\Delta STX16}$: patients with underlying *STX16* deletion; PHP: patients without known genetic deletion. Heatmaps represent 3575 randomly selected CpGs (1% total CpGs).

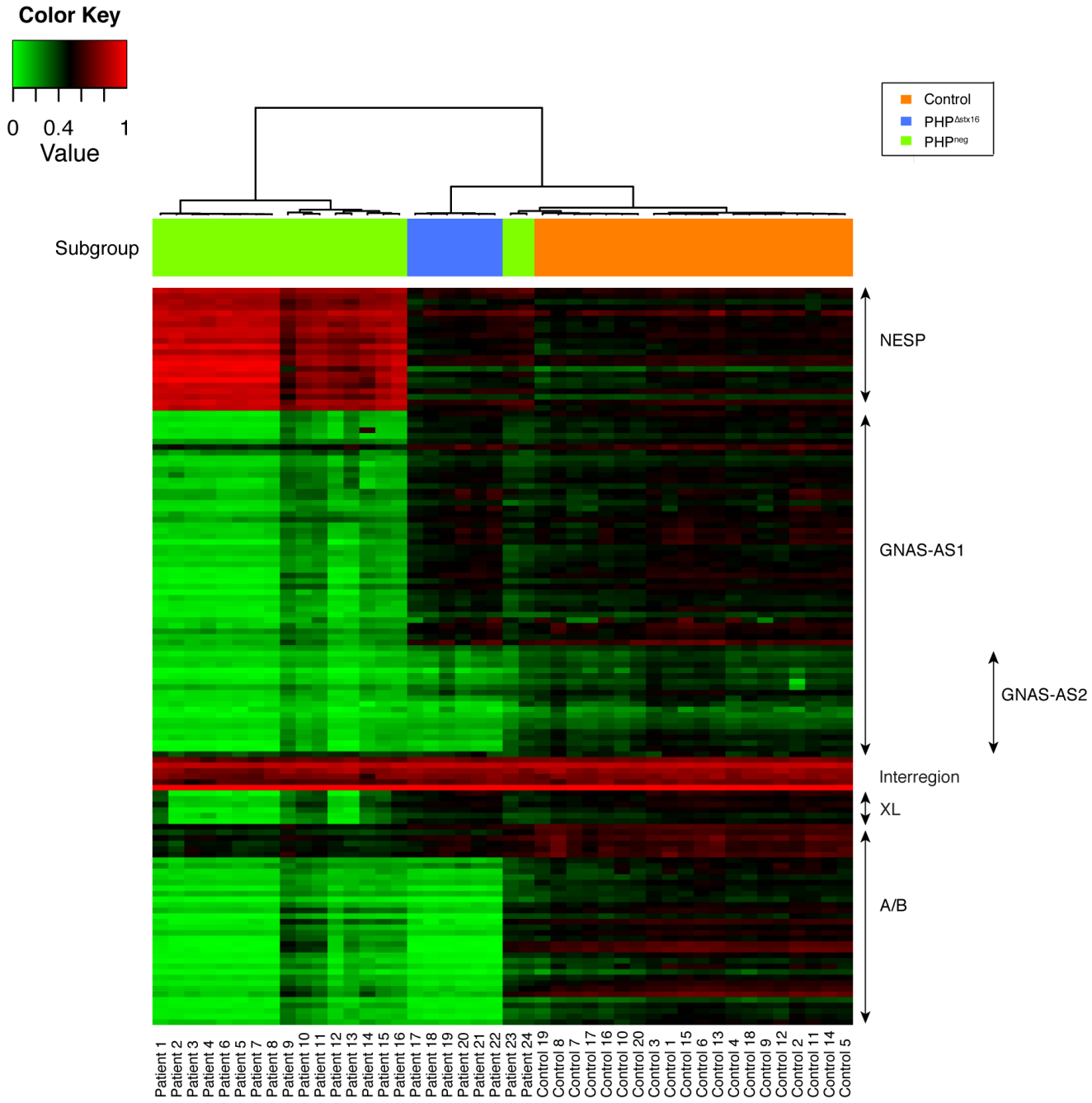

Figure 3. Unsupervised hierarchical clustering of *GNAS* methylation in PHP patients. Methylation values of the individual CpGs of the 4 *GNAS* DMRs are extracted from data obtained with the HM450k. Green and red represent 0 and 1 methylation, respectively. The arrows show the different *GNAS* transcripts.

GNAS methylation analysis based on HM450k data for PHP patients

The methylation values for all CpGs located within the *GNA*S cluster were extracted from data obtained from the genome-wide methylation analysis. The HM450k contains probes mapping to 4 regions that cover the 4 *GNAS* DMRs as specified by red boxes in Figure 1C (referred to as *A/B*, *XL, AS1* and *NESP*). These regions are larger but overlap with the regions that were previously investigated by 5 European centers that have used different technologies including MS-MLPA, Sequenom EpiTYPER or pyrosequencing to quantify the methylation of the *GNAS* DMRs for the 24 PHP patients (see Figure 1C for the location of the studied regions and methodologies and Table 1 for the results for each patient). Unsupervised hierarchical cluster analysis of *GNAS* methylation data obtained from the HM450k for the 24 PHP patients divided these patients in 2 groups according to the presence/absence of *STX16* deletion ($PHP^{\Delta stx16}$ versus PHP^{neg}) (Figure 3). As known in literature [143,144] and confirming the previous diagnosis that was made by the 5 laboratories, $PHP^{\Delta stx16}$ only showed hypomethylation of DMR *A/B* while PHP^{neg} patients had abnormal methylation for all 4 *GNAS* DMRs. However, 2 PHP^{neg} patients (23 and 24) were clustered closer to the healthy control population having normal methylation values for the all *GNAS* DMRs (Table 1 and Figure 3). These patients were previously identified with a 'partial' *GNAS* methylation defect using MS-MLPA and pyrosequencing respectively. After analyzing the separate CpGs from the HM450k, no significant differences were found compared to the control population (separated CpGs are visualized in Figure 3). At the individual probe level we noticed that both patients were mosaic and patient 23 was slightly more hypomethylated than patient 24.

Interestingly, a smaller region we referred to as *AS2* within the *AS1* amplicon had significantly lower methylation values for both $PHP^{\Delta stx16}$ and PHP^{neg} patients compared to the controls (Figure 3 and Table 1). This *AS2* region does not overlap with amplicons that were previously studied for the *AS* region by MS-MLPA, Sequenom EpiTYPER or pyrosequencing by the different laboratories (Figure 1B/C). The *AS2* region is separated from *XL* by a hypermethylated region (Figure 3 and Figure 4). To confirm *AS2* hypomethylation, a validation study was developed using the Sequenom EpiTYPER to quantify methylation in the *AS2* region in 42 PHP patients with PTH resistance that were previously diagnosed with a *GNAS*

epimutation and 20 age- and gender-matched healthy controls. These 42 PHP patients include 20 PHP$^{\Delta stx16}$ and 22 PHP^{neg} patients, of which 3 patients in each group were also analyzed by HM450k array (Table 2). The 22 PHP^{neg} comprise 20 PHP1B with full or partial broad *GNAS* methylation defect and 2 PHP1B patients with isolated A/B methylation defect but having no *STX16* deletion. Significant *AS2* hypomethylation (P-value < 0.0001) was detected for both PHP$^{\Delta stx16}$ and PHP^{neg} patient groups compared to controls (Figure 5). No significant difference in *AS2* methylation was found between PHP$^{\Delta stx16}$ and PHP^{neg} patients with mean methylation values of 10% (95% CI: 7-13%) vs. 8% (95% CI: 5-11%), respectively. This suggests that the imprinting defect for this interval is not determined by the *STX16* deletion and is specific for PHP1B. To investigate if *AS2* hypomethylation changed *XL* expression, we performed *GNAS* versus *XL* mRNA expression studies using total blood mRNA from a PHP^{neg} patient and control heterozygous for *GNAS* SNP (rs7121), but we could not detect *XL* expression in blood cells.

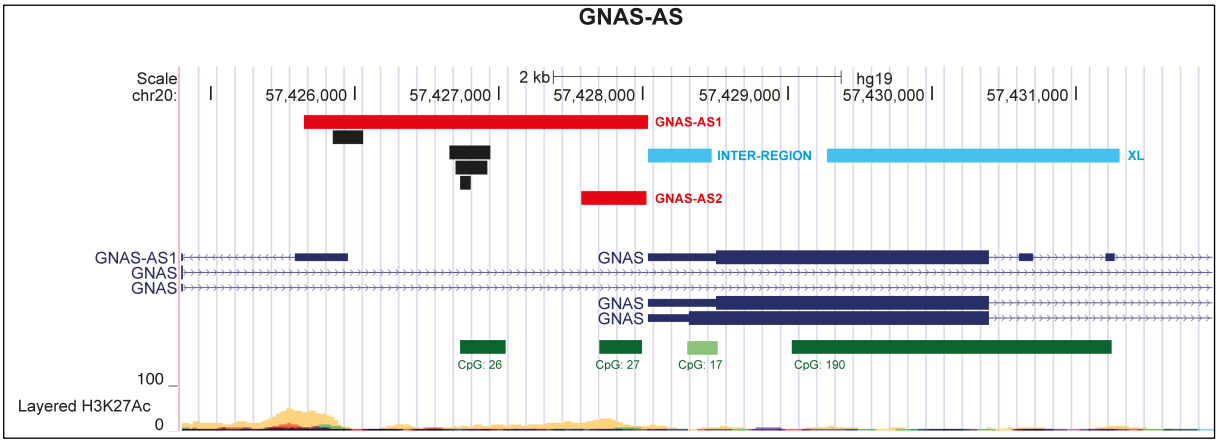

Figure 4. Detailed schematic representation of the human GNAS-AS region. Bars indicate the different *GNAS-AS* methylation studies that were performed in this study using the 450K BeadChip (GNAS-AS1) and Sequenom EpiTYPER (GNAS-AS2) and previously, by the different European centers (black bars). Nucleotide positions accord to NCBI build 37/hg19.

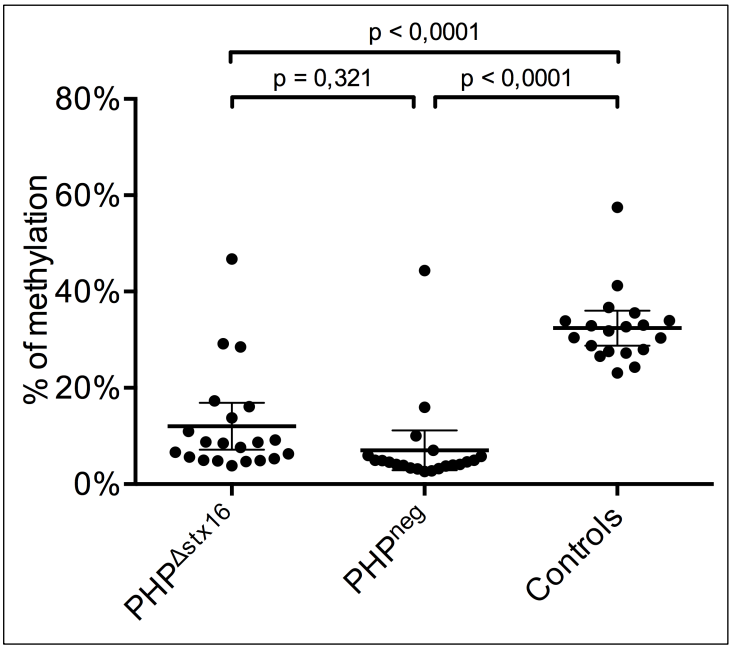

Figure 5. Scatter plot of *NESP-AS2* methylation in PHP patients and controls. Methylation values are obtained with the Sequenom EpiTYPER. Horizontal bars indicate the mean and SD of the group. PHP patients are separated according to underlying *STX16* deletion.

Methylation studies of other imprinted genes for PHP patients

As multi-locus abnormalities have also been described for PHP1B patients [164], we analysed the methylation values for all CpGs located within 58 imprinted DMRs for humans that are covered by the HM450k (Table 3). In addition to methylation abnormalities for the 4 *GNAS* DMRs, we found multi-locus methylation defects in 8 PHP^{neg} and 1 $PHP^{\Delta stx16}$ patients (Figure 6). Abnormal methylation was found for 19 of the 58 human imprinted DMRs and this included significant hypomethylation for *PPIEL:*Ex1-DMR*, DIRAS3:*Ex2-DMR*, DIRAS3:*TSS-DMR*, JAKMIP1, NAP1L5:*TSS-DMR*, FAM50B:*TSS-DMR*, SVOPL, FANCC:*Int1-DMR*, SNRPN:*alt-TSS-DMR*, IGF1R:*Int2-DMR*, LOC100130522/PARD6G-AS1, WRB:*alt-TSS-DMR*, and NHP2L1:*alt-TSS-DMR and significant hypermethylation for *ZBDF2/GPR1:*IG-DMR*, PEG13:*TSS-DMR*, RB1:*Int2-DMR*, SNRPN intragenic CpG40, SNRPN_2 and SNRPN_3. ZBDF2/GPR1:*IG-DMR hypermethylation is likely due to *GPR1-AS:*TSS-DMR hypomethylation. The *GPR1-AS*:TSS-DMR is not included in our screening, as it acquires immediate biparental methylation following implantation, therefore we can only infer loss of methylation due to hypermethylation of *ZBDF2* [170]. The clinical phenotype of the patients with multi-locus methylation abnormalities was not different from the PHP patients with *GNAS* specific epimutations (Table 1).

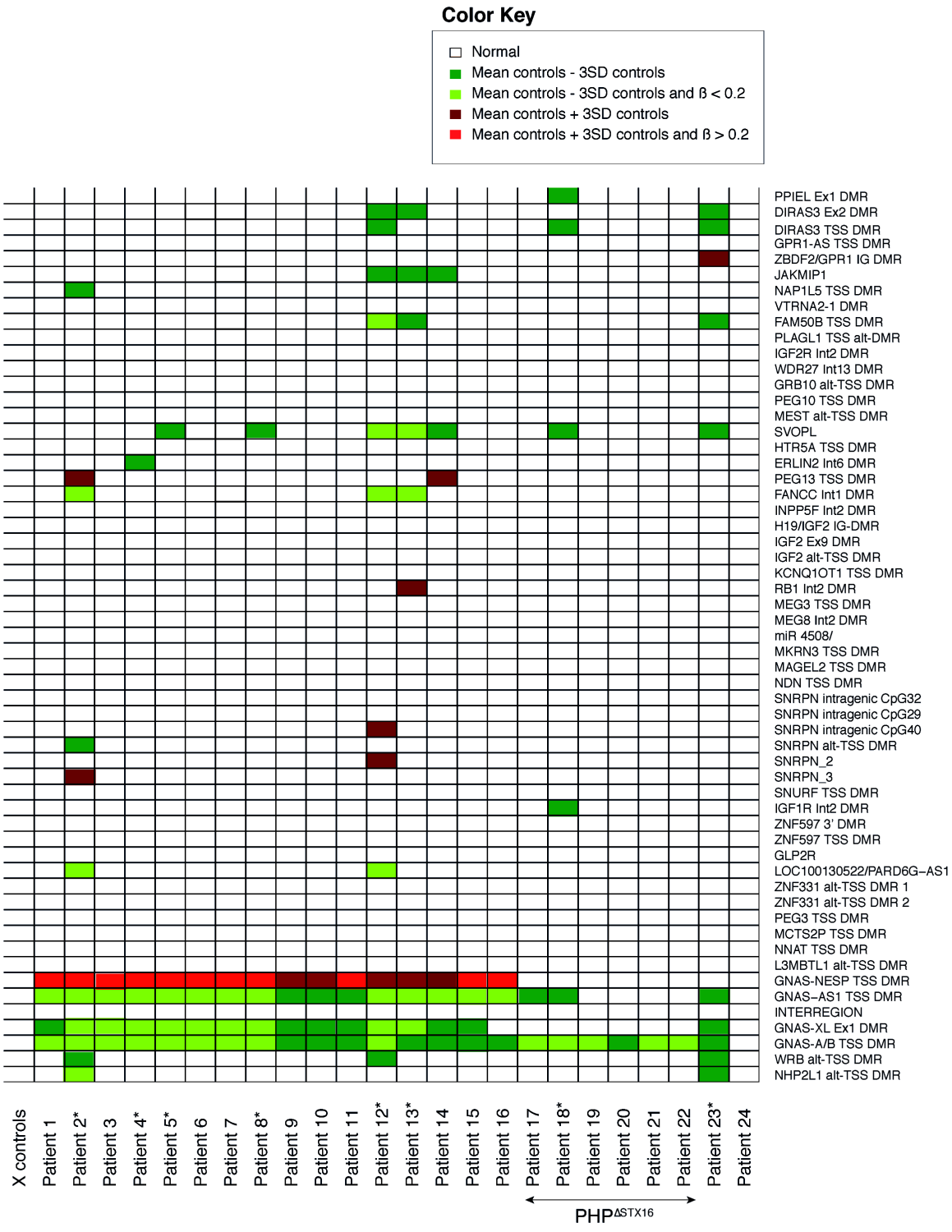

Figure 6. Heatmap showing methylation of known imprinted genes in PHP patients. Methylation values of the genes are extracted from data obtained with the HM450k. Dark green and red respresent -3SD and +3SD, respectively, of the mean as determined in 20 controls. Lighter green and red represent additional cut-offs for absolute methylation < 0.20 and > 0.80. Patients* have multi-locus methylation abnormalities. PHP$^{\Delta STX16}$: patients with underlying *STX16* deletion.

To confirm the findings of multi-locus abnormalities, we performed a validation study using the Sequenom EpiTYPER for 26 PHP patients and 12 healthy controls. We have selected *FANCC* and *SVOPL* as hypomethylation was seen in 3 and 7 PHP patients, respectively. We also validated the methylation of *WDR27* amplicon as negative control. The 26 PHP patients included 5 $PHP^{\Delta stx16}$ and 21 PHP^{neg} patients, 3 patients of each group were also analyzed by HM450k (Table 2). Eight patients had multi-locus methylation abnormalities (Figure 7). The most significant methylation difference was found for *SVOPL* in three PHP^{neg} patients.

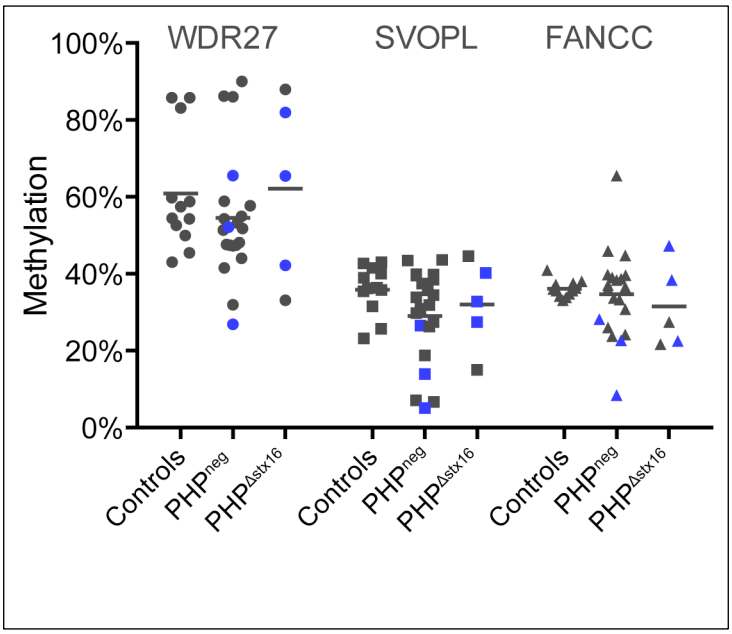

Figure 7. Scatter plot of *FANCC* and *SVOPL* methylation in PHP patients and controls. Methylation values are obtained with the Sequenom EpiTYPER. Bar indicates the mean of the group. PHP patients are separated according to underlying *STX16* deletion. Patients that were investigated with the HM450k are indicated in blue.

5.5 Discussion

Genome-wide studies to identify genetic alterations have successfully entered the field of rare diseases [171]. Similar attempts to elucidate the epigenome are expected to improve our limited knowledge about imprinting disorders (IDs). There has been a revolution in DNA methylation analysis technology over the past decade as genome-wide and entire methylomes can be characterized at single-base-pair resolution [172]. Their implementation to study IDs has only just started. A custom Illumina GoldenGate array targeting 27 imprinted DMRs has been used to study 65 patients with an ID (that include Beckwith-Wiedemann syndrome (BWS), transient neonatal diabetes mellitus (TNDM), PHP1B, Silver-Russell (SRS), Angelman syndrome (AS) and Prader-Willi syndrome (PWS)) and found multi-locus hypomethylation in patients with BWS, SRS, TNDM, and PHP1B, but not in AS and PWS [163]. Two studies have used the HM450k array to quantify genome-wide DNA methylation for BWS and TNDM [169] or SRS patients [173] and concluded that multiple and even novel imprinted genes were abnormally methylated in IDs.

Here, we have studied DNA methylation at about 485.000 CpGs genome-wide in 24 PHP patients with proven but different types of *GNAS* epimutations. The methylomes analyzed for 58 imprinted DMRs revealed in addition to the expected *GNAS* methylation defect, also a multi-locus methylation abnormality in 9 of the 24 patients for 19 other imprinted DMRs that were not previously known for these PHP cases. However, patients did not share a common pattern for these multi-locus methylation abnormalities and there was a high variability in the degree of methylation difference and the number of amplicons per patient that were abnormally methylated. A validation study with the EpiTYPER for the most common abnormally methylated DMRs *FANCC* and *SVOPL* indeed showed significant methylation differences in a replication cohort of PHP patients. The *FANCC* and *SVOPL* DMRs are not well studied and further studies are needed to define the functional relevance of these methylation changes. Though larger cohorts are needed to be conclusive, based on results from both the HM450k and the EpiTYPER study, it seems that PHP^{neg} patients are more sensitive to these multi-locus defects compared to $PHP^{\Delta stx16}$ patients. Other studies that have used targeted approaches with a limited number of known imprinted DMRs have also reported multi-locus defects in PHP patients. Perez-Nanclares et al reported the first two PHP patients with multi-locus

hypomethylation; one patient at *PEG1/MEST* and the other at *GTL2* [165]. Court et al identified five PHP patients with hypomethylation at other imprinted loci: *PEG1/MEST*, *MCTS2, IGF2R, ZNF331, L3MTBL1* and *MEG3* [163]. Maupetit-Méhouas et al studied a larger cohort of 63 PHP patients for the methylation pattern at eight imprinted loci and found multi-locus imprinting defects for 4 PHP patients at *PEG1/MEST*, *L3MBTL1* and *DLK1/GTL2* [164]. Though in our PHP cohort we observe a higher rate of multi-locus methylation defects (38% of all patients), this is probably due to the fact that more DMRs were studied but remarkably, most of these previously reported abnormal DMRs are also abnormal in our study. Docherty et al identified novel candidate imprinted genes in patients with imprinting disorders and multi-locus methylation defects [169]; we identified hypomethylation of three candidate regions (*PPIEL:*Ex1-DMR*, WRB:*alt-TSS-DMR and *NHP2L1:*alt-TSS-DMR) from this study in our patients with PHP1B. The clinical relevance of these regions has not yet been determined. It is possible that these genes are common in most imprinting disorders. Interestingly, we identified two patients with methylation changes in the *SNRPN* DMRs. These two patients also have hypomethylation of the novel candidate DMR *LOC100130522/PARD6G-AS1 [169].* Methylation changes in *SNRPN* DMRs are associated with PWS and AS, but these patients are very infrequent and moreover loss of methylation of the *SNRPN* DMR is rarely described in other imprinting disordes with multilocus methylation disturbances. It has only been observed in two patients with SRS [174], two patients with BWS [163,169] and one patient with TNDM [169]. In accordance with previous studies, our PHP patients with multi-locus methylation defects do not show evidence for phenotype differences with patients having only a *GNAS* methylation defect. Further studies including biochemical analyses are necessary to confirm these findings. The patient with the highest number of genes presenting with a methylation defect has severe hypertension with organ damage but a link with the methylation defect is not obvious. The other patients with multi-locus methylation defects have no additional clinical or molecular features. We identified five patients with simultaneous hypo- and hypermethylation. This finding is consistent with the report of Maupetit-Méhouas [164]. The epidominance hypothesis suggests that the phenotype is determined by the most strongly affected imprinted locus [164]. Patients with hypomethylation of multiple imprinted loci have been associated with increased frequency of developmental delay and congenital anomalies [175] but based on our current study,

we have no evidence for a clinical impact. Of particular interest is the fact that methylation disturbances at multiple imprinted loci are now described in a subset of patients affected with different IDs and this could point to a common pathogenic mechanism for IDs [176].

According to the original classification for PHP, we have included PHP1B patients with A/B only and partial or full broad methylation defects and PHP1A patients with a broad partial methylation defect. During the last years, it became clear for reasons specified in the introduction that this classification is no longer accurate. All CpGs from the genome-wide data within the *GNAS* cluster were analyzed using unsupervised hierarchical cluster analysis. This analysis divided our patients in two groups seemingly only dependent on having the *STX16* deletion or not (referred to as $PHP^{\Delta stx16}$ and PHP^{neg}). The studied intervals cover the 4 DMRs in *GNAS* but these loci are much larger compared to the amplicons that were previously studied by the different labs that have used MS-MLPA, Sequenom EpiTYPER or pyrosequencing (for details see Figure 1). PHP1B patients 23 and 24 that were diagnosed by MS-MLPA and pyrosequencing having a partial broad GNAS methylation defect are now clustered more closer to the control group. The most intriguing finding is however the discovery of a novel previously not described DMR (named *GNAS-AS2*) in the *GNAS* cluster that was found hypomethylated for both $PHP^{\Delta stx16}$ and PHP^{neg} patients. *GNAS-AS2* is located within the large *GNAS-AS1* region and is actually located in the promoter region of the *XL* exon 1 (Figure 4), but is separated from *XL* by a hypermethylated region. Many studies have described that PHP1B patients with *STX16* deletion only have hypomethylation of the *A/B* DMR while the DMRs *XL, GNAS-AS1* and *NESP* are normal [151-154]. This is also the case for the present HM450k data except for the CpGs that are located in the *GNAS-AS2* region. *GNAS-AS2* hypomethylation for both $PHP^{\Delta stx16}$ and PHP^{neg} patients was validated with the EpiTYPER. Only 1/24 (1 with partial PHP1B - broad) and 4/42 PHP (3 with PHP1B - A/B only and 1 with partial PHP1B - broad) patients had a normal *GNAS-AS2* methylation based on HM450k and EpiTYPER data, respectively. Methylation defects affecting the maternal *A/B* DMR lead to the loss of Gsα expression in renal proximal tubules and renal PTH resistance. It is however not clear at this moment whether hypomethylation of the *GNAS-AS2* DMR has a

phenotype impact or whether methylation studies of this region can be useful for a better characterization of PHP patients. Further experiments are also needed to determine if loss of methylation of DMR *GNAS-AS2* influences the expression of *GNAS-XL.*

5.6 Conclusion

We here present the first genome-wide methylation study in different types of PHP. It seems that only the presence of the *STX16* deletion is of significant importance to divide PHP in 2 groups of patients with significantly different methylation profiles. Methylation changes in other imprinted DMRs seem to be enriched in especially PHP^{neg} patients. We identified a novel *GNAS-AS2* DMR in the *GNAS* locus that is hypomethylated in all PHP patients, independently from *STX16* deletion. Further studies must be undertaken to unravel the function and clinical impact of methylation changes in the *GNAS-AS2* region that in addition to the *A/B* DMR can also be hypomethylation in PHP patients with *STX16* deletion.

DISCUSSION

It is good to have an end to journey toward;
but it is the journey that matters, in the end.
Ernest Hemingway (1899-1961)

Despite the high incidence and severity of neural tube defects (NTDs), the exact underlying mechanism is still unknown. Multiple candidate genes and pathways are known to be involved, but growing evidence is also available for an important role of epigenetics and DNA methylation in the origin of NTDs.

The aim of this doctoral thesis was to determine which DNA regions and signaling pathways are more sensitive to DNA methylation changes during embryogenesis and lead to NTDs. Therefore, in addition to the core study of genome-wide DNA methylation, we designed locus-specific and functional validation studies to identify the most interesting candidate genes and in order to unravel the impact of DNA methylation in neural tube development and disease.

Starting with a literature review in **Chapter 2** on "Folate, DNA methylation and neural tube defects" we noticed that human studies investigating DNA methylation in patients with NTDs vary widely in study design. These studies investigated heterogeneous study populations and types of tissues and use different methylation quantification assays. Although findings of global DNA hypomethylation and LINE-1 hypomethylation suggest that disruption of genomic stability may play a role in neural tube closure, it is still unclear how specific regions of the genome are prone to folic acid and DNA methylation changes during embryonic development. Therefore we designed a genome-wide DNA methylation study in patients with lumbosacral MMC using leukocyte DNA.

Genome-wide data can be analyzed using both a *candidate-gene specific approach* whereby single gene information is extracted from the genome-wide analysis (Chapter 3 and 5) or a 'true' *genome-wide approach* to identify differentially methylated regions between patients and controls (Chapter 4 and 5). As analyzing HM450k data is complex and data processing needs particular care [83], I visited the lab of Prof. D. Monk to obtain expertise in data analysis and filtering. During this research stay we developed bioinformatics tools for both a candidate-gene specific as a genome-wide analysis. This study was performed on patients with the imprinting disease pseudohypoparathyroidism and results are presented in **Chapter 5**. Imprinting disorders include a broad spectrum of growth and development defects that are dependent on (epi)genetic disruption of imprinted genes. Recently, it

became clear that the original PHP classification was no longer accurate due to (epi)genetic overlap and moreover some patients with PHP were identified to have broader methylation defects involving more than one imprinted gene, a phenomenon called “multi-locus imprinting defects”. Differences in DNA methylation were investigated for the *GNAS* locus, all known imprinted genes and DNA repetitive elements (*LINE-1* and *LINE-2*). In addition, different normalization methods were compared for the genome-wide DNA methylation analysis. Validation studies using Sequenom EpiTYPER were also performed for this study. Obtained expertise in data analysis and filtering was used for this doctoral thesis.

In **Chapter 3** we used a *candidate-gene specific approach* to analyze the genome-wide DNA methylation data of the patients with lumbosacral MMC. As Homeobox (*HOX*) genes play a central role in spinal cord development, and are tightly regulated in a spatiotemporal and collinear manner, partly by epigenetic modifications, we studied changes in DNA methylation for the different *HOX* genes. Interestingly, almost all CpGs were hypomethylated for the MMC patients with *HOXB7* as the most significant locus. We confirmed *HOXB7* hypomethylation in a larger cohort but also in 12 unaffected siblings each related to a MMC patient. The validation study confirmed a significant association between MMC and *HOXB7* hypomethylation (-14,4%; 95% CI [11,9%, 16,9%]; P-value < 0.0001). Biological validation using a zebrafish model showed that Hoxb7a overexpression but not depletion results in dysmorphic neural tube formation. Interestingly, *HOXB7* hypomethylation was also present in 12 unaffected siblings, each related to a MMC patient. This could confirm the hypothesis that children born from mothers with folic acid resistance and a disturbed one-carbon metabolism, can present with alterations in DNA methylation with high risk for abnormal embryonic development. Moreover, this finding is suggestive of a multifactorial etiology of NTDs. No association was found between the *MTHFR* genotype and *HOXB7* methylation, which suggests that an intrinsic defect in the folic acid pathway related to *MTHFR* activity is not involved.

To investigate whether genome-wide DNA methylation analysis without focusing on candidate pathways could reveal novel genes associated with NTDs; we subsequently used a *genome-wide approach* in **Chapter 4** to identify differentially methylated regions between patients with lumbosacral MMC and controls. We

analyzed the HM450k data using two pipelines (IMA and WateRmelon) and found that 75 CpGs (mapping to 45 genes) were significantly differentially methylated in patients with MMC. The *HOX* genes were not included in this list, but *HOXB7* could be retrieved when only one filter was relieved. *HOXB7* was significantly hypomethylated in MMC patients with significant p-values of 0.007 for both pipelines but with a mean difference in methylation of -0.24 for IMA and -0.06 for the WateRmelon pipeline. Gene enrichment analysis showed multiple gene ontology classes related to neurodevelopmental processes. Moreover, genes are often involved in multiple gene ontology classes and seem to act together through various biological pathways. Validation studies were subsequently applied for the top genes selected from the genome-wide analysis: *ABAT, CNTNAP1, SLC1A6, SNED1, SOX18* and *TEPP.* For each locus, CpG specific methylation differences could be replicated, but the only significant overall methylation difference was found for *SOX18* (- 14%; 95% CI [-8%, -20%], P-value = 0.0003). No additive effect was found for the *MTHFR C/T* variant. Based on the findings between the siblings, we performed an additional analysis to study the inheritance of *SOX18* methylation changes in 5 families of patients with NTDs. Interestingly, the unaffected siblings showed *SOX18* hypomethylation in the same range as the MMC patients while the parents had normal methylation values comparable to the values found for the unrelated healthy controls. To further investigate the influence of an underlying genetic factor, we quantified *SOX18* methylation in a boy with MMC and a paternally inherited *BMP4* deletion and his parents. Interestingly, the patient with the *BMP4* deletion had very low methylation values that were also present in his healthy mother while his father had normal methylation. Though further studies are essential to support a role for *BMP4* deletion and *SOX18* overexpression, this family illustrates that the inheritance of genetic and epigenetic factors could co-act in neural tube development. Notable, regulators of angiogenesis are found for both *SOX18* [135] and *BMP4* [138] what could clarify an old concept that there might be a vascular basis for NTDs [140]. Biological validation of *SOX18* using chemically induced DNA demethylation in HEK cells resulted in *SOX18* hypomethylation and increased expression. Furthermore, overexpression in zebrafish embryos resulted in a dysmorphic neural tube that could not be rescued by addition of folic acid. As it might be informative in which pathways maternal folate impacts neural tube development, we replicated the top findings of our study with data from a recent meta-analysis that

examined the relation between maternal plasma folate and newborn DNA methylation. This study showed that DNA methylation of genes involved in multiple developmental processes, including neural tube development, are influenced by maternal folate. Interestingly, we share one of the top differentially methylated CpGs that is located within *SLC1A6*. *SLC1A6 (High Affinity Aspartate/Glutamate Transporter, Member 6)* is a member of the family of excitatory amino acid transporters, which are widely distributed throughout the brain and spinal cord [177]. Transporter dysfunction is linked to excitotoxic concentrations of glutamate that could be a mechanism of neurodegeneration and cell death [178]. *SLC1A6* seems to be sensitive to maternal plasma folate influences in both healthy controls as in patients with MMC.

STUDY LIMITATIONS

Some limitations need to be taken into account when interpreting our data.

First of all, although the HM450k represents so far the most standardized methodology to assess DNA methylation at genome-wide level, it has some inherent limitations. Some probes can generate artifactual data as some probes co-hybridize at additional locations on the genome than the targeted CpGs, some probes contain common SNPs and probes with a high average intensity are more prone to inconsistent measurements. In addition, divergence between the two Infinium assays generates two different types of data [126]. Different correction and normalization methods are suggested to make the two data sets comparable. Therefore, careful preprocessing and normalization of HM450k data is important to remove any source of variation that is related to technical limitations [83]. The HM450k relies also on traditional bisulfite treatment that cannot discriminate between 5-methylcytosine and 5-hydroxymethylcytosine. As recently became clear that DNA methylation is highly dynamic during brain development, it would also be interesting to investigate 5-hydroxymethylation in patients with NTDs [179].

Secondly, the sample size of our genome-wide DNA methylation study is relatively small. Therefore, after filtering out problematic probes, we applied two different pipelines using different data normalization methods. In a larger cohort of patients

and controls, we subsequently performed validation studies using another methodology to quantify DNA methylation (EpiTYPER).

Thirdly, leukocyte blood was used as surrogate tissue. The ideal tissue would be to use brain or spinal cord, which can only be obtained post-mortem. But various other studies report concordant methylation profiles in brain and blood what suggests that DNA methylation in blood might reflect brain DNA methylation [112-114,142]. DNA methylation in blood is significantly more variable than DNA methylation in brain tissues [141]. Studies in brain tissue of patients with NTDs are essential to investigate the presence of more stable gene expression levels in brain versus blood. Farré et al [141] also identified an epigenetic signature of age that is not related to cell type composition and that did not require a correction for cellular heterogeneity. This is an interesting finding, as until now there was still no clear evidence that epigenetic marks of different cell types respond in a similar way to environmental influences.

Finally, in the current study we were not able to control for genotype. It is estimated that DNA methylation variability differs between 22-80% upon DNA sequence variability [131]. We did not find an association with the *MTHFR* genotype, but we illustrated a possible interaction of (epi)genetic variants in the family of the patient with the *BMP4* deletion. Further studies combining (epi)genetics and environmental modulators are essential to unravel NTD etiology.

CLINICAL AND SCIENTIFIC RELEVANCE OF THE THESIS

A. Clinical relevance

NTDs arise from a complex combination of genetic and environmental interactions. Although we are only beginning to understand their etiology, two major advances have been made in their prevention and treatment. First periconceptional folate supplements prevent both NTD occurrence as recurrence [180] and second, recent surgical advances demonstrate that prenatal surgery improves patient outcomes [4].

Despite these advances, NTDs still represent the second most common group of human birth defects and result in enormous clinical, emotional, financial and societal costs [181]. Each year, 300 000 to 400 000 infants worldwide are born with a NTD. Patients suffer from hydrocephalus, neurogenic bladder, kidney disease, orthopedic complications and psychosocial problems. Treatment includes surgery, medication and physiotherapy. Recent advances resulted in an increased life expectancy and improved quality of life, but no treatment exists that completely eliminates the serious disability or premature mortality. The weighted average lifetime cost for a child with a NTD in the Netherlands is calculated to be €242 948, the quality of life and the life expectancy are included in the weighted average [182]. Furthermore this study recommends folic acid food fortification in the Netherlands, being still cost-effective even if only one case is averted. In Belgium, prenatal diagnosis of NTDs leads to termination of pregnancy in 61% of cases. For a full evaluation of quality-adjusted life years (QALYs) and the economical signature of NTDs, associated costs should be taken into account. Such analysis has not yet been performed in Belgium or other European countries.

For all these reasons, identifying (epi)genetic predictors of NTDs is of great importance for the counseling of women of childbearing age. An understanding of (epi)genetic risk factors would also have implications for identifying potential protective treatments. The key challenge is to understand the developing neural tube, to help generate new intervention strategies to tackle the clinical challenges and to alleviate the economical and societal burdens that accompany these defects.

B. Scientific biological relevance

As already pointed out, both genetic and non-genetic factors are implicated in the causes of NTDs. The genomics revolution provides methods to investigate candidate genes for NTD causation. Numerous mouse NTD models aid to understand the process of neurulation and point to several candidate pathways for the study in human NTDs [16,22]. The impact of maternal folic acid supplementation highlights the importance of environmental factors in human NTD etiology [31,55]. Mouse mutants show a more diverse range of responses to folic acid supplementation, suggesting that the response to folic acid fortification may be more complex than previously suggested and that the length of folic acid exposure and the individual

genetic background plays a central role for a phenotypic response [183]. Mutations in genes that affect DNA methylation, histone modification or chromatin remodeling, result in NTDs in mice [16,22]. The *MTHFR 677C>T* genotype reduces global DNA methylation and is a risk factor for NTDs. Methyl-donor enriched diets can induce alterations in gene expression, and long-term generational exposure can result in increasing variation in DNA methylation.

Epigenetic studies bring new insights in how folic acid may affect transcriptional programs during neural tube closure and identify genes and pathways that are differentially regulated in this way.

C. Advantages of this study

The first important advantage of these studies is the use of the genome-wide DNA methylation approach. The HM450k is highly accurate and reproducible for genome-wide DNA methylation profiling. It covers almost half a million cytosines in 99% of RefSeq genes and 96% of CpG islands, as well as multiple CGI shores and isolated CpGs. The interrogated CpGs cross promoter regions, 5' and 3' UTRs, gene bodies and intergenic regions. The HM450k allows a precise quantification of the methylation level and generates data more quickly and easily analyzable than sequencing data. Therefore this technology represents so far the most standardized high-throughput methodology for quantification of DNA methylation [82,126].

High-throughput technology is inherently imprecise and noisy, and the complexity of the data requests careful consideration in separating signal from noise. Therefore, the second important advantage of our study is that we performed locus-specific validation studies in a large cohort of patients with MMC. Of note is the advantage of the use of a different technique to validate the findings, as technical problems or inadequate statistical analysis might introduce bias [82]. In addition, the population for the locus-specific validation study was carefully selected based on the same phenotype: all patients had an open lumbosacral MMC. Gender- and age matched controls were selected, as aging affects DNA methylation [142,184].

The last advantage is the use of a zebrafish model for functional validation of the findings from our DNA methylation studies. The similarity between zebrafish and

vertebrate neurulation in combination with the practical advantages of working with zebrafish, renders it as a viable and useful model to investigate human neurulation in health and disease.

D. Future research perspectives

Neural tube defects are suggested to have a highly multifactorial and polygenic inheritance pattern. Therefore, it would be interesting to combine next-generation sequencing approaches and epigenetic studies in large families with both affected and unaffected individuals and to investigate the influence of environmental factors in these studies.

First of all, we are contributing to a large international study entitled “An investigation of genetic factors predisposing to valproic acid-associated neural tube defects” (Prof. Frank Vajda, The Royal Melbourne Hospital, Melbourne, Australia). In this study, whole-exome sequencing and genome-wide DNA methylation studies will be combined to investigate whether highly penetrant maternal, paternal or de novo genetic variants influence NTD occurrence and whether there is a link with altered DNA methylation patterns.

It is known that prenatal exposure to the anti-epileptic drug valproic acid is associated with a 10- to 20-fold increased risk of spina bifida [185]. Although the underlying teratogenic mechanism remains unknown, it has been proposed that histone deacetylase inhibition, folate antagonism and competition for the folate receptor binding are included [186]. However, folate does not seem to be effective in preventing NTDs associated with valproic acid exposure [187]. Epigenetic modifications have been postulated to play a role in valproic acid-induced teratogenesis [188]. A study of valproic acid teratogenicity in mice resulted in many homeotic malformations and altered expression of *HOX* genes, in addition they found that genetic susceptibility for valproic acid induced malformations could reside in both the fetal and the parental genomes [189]. We found that *HOXB7* hypomethylation is a potential risk factor for NTDs and also that (epi)genetic susceptibility might interplay as a cause for NTDs.

Secondly, work with inducible pluripotent stem (iPS) cells would be interesting for the development of alternative preventive or curative therapies. After the identification of

the key players in neurulation and NTDs, iPS cells allow direct study of basic biological processes in cells derived from human patients. Stem cell research provides abundant material and a relatively fast time frame to analysis, which provides the possibility to screen small molecules for therapeutic or preventive potential. Mesenchymal stem cells occur naturally in the amniotic fluid and are good candidates for tissue engineering strategies for the repair of neural tube defects [190,191]. These new treatment modalities with iPS cells have to be confirmed in rigorous animal experimental studies before the use in human clinical trials.

Thirdly, not all NTDs are preventable with folic acid treatment in human or in animal models. Spina bifida is reduced in the Axd mutant by methionine and in Curly tail by inositol [22]. The mouse models suggested that genetic heterogeneity could explain this differential response to folic acid action. More studies including additional micronutrients carry the possibility of defining which genetic risk factors may be best targeted by therapies beyond folic acid, in order to develop alternative preventive therapies.

GENERAL CONCLUSION

This doctoral thesis investigated the relation between DNA methylation and NTDs. We believe that our data support the multifactorial polygenic inheritance pattern of NTDs and the importance of epigenetic changes in neural tube development and disease. To our knowledge this is the first study investigating genome-wide DNA methylation in leukocyte DNA of patients with NTDs including a large locus-specific validation study and functional validation in a zebrafish model. Further combined (epi)genetic studies are essential to unravel the complex etiology of NTDs and to alleviate the clinical, economical and psychological burdens for patients with NTDs.

REFERENCES

1. Smith GK (2001) The history of spina bifida, hydrocephalus, paraplegia, and incontinence. Pediatr Surg Int 17: 424-432.
2. Goodrich (2008) A historical review of the surgical treatment of spina bifida. In: Memet Özek M, Cinalli G, Maixner WJ, SpringerLink (Online service), editors. The Spina Bifida Management and Outcome. Milano: Springer-Verlag Italia,.
3. Copp AJ, Greene ND (2013) Neural tube defects--disorders of neurulation and related embryonic processes. Wiley Interdiscip Rev Dev Biol 2: 213-227.
4. Adzick NS, Thom EA, Spong CY, Brock JW, 3rd, Burrows PK, et al. (2011) A randomized trial of prenatal versus postnatal repair of myelomeningocele. N Engl J Med 364: 993-1004.
5. Mitchell LE (2005) Epidemiology of neural tube defects. Am J Med Genet C Semin Med Genet 135C: 88-94.
6. Prevention of neural tube defects: results of the Medical Research Council Vitamin Study. (1991) MRC Vitamin Study Research Group. Lancet 338: 131-137.
7. Czeizel AE, Dudas I (1992) Prevention of the first occurrence of neural-tube defects by periconceptional vitamin supplementation. N Engl J Med 327: 1832-1835.
8. Atta CA, Fiest KM, Frolkis AD, Jette N, Pringsheim T, et al. (2016) Global Birth Prevalence of Spina Bifida by Folic Acid Fortification Status: A Systematic Review and Meta-Analysis. Am J Public Health 106: e24-34.
9. Khoshnood B, Loane M, Walle H, Arriola L, Addor MC, et al. (2015) Long term trends in prevalence of neural tube defects in Europe: population based study. BMJ 351: h5949.
10. Crider KS, Bailey LB, Berry RJ (2011) Folic acid food fortification-its history, effect, concerns, and future directions. Nutrients 3: 370-384.
11. Greene ND, Copp AJ (2009) Development of the vertebrate central nervous system: formation of the neural tube. Prenat Diagn 29: 303-311.
12. Macdonald KB, Juriloff DM, Harris MJ (1989) Developmental study of neural tube closure in a mouse stock with a high incidence of exencephaly. Teratology 39: 195-213.
13. Copp AJ, Greene ND (2010) Genetics and development of neural tube defects. J Pathol 220: 217-230.
14. Juriloff DM, Harris MJ (2012) A consideration of the evidence that genetic defects in planar cell polarity contribute to the etiology of human neural tube defects. Birth Defects Res A Clin Mol Teratol 94: 824-840.
15. Copp AJ, Greene ND, Murdoch JN (2003) The genetic basis of mammalian neurulation. Nat Rev Genet 4: 784-793.
16. Harris MJ, Juriloff DM (2007) Mouse mutants with neural tube closure defects and their role in understanding human neural tube defects. Birth Defects Res A Clin Mol Teratol 79: 187-210.
17. Wyszynski DF (2006) Neural Tube Defects: From Origin to Treatment: Oxford University Press. 399 p.
18. Goetzinger KR, Stamilio DM, Dicke JM, Macones GA, Odibo AO (2008) Evaluating the incidence and likelihood ratios for chromosomal abnormalities in fetuses with common central nervous system malformations. Am J Obstet Gynecol 199: 285 e281-286.
19. Chen CP (2007) Chromosomal abnormalities associated with neural tube defects (I): full aneuploidy. Taiwan J Obstet Gynecol 46: 325-335.
20. Chen CP (2007) Chromosomal abnormalities associated with neural tube defects (II): partial aneuploidy. Taiwan J Obstet Gynecol 46: 336-351.
21. Logan CV, Abdel-Hamed Z, Johnson CA (2011) Molecular genetics and pathogenic mechanisms for the severe ciliopathies: insights into neurodevelopment and pathogenesis of neural tube defects. Mol Neurobiol 43: 12-26.
22. Harris MJ, Juriloff DM (2010) An update to the list of mouse mutants with neural tube closure defects and advances toward a complete genetic perspective of neural tube closure. Birth Defects Res A Clin Mol Teratol 88: 653-669.

23. Copp AJ (2005) Neurulation in the cranial region--normal and abnormal. J Anat 207: 623-635.
24. Detrait ER, George TM, Etchevers HC, Gilbert JR, Vekemans M, et al. (2005) Human neural tube defects: developmental biology, epidemiology, and genetics. Neurotoxicol Teratol 27: 515-524.
25. Harris MJ (2009) Insights into prevention of human neural tube defects by folic acid arising from consideration of mouse mutants. Birth Defects Res A Clin Mol Teratol 85: 331-339.
26. Greene ND, Stanier P, Copp AJ (2009) Genetics of human neural tube defects. Hum Mol Genet 18: R113-129.
27. Boyles AL, Hammock P, Speer MC (2005) Candidate gene analysis in human neural tube defects. Am J Med Genet C Semin Med Genet 135C: 9-23.
28. Au KS, Ashley-Koch A, Northrup H (2010) Epidemiologic and genetic aspects of spina bifida and other neural tube defects. Dev Disabil Res Rev 16: 6-15.
29. Greene ND, Leung KY, Gay V, Burren K, Mills K, et al. (2016) Inositol for the prevention of neural tube defects: a pilot randomised controlled trial. Br J Nutr: 1-10.
30. Copp AJ, Stanier P, Greene NDE (2013) Neural tube defects: recent advances, unsolved questions, and controversies. The Lancet Neurology 12: 799-810.
31. Blom HJ, Shaw GM, den Heijer M, Finnell RH (2006) Neural tube defects and folate: case far from closed. Nat Rev Neurosci 7: 724-731.
32. Greene NDE, Stanier P, Moore GE (2011) The emerging role of epigenetic mechanisms in the aetiology of neural tube defects. Epigenetics 6: 875-883.
33. Teperino R, Lempradl A, Pospisilik JA (2013) Bridging epigenomics and complex disease: the basics. Cell Mol Life Sci 70: 1609-1621.
34. Okano M, Bell DW, Haber DA, Li E (1999) DNA methyltransferases Dnmt3a and Dnmt3b are essential for de novo methylation and mammalian development. Cell 99: 247-257.
35. Dunlevy LP, Burren KA, Chitty LS, Copp AJ, Greene ND (2006) Excess methionine suppresses the methylation cycle and inhibits neural tube closure in mouse embryos. FEBS Lett 580: 2803-2807.
36. Gurvich N, Berman MG, Wittner BS, Gentleman RC, Klein PS, et al. (2005) Association of valproate-induced teratogenesis with histone deacetylase inhibition in vivo. FASEB J 19: 1166-1168.
37. Murko C, Lagger S, Steiner M, Seiser C, Schoefer C, et al. (2013) Histone deacetylase inhibitor Trichostatin A induces neural tube defects and promotes neural crest specification in the chicken neural tube. Differentiation 85: 55-66.
38. Coelho CN, Klein NW (1990) Methionine and neural tube closure in cultured rat embryos: morphological and biochemical analyses. Teratology 42: 437-451.
39. Afman LA, Blom HJ, Drittij MJ, Brouns MR, van Straaten HW (2005) Inhibition of transmethylation disturbs neurulation in chick embryos. Brain Res Dev Brain Res 158: 59-65.
40. Rochtus A, Jansen K, Geet CV, Freson K (2015) Nutri-epigenomic Studies Related to Neural Tube Defects: Does Folate Affect Neural Tube Closure Via Changes in DNA Methylation? Mini Rev Med Chem 15: 1095-1102.
41. Lowery LA, Sive H (2004) Strategies of vertebrate neurulation and a re-evaluation of teleost neural tube formation. Mech Dev 121: 1189-1197.
42. Kibar Z, Bosoi CM, Kooistra M, Salem S, Finnell RH, et al. (2009) Novel mutations in VANGL1 in neural tube defects. Hum Mutat 30: E706-715.
43. Reynolds A, McDearmid JR, Lachance S, De Marco P, Merello E, et al. (2010) VANGL1 rare variants associated with neural tube defects affect convergent extension in zebrafish. Mech Dev 127: 385-392.
44. Ueno N, Greene ND (2003) Planar cell polarity genes and neural tube closure. Birth Defects Res C Embryo Today 69: 318-324.
45. Jirtle RL, Skinner MK (2007) Environmental epigenomics and disease susceptibility. Nat Rev Genet 8: 253-262.

46. Baubec T, Schubeler D (2014) Genomic patterns and context specific interpretation of DNA methylation. Curr Opin Genet Dev 25: 85-92.
47. Lister R, Pelizzola M, Dowen RH, Hawkins RD, Hon G, et al. (2009) Human DNA methylomes at base resolution show widespread epigenomic differences. Nature 462: 315-322.
48. Schubeler D (2015) Function and information content of DNA methylation. Nature 517: 321-326.
49. Rakyan VK, Down TA, Balding DJ, Beck S (2011) Epigenome-wide association studies for common human diseases. Nat Rev Genet 12: 529-541.
50. Gabory A, Attig L, Junien C (2011) Developmental programming and epigenetics. Am J Clin Nutr 94: 1943S-1952S.
51. Waterland RA, Jirtle RL (2004) Early nutrition, epigenetic changes at transposons and imprinted genes, and enhanced susceptibility to adult chronic diseases. Nutrition 20: 63-68.
52. Imbard A, Benoist JF, Blom HJ (2013) Neural tube defects, folic acid and methylation. Int J Environ Res Public Health 10: 4352-4389.
53. Guéant JL, Namour F, Guéant-Rodriguez RM, Daval JL (2013) Folate and fetal programming: a play in epigenomics? Trends Endocrinol Metab 24: 279-289.
54. Botto LD, Lisi A, Robert-Gnansia E, Erickson JD, Vollset SE, et al. (2005) International retrospective cohort study of neural tube defects in relation to folic acid recommendations: are the recommendations working? BMJ 330: 571.
55. Blom HJ (2009) Folic acid, methylation and neural tube closure in humans. Birth Defects Res A Clin Mol Teratol 85: 295-302.
56. van der Put NM, Steegers-Theunissen RP, Frosst P, Trijbels FJ, Eskes TK, et al. (1995) Mutated methylenetetrahydrofolate reductase as a risk factor for spina bifida. Lancet 346: 1070-1071.
57. Molloy AM, Brody LC, Mills JL, Scott JM, Kirke PN (2009) The search for genetic polymorphisms in the homocysteine/folate pathway that contribute to the etiology of human neural tube defects. Birth Defects Res A Clin Mol Teratol 85: 285-294.
58. Botto LD, Yang Q (2000) 5,10-Methylenetetrahydrofolate reductase gene variants and congenital anomalies: a HuGE review. Am J Epidemiol 151: 862-877.
59. Beaudin AE, Stover PJ (2007) Folate-mediated one-carbon metabolism and neural tube defects: balancing genome synthesis and gene expression. Birth Defects Res C Embryo Today 81: 183-203.
60. Nazki FH, Sameer AS, Ganaie BA (2014) Folate: metabolism, genes, polymorphisms and the associated diseases. Gene 533: 11-20.
61. Padmanabhan N, Jia D, Geary-Joo C, Wu X, Ferguson-Smith AC, et al. (2013) Mutation in folate metabolism causes epigenetic instability and transgenerational effects on development. Cell 155: 81-93.
62. Fisk Green R, Byrne J, Crider KS, Gallagher M, Koontz D, et al. (2013) Folate-related gene variants in Irish families affected by neural tube defects. Front Genet 4: 223.
63. Steegers-Theunissen RP, Boers GH, Trijbels FJ, Finkelstein JD, Blom HJ, et al. (1994) Maternal hyperhomocysteinemia: a risk factor for neural-tube defects? Metabolism 43: 1475-1480.
64. Mills JL, McPartlin JM, Kirke PN, Lee YJ, Conley MR, et al. (1995) Homocysteine metabolism in pregnancies complicated by neural-tube defects. Lancet 345: 149-151.
65. Ishida M, Moore GE (2013) The role of imprinted genes in humans. Mol Aspects Med 34: 826-840.
66. Peters J (2014) The role of genomic imprinting in biology and disease: an expanding view. Nat Rev Genet 15: 517-530.
67. Lee HJ, Hore TA, Reik W (2014) Reprogramming the methylome: erasing memory and creating diversity. Cell Stem Cell 14: 710-719.
68. Bock C (2012) Analysing and interpreting DNA methylation data. Nat Rev Genet 13: 705-719.

69. Price EM, Cotton AM, Penaherrera MS, McFadden DE, Kobor MS, et al. (2012) Different measures of "genome-wide" DNA methylation exhibit unique properties in placental and somatic tissues. Epigenetics 7: 652-663.
70. Brooks PJ, Marietta C, Goldman D (1996) DNA mismatch repair and DNA methylation in adult brain neurons. J Neurosci 16: 939-945.
71. Li GM (2008) Mechanisms and functions of DNA mismatch repair. Cell Res 18: 85-98.
72. Liu Z, Wang Z, Li Y, Ouyang S, Chang H, et al. (2012) Association of genomic instability, and the methylation status of imprinted genes and mismatch-repair genes, with neural tube defects. Eur J Hum Genet 20: 516-520.
73. Wu L, Wang L, Shangguan S, Chang S, Wang Z, et al. (2013) Altered methylation of IGF2 DMR0 is associated with neural tube defects. Mol Cell Biochem 380: 33-42.
74. Stolk L, Bouwland-Both MI, van Mill NH, Verbiest MM, Eilers PH, et al. (2013) Epigenetic profiles in children with a neural tube defect; a case-control study in two populations. PLoS One 8: e78462.
75. Wang L, Wang F, Guan J, Le J, Wu L, et al. (2010) Relation between hypomethylation of long interspersed nucleotide elements and risk of neural tube defects. Am J Clin Nutr 91: 1359-1367.
76. Kim JH, Kang GH (2014) Molecular and prognostic heterogeneity of microsatellite-unstable colorectal cancer. World J Gastroenterol 20: 4230-4243.
77. Chang H, Zhang T, Zhang Z, Bao R, Fu C, et al. (2011) Tissue-specific distribution of aberrant DNA methylation associated with maternal low-folate status in human neural tube defects. J Nutr Biochem 22: 1172-1177.
78. Chen X, Guo J, Lei Y, Zou J, Lu X, et al. (2010) Global DNA hypomethylation is associated with NTD-affected pregnancy: A case-control study. Birth Defects Res A Clin Mol Teratol 88: 575-581.
79. Tran S, Wang L, Le J, Guan J, Wu L, et al. (2012) Altered methylation of the DNA repair gene MGMT is associated with neural tube defects. J Mol Neurosci 47: 42-51.
80. Farkas SA, Bottiger AK, Isaksson HS, Finnell RH, Ren A, et al. (2013) Epigenetic alterations in folate transport genes in placental tissue from fetuses with neural tube defects and in leukocytes from subjects with hyperhomocysteinemia. Epigenetics 8: 303-316.
81. Wang Z, Wang L, Shangguan S, Lu X, Chang S, et al. (2013) Association between PTCH1 polymorphisms and risk of neural tube defects in a Chinese population. Birth Defects Res A Clin Mol Teratol 97: 409-415.
82. Michels KB, Binder AM, Dedeurwaerder S, Epstein CB, Greally JM, et al. (2013) Recommendations for the design and analysis of epigenome-wide association studies. Nat Methods 10: 949-955.
83. Dedeurwaerder S, Defrance M, Bizet M, Calonne E, Bontempi G, et al. (2013) A comprehensive overview of Infinium HumanMethylation450 data processing. Brief Bioinform.
84. Wallingford JB, Niswander LA, Shaw GM, Finnell RH (2013) The continuing challenge of understanding, preventing, and treating neural tube defects. Science 339: 1222002.
85. Copp AJ, Stanier P, Greene ND (2013) Neural tube defects: recent advances, unsolved questions, and controversies. Lancet Neurol.
86. Kirke PN, Molloy AM, Daly LE, Burke H, Weir DG, et al. (1993) Maternal plasma folate and vitamin B12 are independent risk factors for neural tube defects. Q J Med 86: 703-708.
87. Cavalli P, Copp AJ (2002) Inositol and folate resistant neural tube defects. J Med Genet 39: E5.
88. Friso S, Choi SW, Girelli D, Mason JB, Dolnikowski GG, et al. (2002) A common mutation in the 5,10-methylenetetrahydrofolate reductase gene affects genomic DNA methylation through an interaction with folate status. Proc Natl Acad Sci U S A 99: 5606-5611.
89. Laurent L, Wong E, Li G, Huynh T, Tsirigos A, et al. (2010) Dynamic changes in the human methylome during differentiation. Genome Res 20: 320-331.

90. Volcik KA, Blanton SH, Kruzel MC, Townsend IT, Tyerman GH, et al. (2002) Testing for genetic associations in a spina bifida population: analysis of the HOX gene family and human candidate gene regions implicated by mouse models of neural tube defects. Am J Med Genet 110: 203-207.
91. Carpenter EM (2002) Hox genes and spinal cord development. Dev Neurosci 24: 24-34.
92. Barber BA, Rastegar M (2010) Epigenetic control of Hox genes during neurogenesis, development, and disease. Ann Anat 192: 261-274.
93. Chambeyron S, Bickmore WA (2004) Chromatin decondensation and nuclear reorganization of the HoxB locus upon induction of transcription. Genes Dev 18: 1119-1130.
94. Boudadi E, Stower H, Halsall JA, Rutledge CE, Leeb M, et al. (2013) The histone deacetylase inhibitor sodium valproate causes limited transcriptional change in mouse embryonic stem cells but selectively overrides Polycomb-mediated Hoxb silencing. Epigenetics Chromatin 6: 11.
95. Bibikova M, Barnes B, Tsan C, Ho V, Klotzle B, et al. (2011) High density DNA methylation array with single CpG site resolution. Genomics 98: 288-295.
96. Wang D, Yan L, Hu Q, Sucheston LE, Higgins MJ, et al. (2012) IMA: an R package for high-throughput analysis of Illumina's 450K Infinium methylation data. Bioinformatics 28: 729-730.
97. Izzi B, Decallonne B, Devriendt K, Bouillon R, Vanderschueren D, et al. (2010) A new approach to imprinting mutation detection in GNAS by Sequenom EpiTYPER system. Clin Chim Acta 411: 2033-2039.
98. Izzi B, Francois I, Labarque V, Thys C, Wittevrongel C, et al. (2012) Methylation defect in imprinted genes detected in patients with an Albright's hereditary osteodystrophy like phenotype and platelet Gs hypofunction. PLoS One 7: e38579.
99. Izzi B, Binder AM, Michels KB (2014) Pyrosequencing Evaluation of Widely Available Bisulfite Conversion Methods: Considerations for Application. Med Epigenet 2: 28-36.
100. Frosst P, Blom HJ, Milos R, Goyette P, Sheppard CA, et al. (1995) A candidate genetic risk factor for vascular disease: a common mutation in methylenetetrahydrofolate reductase. Nat Genet 10: 111-113.
101. Baek SJ, Yang S, Kang TW, Park SM, Kim YS, et al. (2013) MENT: methylation and expression database of normal and tumor tissues. Gene 518: 194-200.
102. Westerfield M (1995) The Zebrafish Book. University of Oregon Press, Eugene, OR.
103. Kimmel CB, Ballard WW, Kimmel SR, Ullmann B, Schilling TF (1995) Stages of embryonic development of the zebrafish. Dev Dyn 203: 253-310.
104. Krauss S, Johansen T, Korzh V, Moens U, Ericson JU, et al. (1991) Zebrafish pax[zf-a]: a paired box-containing gene expressed in the neural tube. EMBO J 10: 3609-3619.
105. Prince VE, Joly L, Ekker M, Ho RK (1998) Zebrafish hox genes: genomic organization and modified colinear expression patterns in the trunk. Development 125: 407-420.
106. Prince V (2002) The Hox Paradox: More complex(es) than imagined. Dev Biol 249: 1-15.
107. Philippidou P, Dasen JS (2013) Hox genes: choreographers in neural development, architects of circuit organization. Neuron 80: 12-34.
108. Soshnikova N, Dewaele R, Janvier P, Krumlauf R, Duboule D (2013) Duplications of hox gene clusters and the emergence of vertebrates. Dev Biol 378: 194-199.
109. Vieux-Rochas M, Mascrez B, Krumlauf R, Duboule D (2013) Combined function of HoxA and HoxB clusters in neural crest cells. Dev Biol 382: 293-301.
110. Jessell TM (2000) Neuronal specification in the spinal cord: inductive signals and transcriptional codes. Nat Rev Genet 1: 20-29.
111. Doniach T (1995) Basic FGF as an inducer of anteroposterior neural pattern. Cell 83: 1067-1070.
112. Masliah E, Dumaop W, Galasko D, Desplats P (2013) Distinctive patterns of DNA methylation associated with Parkinson disease: identification of concordant

epigenetic changes in brain and peripheral blood leukocytes. Epigenetics 8: 1030-1038.
113. Tylee DS, Kawaguchi DM, Glatt SJ (2013) On the outside, looking in: a review and evaluation of the comparability of blood and brain "-omes". Am J Med Genet B Neuropsychiatr Genet 162B: 595-603.
114. Ikegame T, Bundo M, Murata Y, Kasai K, Kato T, et al. (2013) DNA methylation of the BDNF gene and its relevance to psychiatric disorders. J Hum Genet 58: 434-438.
115. Avraham A, Sandbank J, Yarom N, Shalom A, Karni T, et al. (2010) A similar cell-specific pattern of HOXA methylation in normal and in cancer tissues. Epigenetics 5: 41-46.
116. Rochtus A, Izzi B, Vangeel E, Louwette S, Wittevrongel C, et al. (2015) DNA methylation analysis of Homeobox genes implicates HOXB7 hypomethylation as risk factor for neural tube defects. Epigenetics 10: 92-101.
117. Kok DE, Dhonukshe-Rutten RA, Lute C, Heil SG, Uitterlinden AG, et al. (2015) The effects of long-term daily folic acid and vitamin B12 supplementation on genome-wide DNA methylation in elderly subjects. Clin Epigenetics 7: 121.
118. Joubert BR, den Dekker HT, Felix JF, Bohlin J, Ligthart S, et al. (2016) Maternal plasma folate impacts differential DNA methylation in an epigenome-wide meta-analysis of newborns. Nat Commun 7: 10577.
119. Touleimat N, Tost J (2012) Complete pipeline for Infinium((R)) Human Methylation 450K BeadChip data processing using subset quantile normalization for accurate DNA methylation estimation. Epigenomics 4: 325-341.
120. Edgar R, Domrachev M, Lash AE (2002) Gene Expression Omnibus: NCBI gene expression and hybridization array data repository. Nucleic Acids Res 30: 207-210.
121. Merico D, Isserlin R, Stueker O, Emili A, Bader GD (2010) Enrichment map: a network-based method for gene-set enrichment visualization and interpretation. PLoS One 5: e13984.
122. Livak KJ, Schmittgen TD (2001) Analysis of relative gene expression data using real-time quantitative PCR and the 2(-Delta Delta C(T)) Method. Methods 25: 402-408.
123. Ma Y, Wu M, Li D, Li XQ, Li P, et al. (2012) Embryonic developmental toxicity of selenite in zebrafish (Danio rerio) and prevention with folic acid. Food Chem Toxicol 50: 2854-2863.
124. Wilde JJ, Petersen JR, Niswander L (2014) Genetic, epigenetic, and environmental contributions to neural tube closure. Annu Rev Genet 48: 583-611.
125. Greene ND, Copp AJ (2014) Neural tube defects. Annu Rev Neurosci 37: 221-242.
126. Dedeurwaerder S, Defrance M, Calonne E, Denis H, Sotiriou C, et al. (2011) Evaluation of the Infinium Methylation 450K technology. Epigenomics 3: 771-784.
127. Irrthum A, Devriendt K, Chitayat D, Matthijs G, Glade C, et al. (2003) Mutations in the transcription factor gene SOX18 underlie recessive and dominant forms of hypotrichosis-lymphedema-telangiectasia. Am J Hum Genet 72: 1470-1478.
128. Lu XL, Wang L, Chang SY, Shangguan SF, Wang Z, et al. (2015) Sonic Hedgehog Signaling Affected by Promoter Hypermethylation Induces Aberrant Gli2 Expression in Spina Bifida. Mol Neurobiol.
129. Joubert BR, Felix JF, Yousefi P, Bakulski KM, Just AC, et al. (2016) DNA Methylation in Newborns and Maternal Smoking in Pregnancy: Genome-wide Consortium Meta-analysis. Am J Hum Genet 98: 680-696.
130. Chen Q, Wang H, Schwender H, Zhang T, Hetmanski JB, et al. (2014) Joint testing of genotypic and gene-environment interaction identified novel association for BMP4 with non-syndromic CL/P in an Asian population using data from an International Cleft Consortium. PLoS One 9: e109038.
131. Gertz J, Varley KE, Reddy TE, Bowling KM, Pauli F, et al. (2011) Analysis of DNA methylation in a three-generation family reveals widespread genetic influence on epigenetic regulation. PLoS Genet 7: e1002228.

132. Bakrania P, Efthymiou M, Klein JC, Salt A, Bunyan DJ, et al. (2008) Mutations in BMP4 cause eye, brain, and digit developmental anomalies: overlap between the BMP4 and hedgehog signaling pathways. Am J Hum Genet 82: 304-319.
133. Lumaka A, Van Hole C, Casteels I, Ortibus E, De Wolf V, et al. (2012) Variability in expression of a familial 2.79 Mb microdeletion in chromosome 14q22.1-22.2. Am J Med Genet A 158A: 1381-1387.
134. Tesson C, Nawara M, Salih MA, Rossignol R, Zaki MS, et al. (2012) Alteration of fatty-acid-metabolizing enzymes affects mitochondrial form and function in hereditary spastic paraplegia. Am J Hum Genet 91: 1051-1064.
135. Petrovic I, Milivojevic M, Popovic J, Schwirtlich M, Rankovic B, et al. (2015) SOX18 Is a Novel Target Gene of Hedgehog Signaling in Cervical Carcinoma Cell Lines. PLoS One 10: e0143591.
136. Cermenati S, Moleri S, Cimbro S, Corti P, Del Giacco L, et al. (2008) Sox18 and Sox7 play redundant roles in vascular development. Blood 111: 2657-2666.
137. Matsui T, Kanai-Azuma M, Hara K, Matoba S, Hiramatsu R, et al. (2006) Redundant roles of Sox17 and Sox18 in postnatal angiogenesis in mice. J Cell Sci 119: 3513-3526.
138. Boyd NL, Dhara SK, Rekaya R, Godbey EA, Hasneen K, et al. (2007) BMP4 promotes formation of primitive vascular networks in human embryonic stem cell-derived embryoid bodies. Exp Biol Med (Maywood) 232: 833-843.
139. Rothhammer T, Bataille F, Spruss T, Eissner G, Bosserhoff AK (2007) Functional implication of BMP4 expression on angiogenesis in malignant melanoma. Oncogene 26: 4158-4170.
140. Stevenson RE, Kelly JC, Aylsworth AS, Phelan MC (1987) Vascular basis for neural tube defects: a hypothesis. Pediatrics 80: 102-106.
141. Farre P, Jones MJ, Meaney MJ, Emberly E, Turecki G, et al. (2015) Concordant and discordant DNA methylation signatures of aging in human blood and brain. Epigenetics Chromatin 8: 19.
142. Horvath S, Zhang Y, Langfelder P, Kahn RS, Boks MP, et al. (2012) Aging effects on DNA methylation modules in human brain and blood tissue. Genome Biol 13: R97.
143. Levine MA (2012) An update on the clinical and molecular characteristics of pseudohypoparathyroidism. Curr Opin Endocrinol Diabetes Obes 19: 443-451.
144. Bastepe M (2013) Genetics and epigenetics of parathyroid hormone resistance. Endocr Dev 24: 11-24.
145. Patten JL, Johns DR, Valle D, Eil C, Gruppuso PA, et al. (1990) Mutation in the gene encoding the stimulatory G protein of adenylate cyclase in Albright's hereditary osteodystrophy. N Engl J Med 322: 1412-1419.
146. Davies SJ, Hughes HE (1993) Imprinting in Albright's hereditary osteodystrophy. J Med Genet 30: 101-103.
147. Mantovani G (2011) Clinical review: Pseudohypoparathyroidism: diagnosis and treatment. J Clin Endocrinol Metab 96: 3020-3030.
148. de Nanclares GP, Fernandez-Rebollo E, Santin I, Garcia-Cuartero B, Gaztambide S, et al. (2007) Epigenetic defects of GNAS in patients with pseudohypoparathyroidism and mild features of Albright's hereditary osteodystrophy. J Clin Endocrinol Metab 92: 2370-2373.
149. Molinaro A, Tiosano D, Takatani R, Chrysis D, Russell W, et al. (2015) TSH elevations as the first laboratory evidence for pseudohypoparathyroidism type Ib (PHP-Ib). J Bone Miner Res 30: 906-912.
150. Romanet P, Osei L, Netchine I, Pertuit M, Enjalbert A, et al. (2015) Case report of GNAS epigenetic defect revealed by a congenital hypothyroidism. Pediatrics 135: e1079-1083.
151. Bastepe M, Pincus JE, Sugimoto T, Tojo K, Kanatani M, et al. (2001) Positional dissociation between the genetic mutation responsible for pseudohypoparathyroidism type Ib and the associated methylation defect at exon A/B: evidence for a long-range

regulatory element within the imprinted GNAS1 locus. Hum Mol Genet 10: 1231-1241.
152. Bastepe M, Frohlich LF, Hendy GN, Indridason OS, Josse RG, et al. (2003) Autosomal dominant pseudohypoparathyroidism type Ib is associated with a heterozygous microdeletion that likely disrupts a putative imprinting control element of GNAS. J Clin Invest 112: 1255-1263.
153. Linglart A, Gensure RC, Olney RC, Juppner H, Bastepe M (2005) A novel STX16 deletion in autosomal dominant pseudohypoparathyroidism type Ib redefines the boundaries of a cis-acting imprinting control element of GNAS. Am J Hum Genet 76: 804-814.
154. Elli FM, de Sanctis L, Peverelli E, Bordogna P, Pivetta B, et al. (2014) Autosomal dominant pseudohypoparathyroidism type Ib: a novel inherited deletion ablating STX16 causes loss of imprinting at the A/B DMR. J Clin Endocrinol Metab 99: E724-728.
155. Richard N, Abeguile G, Coudray N, Mittre H, Gruchy N, et al. (2012) A new deletion ablating NESP55 causes loss of maternal imprint of A/B GNAS and autosomal dominant pseudohypoparathyroidism type Ib. J Clin Endocrinol Metab 97: E863-867.
156. Unluturk U, Harmanci A, Babaoglu M, Yasar U, Varli K, et al. (2008) Molecular diagnosis and clinical characterization of pseudohypoparathyroidism type-Ib in a patient with mild Albright's hereditary osteodystrophy-like features, epileptic seizures, and defective renal handling of uric acid. Am J Med Sci 336: 84-90.
157. Mantovani G, de Sanctis L, Barbieri AM, Elli FM, Bollati V, et al. (2010) Pseudohypoparathyroidism and GNAS epigenetic defects: clinical evaluation of albright hereditary osteodystrophy and molecular analysis in 40 patients. J Clin Endocrinol Metab 95: 651-658.
158. Mariot V, Maupetit-Mehouas S, Sinding C, Kottler ML, Linglart A (2008) A maternal epimutation of GNAS leads to Albright osteodystrophy and parathyroid hormone resistance. J Clin Endocrinol Metab 93: 661-665.
159. Elli FM, de Sanctis L, Bollati V, Tarantini L, Filopanti M, et al. (2013) Quantitative analysis of methylation defects and correlation with clinical characteristics in patients with Pseudohypoparathyroidism type I and GNAS epigenetic alterations. J Clin Endocrinol Metab: jc20133086.
160. Freson K, Izzi B, Labarque V, Van Helvoirt M, Thys C, et al. (2008) GNAS defects identified by stimulatory G protein alpha-subunit signalling studies in platelets. J Clin Endocrinol Metab 93: 4851-4859.
161. Zazo C, Thiele S, Martin C, Fernandez-Rebollo E, Martinez-Indart L, et al. (2011) Gsalpha activity is reduced in erythrocyte membranes of patients with psedohypoparathyroidism due to epigenetic alterations at the GNAS locus. J Bone Miner Res 26: 1864-1870.
162. Garin I, Mantovani G, Aguirre U, Barlier A, Brix B, et al. (2015) European guidance for the molecular diagnosis of pseudohypoparathyroidism not caused by point genetic variants at GNAS: an EQA study. Eur J Hum Genet 23: 438-444.
163. Court F, Martin-Trujillo A, Romanelli V, Garin I, Iglesias-Platas I, et al. (2013) Genome-wide allelic methylation analysis reveals disease-specific susceptibility to multiple methylation defects in imprinting syndromes. Hum Mutat 34: 595-602.
164. Maupetit-Mehouas S, Azzi S, Steunou V, Sakakini N, Silve C, et al. (2013) Simultaneous hyper- and hypomethylation at imprinted loci in a subset of patients with GNAS epimutations underlies a complex and different mechanism of multilocus methylation defect in pseudohypoparathyroidism type 1b. Hum Mutat 34: 1172-1180.
165. Perez-Nanclares G, Romanelli V, Mayo S, Garin I, Zazo C, et al. (2012) Detection of hypomethylation syndrome among patients with epigenetic alterations at the GNAS locus. J Clin Endocrinol Metab 97: E1060-1067.
166. Reinius LE, Acevedo N, Joerink M, Pershagen G, Dahlen SE, et al. (2012) Differential DNA methylation in purified human blood cells: implications for cell lineage and studies on disease susceptibility. PLoS One 7: e41361.

167. Houseman EA, Accomando WP, Koestler DC, Christensen BC, Marsit CJ, et al. (2012) DNA methylation arrays as surrogate measures of cell mixture distribution. BMC Bioinformatics 13: 86.
168. Court F, Tayama C, Romanelli V, Martin-Trujillo A, Iglesias-Platas I, et al. (2014) Genome-wide parent-of-origin DNA methylation analysis reveals the intricacies of human imprinting and suggests a germline methylation-independent mechanism of establishment. Genome Res 24: 554-569.
169. Docherty LE, Rezwan FI, Poole RL, Jagoe H, Lake H, et al. (2014) Genome-wide DNA methylation analysis of patients with imprinting disorders identifies differentially methylated regions associated with novel candidate imprinted genes. J Med Genet 51: 229-238.
170. Kobayashi H, Yanagisawa E, Sakashita A, Sugawara N, Kumakura S, et al. (2013) Epigenetic and transcriptional features of the novel human imprinted lncRNA GPR1AS suggest it is a functional ortholog to mouse Zdbf2linc. Epigenetics 8: 635-645.
171. Boycott KM, Vanstone MR, Bulman DE, MacKenzie AE (2013) Rare-disease genetics in the era of next-generation sequencing: discovery to translation. Nat Rev Genet 14: 681-691.
172. Laird PW (2010) Principles and challenges of genomewide DNA methylation analysis. Nat Rev Genet 11: 191-203.
173. Prickett AR, Ishida M, Bohm S, Frost JM, Puszyk W, et al. (2015) Genome-wide methylation analysis in Silver-Russell syndrome patients. Hum Genet 134: 317-332.
174. Azzi S, Rossignol S, Steunou V, Sas T, Thibaud N, et al. (2009) Multilocus methylation analysis in a large cohort of 11p15-related foetal growth disorders (Russell Silver and Beckwith Wiedemann syndromes) reveals simultaneous loss of methylation at paternal and maternal imprinted loci. Hum Mol Genet 18: 4724-4733.
175. Poole RL, Docherty LE, Al Sayegh A, Caliebe A, Turner C, et al. (2013) Targeted methylation testing of a patient cohort broadens the epigenetic and clinical description of imprinting disorders. Am J Med Genet A 161: 2174-2182.
176. Eggermann T, Elbracht M, Schroder C, Reutter H, Soellner L, et al. (2013) Congenital imprinting disorders: a novel mechanism linking seemingly unrelated disorders. J Pediatr 163: 1202-1207.
177. Queen SA, Kesslak JP, Bridges RJ (2007) Regional distribution of sodium-dependent excitatory amino acid transporters in rat spinal cord. J Spinal Cord Med 30: 263-271.
178. Campiani G, Fattorusso C, De Angelis M, Catalanotti B, Butini S, et al. (2003) Neuronal high-affinity sodium-dependent glutamate transporters (EAATs): targets for the development of novel therapeutics against neurodegenerative diseases. Curr Pharm Des 9: 599-625.
179. Lister R, Mukamel EA, Nery JR, Urich M, Puddifoot CA, et al. (2013) Global epigenomic reconfiguration during mammalian brain development. Science 341: 1237905.
180. De-Regil LM, Pena-Rosas JP, Fernandez-Gaxiola AC, Rayco-Solon P (2015) Effects and safety of periconceptional oral folate supplementation for preventing birth defects. Cochrane Database Syst Rev 12: CD007950.
181. Yi Y, Lindemann M, Colligs A, Snowball C (2011) Economic burden of neural tube defects and impact of prevention with folic acid: a literature review. Eur J Pediatr 170: 1391-1400.
182. Jentink J, van de Vrie-Hoekstra NW, de Jong-van den Berg LT, Postma MJ (2008) Economic evaluation of folic acid food fortification in The Netherlands. Eur J Public Health 18: 270-274.
183. Marean A, Graf A, Zhang Y, Niswander L (2011) Folic acid supplementation can adversely affect murine neural tube closure and embryonic survival. Hum Mol Genet 20: 3678-3683.
184. Bell JT, Tsai PC, Yang TP, Pidsley R, Nisbet J, et al. (2012) Epigenome-wide scans identify differentially methylated regions for age and age-related phenotypes in a healthy ageing population. PLoS Genet 8: e1002629.

185. Jentink J, Loane MA, Dolk H, Barisic I, Garne E, et al. (2010) Valproic acid monotherapy in pregnancy and major congenital malformations. N Engl J Med 362: 2185-2193.
186. Fathe K, Palacios A, Finnell RH (2014) Brief report novel mechanism for valproate-induced teratogenicity. Birth Defects Res A Clin Mol Teratol 100: 592-597.
187. Jentink J, Bakker MK, Nijenhuis CM, Wilffert B, de Jong-van den Berg LT (2010) Does folic acid use decrease the risk for spina bifida after in utero exposure to valproic acid? Pharmacoepidemiol Drug Saf 19: 803-807.
188. Tung EW, Winn LM (2010) Epigenetic modifications in valproic acid-induced teratogenesis. Toxicol Appl Pharmacol 248: 201-209.
189. Faiella A, Wernig M, Consalez GG, Hostick U, Hofmann C, et al. (2000) A mouse model for valproate teratogenicity: parental effects, homeotic transformations, and altered HOX expression. Hum Mol Genet 9: 227-236.
190. Turner CG, Klein JD, Wang J, Thakor D, Benedict D, et al. (2013) The amniotic fluid as a source of neural stem cells in the setting of experimental neural tube defects. Stem Cells Dev 22: 548-553.
191. Li H, Gao F, Ma L, Jiang J, Miao J, et al. (2012) Therapeutic potential of in utero mesenchymal stem cell (MSCs) transplantation in rat foetuses with spina bifida aperta. J Cell Mol Med 16: 1606-1617.

SCIENTIFIC SUMMARY

The laws of science do not distinguish
between the past and the future.
Stephen Hawking (1942)

SCIENTIFIC SUMMARY

Neural tube defects, affecting 1-2 per 1000 pregnancies, are severe congenital malformations that arise during early embryonic development due to failure of neurulation. Neural tube closure is influenced by a complex multifactorial etiology including both genetic and environmental factors. Although more than 250 mice models are known for NTDs and many candidate genes have been investigated in patient cohorts, the molecular basis underlying most human NTDs has still to be unravelled. Obesity, diabetes and anti-epileptic drugs give a higher risk for NTDs. On the other hand, folic acid prevents up to 70% of NTDs. However, most maternal folic acid levels in NTD-affected pregnancies are normal and despite optimal supplementation, the incidence of NTDs remains high. These environmental factors are linked to DNA methylation, an epigenetic modification that changes gene expression. The methylation hypothesis suggests that folate prevents NTDs by stimulating cellular methylation reactions and that a disturbed one-carbon metabolism may underlie NTDs. This brings us to the main question of this thesis: Can folate affect neural tube closure via changes in DNA methylation?

In this doctoral thesis, we wanted to investigate which DNA regions are more sensitive to methylation changes during embryogenesis and can lead to NTDs. Therefore; we performed a genome-wide DNA methylation analysis in patients with a myelomeningocele.

In Chapter 1 we go back to the embryological background of NTDs and we give an overview of the genetic and environmental factors that are known to be involved in NTDs. As we suppose that epigenetics and DNA methylation might fill the gap of knowledge in the search for the pathogenesis of NTDs, Chapter 2 gives an overview of studies that have been investigating the link between folate, DNA methylation and NTDs.

In Chapter 3 and 4 we discuss the results of the genome-wide DNA methylation study in patients with a myelomeningocele (MMC). In Chapter 3 we first investigated DNA methylation of the Homeobox genes in patients with a MMC. Homeobox genes play a central role in neural tube development for the establishment of the anterior-posterior body axis and are tightly regulated in a spatiotemporal and collinear

manner, partly by chromatin structure and epigenetic modifications. This study identified *HOXB7* hypomethylation as a potential risk factor for NTDs. In addition, *HOXB7* hypomethylation was also present in unaffected siblings of patients with a MMC. These findings are suggestive for additional (epi)genetic factors underlying NTDs. Therefore, we further analysed the genome-wide DNA methylation data without prioritizing for candidate genes in Chapter 4. Forty-five genes were significantly differentially methylated, and functional enrichment analysis revealed multiple neurodevelopmentally important gene ontology classes. Validation of the top 6 genes (*ABAT, CNTNAP1, SLC1A6, SNED1, SOX18* and *TEPP*) showed that *SOX18* hypomethylation is a potential risk factor for NTDs. DNA methylation analyses in families of patients with MMC revealed that parents had a significantly higher methylation than both patients with MMC and their unaffected siblings. These findings might suggest a maternal contribution for a disturbed one-carbon metabolism. DNA methylation analysis in a family of a patient with a paternally inherited *BMP4* deletion showed that genetic and epigenetic factors might interplay in the development of NTDs.
In Chapter 5 we present the study of genome-wide DNA methylation in patients with pseudohypoparathyroidism, that was performed to obtain expertise in data analysis and filtering, subsequently used for this thesis.

In conclusion, this doctoral thesis investigated the relation between DNA methylation and NTDs. We believe that our data support the multifactorial polygenic inheritance pattern of NTDs and the importance of epigenetic changes in neural tube development and disease. Further combined (epi)genetic studies are essential to unravel the complex etiology of NTDs and to alleviate the clinical, economical and psychological burdens for patients with NTDs.

NEDERLANDSTALIGE SAMENVATTING

Een open rug, of spina bifida, is het gevolg van een onvolledige sluiting van de primitieve neurale buis en de daarboven gelegen wervelbogen en huid. De term spina bifida is immers afgeleid vanuit het Latijn en betekent letterlijk “gespleten ruggengraat”. Neurale buis defecten (NBD) ontstaan binnen de eerste vier weken van de zwangerschap. Wereldwijd vormen NBD de tweede meest voorkomende congenitale aandoening met een incidentie van 0.5-2 per 1000 zwangerschappen. Ondanks de hoge prevalentie en de traumatische gevolgen voor patiënten met NBD, blijft het exacte ontstaansmechanisme nauwelijks begrepen. Zowel het hoge recurrentie- en occurentie- risico, als de hogere prevalentie in bepaalde etnische groepen, wijzen op het belang van genetische factoren. Daarnaast spelen verschillende omgevingsfactoren een belangrijke rol in het voorkomen van NBD. Maternele foliumzuur suppletie leidde tot 75% reductie van de incidentie, maar het blijft echter onduidelijk hoe foliumzuur neurale buisdefecten voorkomt. De maternele foliumzuurspiegel is in de meeste zwangerschappen met NBD immers normaal. Recent onderzoek verlegt de focus naar epigenetische mechanismen die door deregulatie van genexpressie tot NBD kunnen leiden. Wijzigingen in DNA-methylatie is één van de hoofdmechanismen van de epigenetica. Foliumzuur staat centraal in het één-koolstof-metabolisme dat noodzakelijk is voor DNA-synthese en de productie van s-adenosyl-methionine, de universele methyl groep donor voor alle macromolecules. Kan foliumzuur bijgevolg neurale buis sluiting beïnvloeden door veranderingen in DNA methylatie?

In deze doctorale thesis hebben we onderzocht welke DNA-regio’s meer gevoelig zijn aan veranderingen in DNA methylatie tijdens de vroege embryonale ontwikkeling en zouden kunnen leiden tot NBD. Hiervoor hebben we een genoom-wijde DNA methylatie analyse uitgevoerd in patiënten met spina bifida aperta ofwel myelomeningocele (MMC).

In de introductie van deze thesis gaan we terug naar de embryologie van NBD en geven we een overzicht van de genetische en omgevingsfactoren die een belangrijke rol spelen in de pathogenese. Aangezien we veronderstellen dat epigenetica en DNA methylatie de kenniskloof zouden kunnen sluiten, geven we in

hoofdstuk 2 een overzicht van de studies die al naar verbanden tussen foliumzuur, DNA methylatie en NBD hebben gezocht.

In hoofdstukken 3 en 4 bespreken we vervolgens de resultaten van de genoom-wijde DNA methylatie studie in patiënten met spina bifida. Aangezien Homeobox genen embryologisch een belangrijke rol spelen in de vorming van de neurale buis, en aangezien deze genen epigenetisch gereguleerd zijn, hebben we in hoofdstuk 3 eerst DNA methylatie voor de Homeobox genen onderzocht. Deze studie toont aan dat *HOXB7* hypomethylatie een potentiële risicofactor voor spina bifida is. Aangezien *HOXB7* hypomethylatie ook voorkomt bij niet-aangetaste broers en zussen van patiënten, spelen vermoedelijk bijkomende (epi)genetische factoren eveneens een rol. Daarom hebben we vervolgens in hoofdstuk 4 de genoom-wijde data zonder voorkennis geanalyseerd. Hierbij hebben we 45 genen gevonden, die betrokken zijn in meerdere neurologische ontwikkelingsprocessen. Na verdere validatie van de top 6 genen (*ABAT, CNTNAP1, SLC1A6, SNED1, SOX18* en *TEPP*) blijkt dat *SOX18* een bijkomende potentiële risicofactor voor spina bifida is. Op basis van de bevindingen bij de broers en zussen, hebben we *SOX18* methylatie verder onderzocht in 5 families van patiënten met spina bifida. Hierbij stellen we vast dat de beide ouders een significant hogere methylatie hebben, vergelijkbaar aan de gezonde controles, dan de beide kinderen. Zowel de patiënt als zijn gezonde broer of zus heeft een lagere methylatie dan beide ouders, vergelijkbaar aan de patiënten met spina bifida. Bijkomende analyse in de familie van een patiënt met een paterneel overgeërfde *BMP4* deletie, geeft aanwijzing voor een potentieel samenspel van zowel genetische als epigenetische factoren onderliggend aan spina bifida.

In hoofdstuk 5 beschrijven we de studie van genoom-wijde DNA methylatie in patiënten met pseudohypoparathyroïdie, die werd uitgevoerd om expertise te verwerven in de analyse en filtering van genoom-wijde data.

Tot slot kunnen we stellen dat onze studie de relatie tussen DNA methylatie en NBD heeft onderzocht. Onze data ondersteunen het multifactoriële polygenische overervingspatroon dat aan de oorzaak van NBD ligt en geven aanwijzingen voor de belangrijke rol die DNA methylatie hierin speelt. Bijkomende gecombineerde genetische en epigenetische studies zijn essentieel om de complexe etiologie van

NBD verder te ontrafelen en om de klinische, economische en psychologische last voor patiënten te verlichten. Aangezien het duidelijk is dat foliumzuur een belangrijke rol speelt in het ontstaan van neurale buisdefecten, ondersteunen we de internationale richtlijnen die de dagelijkse inname van 400 microgram foliumzuur vanaf drie maanden voor tot minstens drie maanden na de conceptie adviseren.

DANKWOORD

You gave me your time,
the most thoughtful gift of all.
Dan Zandra

Beste collega's, vrienden en familie,

Nu de laatste hand aan de thesis gelegd is, neem ik graag de tijd om stil te staan bij iedereen die heeft bijgedragen aan de realisatie hiervan. De weg naar een doctorale thesis verloopt niet altijd in een rechte lijn. Ze kent immers ook pieken en dalen, bochten en tweesprongen, maar telkens weer stond er iemand klaar om met me mee te gaan. Heel graag wil ik iedereen danken, langs de kant van de weg of op belangrijke kruispunten, om er voor mij te zijn.

Eerst en vooral dank ik van harte mijn promotor en copromotor, Prof. Kathleen Freson en Prof. Chris Van Geet. Kathleen, veel dank voor uw visie, die de belangrijkste richtingwijzer voor mijn thesis vormde de afgelopen vier jaar. Hartelijk dank om er voor me te zijn, voor uw deur die altijd open stond, voor uw tijd en snelle en nauwgezette antwoorden. Prof. Chris Van Geet, hartelijk dank om me in eerste instantie de kans te geven de opleiding pediatrie te volgen en om deze vervolgens te verrijken in de wereld van de wetenschappen. Al hoorde het onderwerp van mijn thesis misschien niet echt onder de koepel van de 'plaatjes', het was fijn om van deze warme groep deel uit te maken en kennis te verwerven binnen de epigenetica. Dank voor uw steun en enthousiasme voor mijn onderzoek.

Vervolgens dank ik de leden van de interne en externe begeleidings- commissies. Prof. Katrien Jansen, dank voor uw interesse en aanmoediging en om me te laten meevolgen in de spina bifida conventie, ik heb er veel van geleerd. Hartelijk dank Prof. Aleyde Van Eynde, Prof. Oebo Brouwers en Prof. Wilma Steegenga om mijn thesis na te lezen, voor uw constructieve opmerkingen en uw tijd om hier vandaag aanwezig te zijn.

Binnen het departement cardiovasculaire wetenschappen dank ik Prof. Herijgers en Prof. Budts, om me de kans te bieden mijn doctoraat te volbrengen en om vandaag mijn verdediging voor te zitten. Binnen het Centrum voor Moleculaire en Vasculaire Biologie (CMVB) dank ik Prof. Lijnen en zijn voorgangers Prof. Em. Verstraeten, Vermylen en Collen om in hun inspiratie en visie te mogen werken. Veel dank ook aan de andere proffen van onze eigen plaatjesgroep: Prof. Hoylaerts, Prof. Verhamme, Prof. Heying, Prof. Peerlinck en Prof. Jacquemin voor de interesse in mijn onderzoek en voor de constructieve opmerkingen tijdens de talloze labmeetings. In het bijzonder dank ik An, Diane, Karen, Gabriela, Annick en Ingrid om al de praktische regelingen heel vlot te laten verlopen.

In het laboratorium dank ik van harte Chantal en Christine om me al de technische vaardigheden aan te leren zoals DNA extraheren en zebravisjes injecteren. Veel dank om me wegwijs te maken en me op te leiden in het laboratorium. Soetkin, Katrien, Marleen, Mara, … dank voor jullie praktische hulp en voor de goede organisatie van ons laboratorium. Dank aan allen voor de goede sfeer, de gezellige

babbels en de leuke feestjes. Thomas en Gilian, bedankt voor jullie hulp bij het afschieten van de Sequenom platen. Sophie, bedankt voor je begeleiding bij de zebravisjes.

Graag dank ik al de collega PhD studenten, postdocs en masterstudenten in en buiten het CMVB. Anouck, bedankt voor je vele babbels en steun. Jorien, bedankt voor je eeuwige optimisme. Marijke, bedankt om er altijd te zijn en voor je luisterende oor. Special thanks to Benedetta, thanks a lot for your support, all your information and your good “boxes of sorrows”. With you the Epigenetics world became more clear. Elise en Evelien, bedankt voor ons mini-epigenetica-clubje en voor de toffe tijd (op congres) samen, het deed deugd om samen te discussiëren en overleggen. Raf en Griet, bedankt voor jullie hulp bij de analyse van de HM450k. Christophe, Thomas, Manisha, Jessica, Sophie, Nora, Maarten, Laurens, Rafael, Lorenz, Lotte, Dries, Sander, Maarten, Bianca, Ilse … bedankt voor de leuke momenten en de goede sfeer. Ik wens jullie veel succes toe met jullie onderzoeksprojecten.

Alex, thank you for helping me with the analysis of the 450k, all the scripts in R and the many many heatmaps. Thanks a lot to all the people from the lab of Prof. Dave Monk for having a wonderful period in Spain. Dave, thank you for giving me the opportunity to stay in your lab. It was a rich experience, both on scientific as on human level.

In het ziekenhuis dank ik de ouders en kinderen die hebben meegewerkt aan onze studie. Myleen, veel dank voor de hulp bij het verzamelen van de patiëntenstalen. Daarnaast dank ik het hele team van de pediatrie voor het samenwerken tijdens de talrijke wachtdiensten en raadplegingen. Het was deugddoend en moedgevend om geregeld in de pediatrie thuis te komen tussen het labo-werk door. In het bijzonder dank ik Prof. Lieven Lagae voor het vertrouwen en de begeleiding naar de toekomst.

Naast ‘doctoreren’ en ‘specialiseren’ was er nog tijd voor andere ‘projecten’.

Hierbij dank ik de leden van het bestuur van de Vlaamse Vereniging voor Kindergeneeskunde (VVK) voor de leerrijke en constructieve vergaderingen, waar doorheen de talrijke discussies mooie projecten werden gerealiseerd. Het was een genoegen om voorzitter te zijn van de VVK jongeren en om hierbij jullie volle steun te ervaren. Bedankt voor de aangename samenwerking, voor de goede sfeer en bovenal voor het blijven streven naar verbetering van welzijn van zowel Kind als Kinderarts. In het bijzonder dank ik de VVK jongeren voor de vlotte samenwerking en toffe tijd samen.

Daarnaast dank ik al de medeleden van de Leuvense Vereniging voor Geneesheer Assistenten (LVGA) voor de interessante discussies en constructieve samenwerking

in het belang van de Leuvense assistenten. Proficiat met de verwezenlijkingen en veel succes verder.

Hartelijk dank Prof. Marc Vervenne om me de kans te bieden om tijdens mijn hele doctoraatsopleiding in de gemeenschap van het Groot Begijnhof te mogen wonen. Het is een heerlijke plaats om ’s avonds tot rust te komen.

Daarnaast dank ik de vriendinnen van Leuven, de hele Rotaract-crew en de vele andere vrienden voor de fijne avondjes, weekendjes, telefoontjes, sms’jes die voor de nodige steun en uitlaatklep zorgden.

In het bijzonder wil ik van ganser harte mijn familie danken. Bedankt lieve ouders voor de kansen die jullie me gegeven hebben, voor jullie steun en voor de warme thuis. De afgelopen vier jaar doctoraat en specialisatie maakten van de agenda soms een puzzel, maar jullie deur staat altijd open en het was fijn om bij jullie tot rust te komen. Veel dank aan mijn broers, schoonzussen en schoonbroers. Bedankt Koen, Luc en Tom, Jan en Bénédicte, Frederic en Mary-Ann. Het doet zoveel deugd dat ik altijd op jullie kan rekenen en dat we een hechte groep vormen. Dank aan mijn (toekomstige) schoonouders voor jullie warmte, steun en enthousiasme. Hartelijk dank liefste Meter, Moeke, nonkels en tantes voor jullie interesse en het supporteren voor mijn thesis. Tot mijn spijt is mijn oma overleden tijdens mijn thesisjaren, maar ik weet dat je trots zou zijn, Oma, dank je voor je levenslessen en warmte.

Tot slot, liefste Jan, was het ongelooflijk heerlijk om jou tegen te komen en ik hoop dat we nog vele jaren samen verder op stap gaan en een nieuw boek kunnen neerschrijven. Bedankt voor je steun en je liefde.

Anne
Leuven, 14 juli 2016

CURRICULUM VITAE

To see a world in a grain of sand
And a heaven in a wild flower
Hold infinity in the palm of your hand
And eternity in an hour
William Blake (1757-1827)

PERSONAL INFORMATION

Last name	Rochtus
First names	Anne Maria Magda Marc
Place and date of birth	Dendermonde, December 24th, 1985
Nationality	Belgian
Contact mail	anne.rochtus@kuleuven.be annerochtus@gmail.com
Telephone	+32 (0)472 946 125

EDUCATION

2003-2010 Medical Doctor, Magna cum laude
University of Leuven

2010-2017 Specialist Training Pediatrics
University Hospital of Leuven

2012-2016 Doctoral Research
PhD project: 'DNA methylation studies in Spina Bifida'
University of Leuven

ADDITIONAL TRAINING

2005-2006 Spanish intensive courses, University of Leuven
2006-2007 Introduction to Child Psychiatry, University of Leuven
2007-2008 Medical French, University of Leuven
2011-2012 Advanced Pediatric Life Support Course, Antwerpen
2011-2012 Newborn Life Support Course, Antwerpen
2012-2013 Biostatistics and statistical bio-informatics, ESAT, University of Leuven
2012-2013 Laboratory Animal Science, University of Leuven
2012-2013 Ingenuity Pathway Analysis, VIB Leuven
2012-2013 Epigenetics, online intensive course, University of Melbourne
2013-2014 Introduction to R, ESAT, University of Leuven
2015-2016 European Paediatric Neurology Training Course 2016, Budapest, Hungary

SCIENTIFIC STUDIES AND VISITS

Master paper 2008-2009: **A. Rochtus**, A. De Ferm. Profylactische fixatie van de contralaterale heup bij patiënten met unilaterale epifysiolyse van de heupkop.

Master paper in preparation for specialty training Pediatrics 2009-2010: **A. Rochtus**, C. Van Geet. 'Immature Platelet Fraction' als parameter van megakaryopoïese.

Short Term Scientific Mission (STSM) funded by the EU COST action from the European Network of Human Imprinting Disorders in the laboratory of Genomic Imprinting and Cancer at IDIBELL in Barcelona, Spain, under supervision of Dr. Dave Monk: Genome-wide methylation in pseudohypoparathyroidism patients to

determine if their GNAS methylation defect is locus-specific or associated with multiple methylation defects. (20/04/2014 – 09/05/2014)

PUBLICATIONS

A. Rochtus, Ph. Alliet. Een 14-jarige jongen met thoracale pijn. Tijdschr Belg Kinderarts 2009:11(3);44-45

A. Rochtus, K. Vanrykel, A. Van De Casteele. Acute mastoiditis. Tijdschr Belg Kinderarts 2013:15(2);153-157

A. Rochtus, B. Izzi, E. Vangeel, S. Louwette, C. Wittevrongel, D. Lambrechts, Y. Moreau, R. Winand, C. Verpoorten, K. Jansen, C. Van Geet, K. Freson. DNA methylation analysis of Homeobox genes implicates *HOXB7* hypomethylation as risk factor for neural tube defects. Epigenetics. 2015;10(1):92-101.

A. Rochtus, K. Jansen, C. Van Geet, K. Freson. Nutri-epigenomic studies related to neural tube defects: does folate affects neural tube closure via changes in DNA methylation? Mini Rev Med Chem. 2015;15(13):1095-102.

A. Rochtus, A.M. Trujillo, B. Izzi, F.M. Elli, A. Linglart, G. Mantovani, G. Perez de Nanclares, S. Thiele, B. Decallonne, C. Van Geet, D. Monk, K. Freson. Genome-wide DNA methylation analysis of pseudohypopara-thyroidism patients with *GNAS* imprinting defects. Clin Epigenetics. 2016 Jan 26;8:10.

A. Rochtus, R. Winand, G. Laenen, E. Vangeel, B. Izzi, C. Wittevrongel, Y. Moreau, C. Verpoorten, K. Jansen, C. Van Geet, K. Freson. Methylome analysis for spina bifida shows *SOX18* hypomethylation as risk factor with evidence for a complex (epi)genetic interplay to affect neural tube development. *In Review.*

ORAL PRESENTATIONS

MDG Student Symposium (Leuven - October 2014). **A. Rochtus**. DNA methylation analysis of Homeobox genes implicates HOXB7 hypomethylation as risk factor for neural tube defects.

Second European Imprinting Disorders School (Paris – May 2015). **A. Rochtus**, A.M. Trujillo, F.M. Elli, V. Grybek, B. Izzi, G. Perez de Nanclares, S. Thiele, C. Van Geet, D. Monk, K. Freson on behalf of the EuroPHP consortium. Genome-wide DNA methylation in patients with Pseudohypoparathyroidism.

First Joint Meeting of Belgium and Dutch Child Neurology Societies (Tilburg – November 2015). **A. Rochtus**, R. Winand, G. Laenen, E. Vangeel, B. Izzi, C. Wittevrongel, Y. Moreau, C. Verpoorten, K. Jansen, C. Van Geet, K. Freson. DNA hypomethylation is linked to distinct pathways related to neural tube defects.

POSTER PRESENTATIONS

Conference Belgische Vereniging Kindergeneeskunde (Brussels – March 2011). **A. Rochtus**, E. Ortibus. Growth and nutrition in Cerebral Palsy.

European Imprinting Disorders School (Paris – May 2014). **A. Rochtus**, B. Izzi, R Winand, E Van Geel, Y. Moreau, K. Jansen, C. Van Geet, K. Freson. Genome-wide DNA methylation studies in patients with a myelomeningocoele.

Department of Cardiovascular sciences meeting (Leuven - October 2014). **A. Rochtus**, B. Izzi, C. Van Geet, K. Freson. A methodology to quantify genome-wide methylation using the HumanMethylation 450K BeadChip: development of analysis methods with imprinting disease PseudoHypoParathyroidism as model.

Epigenetics plasticity: implications in neural (dys)function (ICVS Braga – October 2014). **A. Rochtus**, B. Izzi, E. Vangeel, S. Louwette, C. Wittevrongel, D. Lambrechts, Y. Moreau, R. Winand, C. Verpoorten, K. Jansen, C. Van Geet, K. Freson. DNA methylation analysis of Homeobox genes implicates HOXB7 hypomethylation as risk factor for neural tube defects.

ESHG (Glasgow - June 2015). Methylome analysis for spina bifida identified hypomethylation of multiple genetic loci and distinct pathways linked to neural tube defects. **A. Rochtus**, B. Izzi, C. Wittevrongel, Y. Moreau, R. Winand, G. Laenen, C. Verpoorten, K. Jansen, C. Van Geet, K. Freson

Department of Cardiovascular sciences meeting (Leuven – October 2015). **A. Rochtus**, A. Martin-Trujillo, B. Izzi, F. Elli, I. Garin, A. Linglart, G. Mantovani, G. Perez de Nanclares, S. Thiele, B. Decallonne, C. Van Geet, D. Monk, K. Freson. Genome-wide DNA methylation analysis of pseudohypopara-thyroidism patients with GNAS imprinting defects.

Epigenomics of Common Diseases (Cambridge – November 2015). **A. Rochtus**, R. Winand, G. Laenen, E. Vangeel, B. Izzi, C. Wittevrongel, Y. Moreau, C. Verpoorten, K. Jansen, C. Van Geet, K. Freson. DNA hypomethylation in spina bifida is linked to distinct pathways related to neural tube defects.

Conference Belgische Vereniging Kindergeneeskunde (Brussels – March 2016). K. Huysentruyt, L. Dossche, **A. Rochtus**. Enquête “Kinderarts van morgen” 2015.

AWARDS

First Joint Meeting of Belgium and Dutch Child Neurology Societies (Tilburg – November 2015).

FREELANCE SCIENTIFIC EUROPEAN CORRESPONDENT FOR EPIGENIE.COM

10/2012 Epigenetics and Stem Cells – Robinson College Cambridge UK
04/2013 Non-coding RNA, Epigenetics and Transgenerational Inheritance – Churchill College Cambridge UK
10/2013 Epigenomics of Common Diseases – Wellcome Trust Institute Cambridge UK
10/2014 Epigenetics plasticity: implications in neural (dys)function – ICVS Braga
10/2014 Epigenomics of Common Diseases – Wellcome Trust Institute Cambridge UK
11/2015 Epigenomics of Common Diseases – Wellcome Genome Campus Cambridge UK

EXTRA-CURRICULAR ACTIVITIES

2013 – present President of the Resident Committee of the Flemisch Association of Pediatrics - Vlaamse Vereniging Kindergeneeskunde (VVK) Jongeren

2013 – present Member of Medical Resident Association of Leuven - Leuvense Vereniging Geneesheer Assistenten (LVGA)

2013 – present Member of Permanent Education Committee (POC) for the Master of Specialist Training in Medicine

2012 – present Member of Rotaract Leuven and president of the Social Committee for the organization of events for charity